Beatrice Offshore Wind Farm

Year 1 Post-construction Ornithological Monitoring Report 2019

Date:	28/04/2021
Tel:	0141 342 5404
Web:	www.macarthurgreen.com
Address:	93 South Woodside Road |Glasgow | G20 6NT

Document Quality Record

Version	Status	Person Responsible	Date
0.1	Draft	Mark Trinder	10.06.2020
0.2	Reviewed	Ross McGregor, Bob Furness	11.06.2020
0.3	Updated	Mark Trinder	12.06.2020
1	Internal Approval	Mark Trinder	12.06.2020
1.1	External Review	Joe Deimel	19.06.2020
1.2	Final	Mark Trinder	22.06.2020
2.0	Update following SNH and MSS comments	Mark Trinder	10.12.2020
2.1	Update to include turbine RPM data	Mark Trinder	27.04.2021
2.2	Final following client review	Mark Trinder	28.04.2021

CONTENTS

1 INTRODUCTION

The Beatrice Offshore Wind Farm is located in the Moray Firth, at its closest 13.5 km from the Caithness coast (Figure 2-1). Construction of the offshore elements began in April 2017, the first turbine was installed and operational by July 2018 and the final turbine was installed on the 14th May 2019.

The potential ornithological impacts which were considered of greatest concern during the application process were collision risk to large gulls (great black-backed gull and herring gull) and displacement of foraging auks (guillemots, razorbills and puffins). All these species breed at colonies which comprise the East Caithness Cliffs SPA and some of the birds present at the Wind Farm during the breeding season are likely to be from this SPA population. Through discussion with the Moray Firth Regional Advisory Group Ornithology Subgroup (MFRAG-O), the potential for the above impacts to affect these breeding populations was identified as the focus of ornithological monitoring for the Wind Farm.

A survey area, approximately rectangular in shape aligned parallel to the Caithness coast, was defined and surveyed in 2015 to provide pre-construction data. The surveys follow transects extending from the Caithness coast to 4 km beyond the seaward edge of the Wind Farm site boundary which measure approximately 40 km from north-east to south-west (Figure 2-1). In 2019, following installation of all turbines, the first post-construction survey was conducted. The same survey design and aerial survey contractor (HiDef) were used to ensure data comparability.

All seabirds were recorded during the surveys, however the targets for monitoring identified by MFRAG-O (hereafter, focal species) were great black-backed gull, herring gull, puffin, common guillemot, razorbill, kittiwake and gannet. Therefore, this report only discusses these species.

The primary aims of the aerial surveys were originally defined as:

- To collect seabird distribution data during the breeding season to enable comparisons of seabird abundance distributions before and after construction and estimate the magnitude (if any) of displacement resulting from avoidance of the Wind Farm (with a particular emphasis on puffin);
- Estimate the extent of connectivity between the Wind Farm and the East Caithness Cliffs SPA through analysis of flight directions; and
- Investigate the robustness of flight heights calculated from digital aerial data.

The aerial survey data are most suitable for considering spatial distributions and therefore most of the analyses and reporting presented here focus on this element of potential wind farm impacts. Two independent analyses have been conducted. The first used spatial models to compare the before (pre-construction) and after (post-construction) distributions using the MRSea R package (Scott-Hayward *et al.* 2013). The second used a bespoke turbine avoidance method, developed specifically for this monitoring study. This method, focused on data collected within the wind farm area itself, compared the observed range of seabird-turbine distances with those that might be observed by chance. This provides an indication of if birds are either avoiding, or attracted to, the turbines. Because this analysis does not rely on before-after comparisons (as the spatial analysis described above does), the results are not affected by potential inter-annual variations. The analysis was trialed with the pre-construction data, however this could only consider if the method

was expected to work, since there were no structures for birds to react to at that time. Analysis of the post-construction data presented in this report is the first time this has been used at an operational wind farm.

2 METHODS

The area of interest for surveying was identified as a region extending from the East Caithness coast to beyond the eastern Wind Farm boundary and extending to the north-east and south-west beyond the limits of the Wind Farm (Figure 2-1). Following discussions with MFRAG-O the finalised design of the aerial surveys was submitted to Marine Scotland on 29th May 2015 (Doc Ref: LF000005-SOW-05). Following the successful use of this survey design for the pre-construction surveys[1] this design was used for the post-construction surveys in 2019, the results of which are reported here.

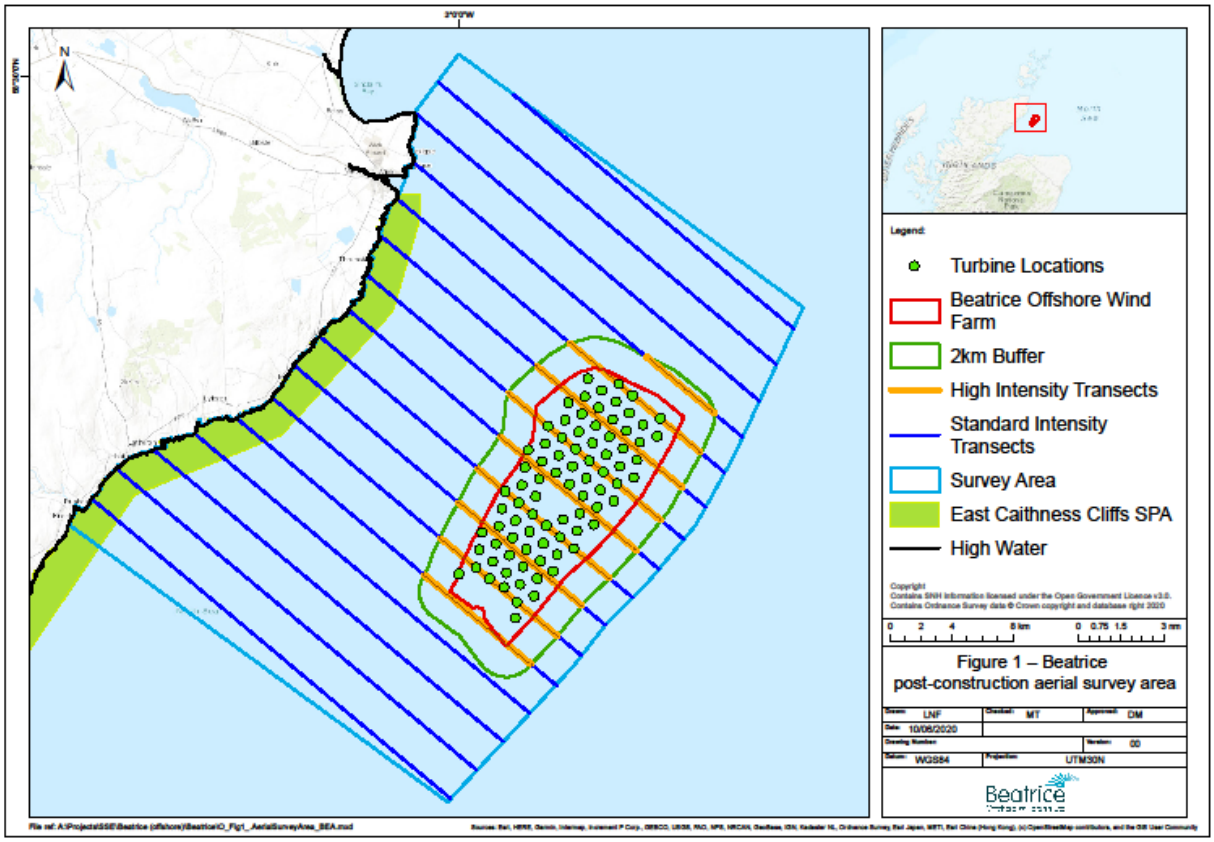

Figure 2-1. Survey area (light blue boundary) for aerial survey coverage of the Beatrice Offshore Wind Farm and the region of sea between the Wind Farm and the Caithness coast. Transects shown in dark blue, Wind Farm boundary (red), 2 km buffer (green) and turbine locations (green circles) shown.

The survey area measures approximately 40 km south-west to north-east and 26 km to 30 km north-west to south-east with 16 transects oriented perpendicular to the coast. The seaward boundary follows a 4 km buffer from the Wind Farm boundary to match the site characterisation

boat survey buffer. The transects which cross the Wind Farm were aligned to ensure that alternate ones crossed rows of turbines, with spacing of the remaining transects taken from this requirement. Hence the transects were separated by 2.5 km, and were between 24.2 and 31.7 km in length, giving a total transect length of 456 km. Approximately 60 km of this crossed the Wind Farm area (i.e. the area within the red line boundary shown in Figure 2-1 and Figure 2-2).

Both pre- and post-construction surveys were conducted by HiDef using high definition video cameras which record data continuously, generating strip transect data with the entire area surveyed within a single day on each occasion. Use of the same contractor ensured the datasets were comparable for analysis.

HiDef utilise up to four cameras mounted in parallel to give a total transect width of up to 500 m (125 m each). For transects within the 2 km Wind Farm buffer, data were provided from all four cameras, giving a coverage of 20% (hereafter 'high intensity survey'). These data were used for the turbine avoidance analysis. For the remainder of the survey area, data were provided from the two central cameras (250 m), giving coverage of 10% (hereafter 'standard intensity survey'). The high intensity transects were positioned so that alternate ones crossed rows of planned (in 2015) and subsequently constructed (2019) turbine locations (Figure 2-2). The total area surveyed was approximately 1,142 km^2, within which the wind farm area plus buffer covers an area of 383 km^2 and the wind farm covers an area of 131 km^2.

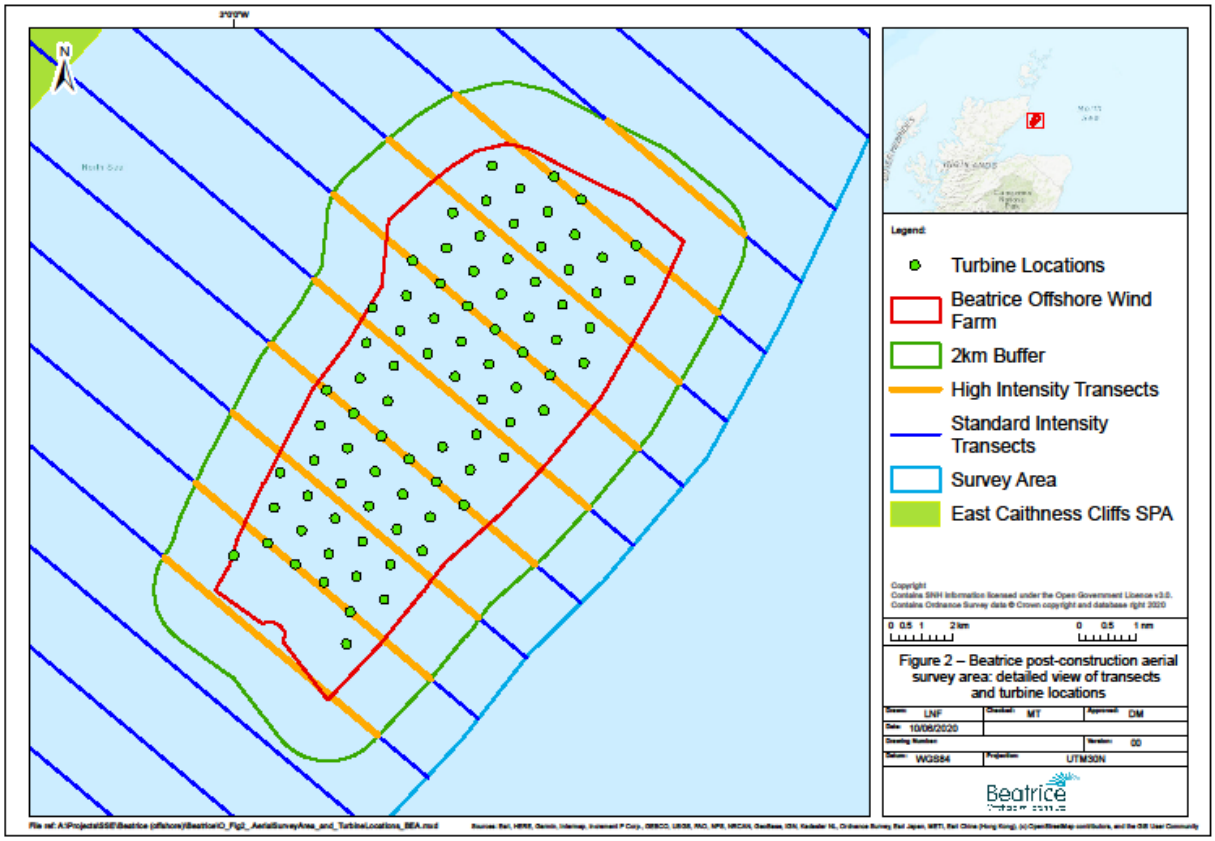

Figure 2-2. Detail of transects for aerial surveys over the Beatrice Wind Farm showing transect alignment in relation to turbine rows.

Data collected during each survey were supplied as spreadsheets and GIS shapefiles following image processing and transcription by HiDef. Each bird observed was identified using a hierarchical classification, down to species level wherever possible, with an associated confidence level. The following data were supplied following the surveys:

- Locations for all individuals observed; and,
- Flight heights for selected species (great black-backed gull, herring gull, gannet and kittiwake).

Additional data which were collected include behaviour (e.g. flying, sitting, etc.), age and sex (if possible).

2.1 Data analysis

For different aspects of the analysis the survey data were divided into the following areas:

- Total survey area – this was the entire survey region within the survey boundary (i.e. 1,142 km^2) making use of the standard intensity survey data;
- Wind Farm and 2 km buffer – this was the area within the 2 km buffer of the Wind Farm and used the high intensity survey data;
- Wind Farm and 500 m buffer – this was a subset of the Wind Farm and 2 km (high intensity) data; and
- Wind Farm – this was the area within the Wind Farm site boundary only.

Data analysis was split into the following components:

1. Assessment of the 2019 distribution and abundance of great black-backed gull, herring gull, puffin, common guillemot, razorbill, kittiwake and gannet across the entire surveyed area using the standard intensity data. Birds on the water and in flight were analysed separately; spatial models were used for birds on the water (if seen in sufficient numbers), permitting the use of explanatory variables to improve model precision; birds seen in lower numbers (on the water) and birds recorded in flight were analysed using design based methods (further details are provided below). Spatial modelling outputs were used to generate density surface maps for the total survey area and estimates of the population abundance in the total survey area and the Wind Farm area;
2. Comparison of the 2015 and 2019 model distributions using MRSea. The two datasets were combined and modelled with explanatory covariates (as above) and additional factor covariates of survey number and impact (defined as before/after the wind farm). To test for a redistribution effect an interaction term for impact and spatial location was included. Outputs from the models are provided as difference surfaces (i.e. the spatially explicit difference in abundance for the before and after surveys);
3. Analysis of seabird distributions within the Wind Farm and 500 m buffer in relation to planned turbine locations. A method to assess within Wind Farm avoidance of turbines was developed using these data and the results of this approach are included (note that this aspect was focused on the potential to detect displacement of foraging birds from areas around turbine bases rather than estimation of collision avoidance rates); and,

4. Analysis of flight height data for collision risk species (great black-backed gull, herring gull, kittiwake and gannet), to explore relationships between height and proximity to the turbines.

2.2 Spatial modelling and design-based analysis of birds on the water

The distributions of the focal species across the survey area were analysed using the MRSea Package for R, developed by Scott-Hayward *et al.* (2013). This package was developed under contract to Marine Scotland for analysis of data collected for marine renewable developments and is therefore directly applicable to the current study.

Spatial modelling permits the use of explanatory variables to be included in the analysis to identify significant relationships between the variables and the recorded distributions. Any significant covariates identified can then be used to predict distributions in areas not surveyed, either between transects or to areas beyond the surveyed area (in the current analysis only the former was undertaken). Thus, the observations made along transects can be used to estimate the density between transects and thereby to derive predictive maps and abundance estimates for the whole survey area.

The candidate covariates used in the analysis were sea depth (obtained from EMODnet, 13/12/2019) and distance to coast, together with a spatial term (a combined x-y position), which captures additional spatial patterns not explained by the other covariates. To conduct this analysis the transect data were divided into 500 m long segments. Segment width for analysis of the total survey area was 250 m, and for the data collected on the Wind Farm and 2 km buffer was 500 m. Covariate values for use in the modelling (e.g. distance to coast and depth) were obtained for the midpoint of each segment. The depth value was the average value for the 90x90 m cell in which the segment midpoint was located.

Spatial analysis was conducted using only birds recorded on the sea surface since the explanatory covariates were selected on the basis of potential relationships with foraging locations, and hence these would not be expected to show strong correlations with the distribution of flying birds (particularly auks). Analysis of the density and abundance of flying birds was conducted separately (see Section 2.3).

Spatial model fitting followed the methods set out in Scott-Hayward *et al.* (2013). To generate maps of spatial distributions, each survey was analysed independently, using the smoothed x-y spatial term with depth and minimum distance to coast as additive terms. The MRSea functions automatically test relationships and retain only significant covariates in the final model. The outputs from these models are provided primarily for illustration.

If modelling was unsuccessful (i.e. the model failed to converge) for a particular species on a survey, maps of the observed bird locations are provided without an underlying density surface.

To test for a Wind Farm effect the data from 2015 and 2019 were combined and an impact term (0/1) included as a categorical variable. To accommodate autocorrelation (e.g. along transects) a blocking structure was included in the analysis. This was a composite of survey ID (1 to 6) and transect ID (1 to 16) and allowed for spatial and temporal autocorrelation and also for testing for influential blocks within the data.

The initial model formulation was as follows:

$$y \sim impact + s(depth) + s(disttocoast) + s(x,y, impact)$$

with only significant terms (at $p < 0.05$) retained in the final model.

As well as impact (0/1) this model included smoothed, one-dimensional terms for depth and distance to coast, a two dimensional spatial smooth term (x,y) and an interaction between the spatial smoother and impact to test for a redistribution effect (i.e. rather than simply an overall change in number). It is not possible to determine from the model coefficients what the spatial nature of the changes are. Thus, while a significant interaction between the impact and spatial terms indicates a before-after re-distribution effect, this does not on its own indicate where the change has occurred. To visualise the changes to the spatial distribution, the models were used to make predictions across a grid of cells covering the study area. To ensure the outputs are robust, MRSea employs a bootstrap routine, thereby incorporating parameter uncertainty. The median difference between the pre- and post- surfaces were plotted as maps which indicate where changes in distribution have occurred. Cells which have changed significantly are identified with symbols that also denoted the direction of change (positive/negative).

The spatially explicit abundance predictions were made across a prediction grid of 500 m cells covering the entire survey area each cell of which had a covariate parameter value for depth, distance to coast and the spatial term (i.e. coordinate). The abundance of each species in any spatial subset of cells was obtained by summing the cells within that region (e.g. those in the Wind Farm). By including covariate values for the impact and survey number terms in the model, the abundance for all combinations of survey and impact could also be obtained.

Comparison of predicted cells, for example of the pre and post datasets, allows spatially explicit differences to be derived (i.e. subtracting one from the other to obtain cell by cell differences).

To check the extent to which the before-after results were influenced by individual surveys the *runInfluence* function in MRSea was used to obtain the covratio and press statistics. The summary results are provided in the results section, with the plotted outputs in Appendix D.

In addition to spatial modelling, the abundance of birds in the survey area and the wind farm were calculated for both the 2015 and 2019 surveys. The previous method (used in an earlier draft of this report and in the 2015 report) calculated the density as the number seen divided by the surveyed area and multiplied this by the total survey region to obtain an abundance estimate. In addition, for estimating the wind farm abundance estimates all of the 'high-intensity' survey data (i.e. 4 cameras) were used. This dataset extended across the wind farm and 2km buffer, from which the estimated density was multiplied by the wind farm area to obtain a wind farm abundance. Thus, while the abundance applied to the wind farm only, the density applied to the larger 2km area.

However, in order to be able to estimate confidence intervals around these estimates (at the request of the Moray Firth Regional Advisory Group) it was necessary to modify the calculation method, and this has resulted in modified estimates. The revised method divides each transect into 500m segments (to which observed birds are assigned), which can then be resampled using a bootstrap method, in this case 1,000 times, from which a distribution of 1,000 survey counts was derived, and the 95% confidence intervals obtained. Since the transects are not exactly divisible by the segment length (500m) a small number of observations at the transect ends may fall outside

the surveyed area, and this results in slightly different estimates compared with those in the previous version of this report and in the 2015 monitoring report. In addition, to obtain the wind farm estimates in the revised method only the data collected inside the lease boundary were used, which has also resulted in changes in the estimated abundance in some cases (typically the changes are largest for more patchy, less abundant species and vice versa).

Although design-based estimates are less robust than model-based ones, for species observed in smaller numbers it was not possible to successfully fit models and therefore it was necessary to use design based methods to obtain abundance estimates.

While the spatial modelling repeated and updated the pre-construction analysis originally presented in BOWL 2016, it should be noted that in some cases the pre-construction abundances derived from the spatial models presented in the current report differ from those in the pre-construction report. This is a result of methodological revisions (e.g. to the MRSea library), changes in the orientation of the grid of prediction cells used and the consequent small changes in some of the covariate estimates (see ANNEX A for a comparison of abundance estimates).

For those species for which availability bias may lead to underestimation of absolute abundance (e.g. diving species such as auks), abundance estimates can be multiplied by correction factors to obtain the estimated total abundance allowing for birds which were underwater when the images were recorded. This is useful for comparisons with previous estimates and sites elsewhere (assuming those have also been corrected for potential bias), however as the correction factor is a constant rate for each species, there is no benefit in terms of comparing distributions between surveys or between the spatial modelling and design based estimates. Correction factors for guillemot, razorbill and puffin were taken from Thaxter *et al*. (2010) and Burton *et al*. (2013). The values used were: guillemot, 1.237; razorbill, 1.174; puffin, 1.202. Note that these adjustments were only made to the design-based abundance estimates (as it was considered less appropriate to adjust the model based ones), and therefore partly explain differences between the two sets of abundance estimates for these species.

2.3 Abundance of birds in flight

The abundance of birds in flight was estimated using design-based methods, with the density of birds in each transect calculated as the number observed divided by the area surveyed. To estimate abundance across the total survey area the standard intensity data were used, while for the estimated abundance in the Wind Farm area the high intensity data were used, thereby maximising use of the data. The average density across transects was multiplied by the relevant area to obtain estimates of the abundance of birds in flight. The locations recorded on each survey were plotted and are provided in Annex B.

2.4 Seabird distributions in relation to turbine locations

The high intensity data from the post-construction surveys were analysed using the method developed to investigate within Wind Farm seabird distributions. For each species (guillemot, puffin, razorbill, kittiwake and herring gull; note that there were insufficient observations within the wind farm for gannet or great black-backed gull) the analysis used the locations of each observed individual within 400 m of turbines.

The analysis was focused on seabird usage with the wind farm. Therefore, since birds recorded in flight may have been passing through the wind farm, rather than utilizing the area, only birds recorded on the sea surface were included in the analysis. The minimum distance between each bird and the nearest turbine location was calculated from the density of birds within sequential 100 m radius circles (100, 200, 300 and 400 m) around each turbine. To test if the observed density within each radius differed from a random distribution a two-dimensional bootstrap procedure was developed.

For each bootstrap simulation the grid of actual turbine locations was offset using a uniformly distributed random offset value generated independently for both x and y coordinates within a range of +/-510 m (x) and +/-550 m (y), with an angular offset to generate random locations within adjacent parallelograms around each turbine location (see Figure 2-3). At each iteration of the bootstrap the same offset (x/y) was applied to all turbine locations, thereby 'moving' the Wind Farm as a whole while maintaining all the inter-turbine distances and relative positions. It can be seen in Figure 2-3 that this approach ensured turbine relocations were located within discrete parallelograms up to half the distance to the next turbines.

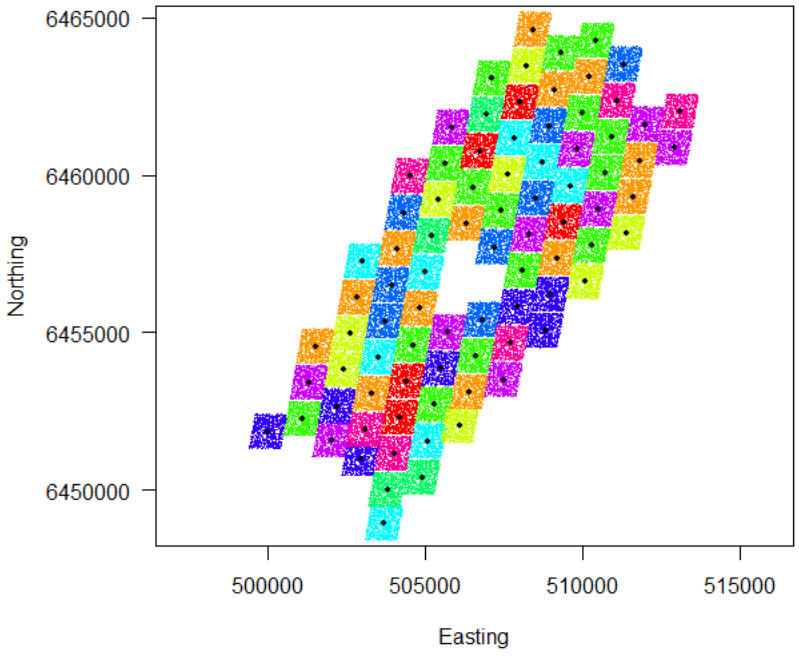

Figure 2-3. Illustration of randomised turbine positions used in the turbine avoidance analysis. Each coloured parallelogram contains 1,000 dots, each one a single realization of the randomized turbine location around the actual turbine locations (black dots).

In order to maximise sample sizes, the initial analysis combined the data for each species across the 6 (post-construction) surveys. In addition, to investigate for the presence of potential variations in density around the turbines under different wind farm operating conditions, the data were analysed in relation to turbine revolution per minute (RPM), using the average value for each turbine recorded during the period each survey was flown. Each bird observation used in the

turbine avoidance dataset had the average RPM of the nearest turbine, as recorded on the same survey, assigned to it (i.e. the RPM for the closest turbine at the time the observation was made). The turbine avoidance analysis was then re-run, but with the data divided into five subsets based on the RPM:

- <2,
- >=2 & <4,
- >=4 & <6,
- >=6 & <8, and
- >=8.

2.5 Flight heights

HiDef provided size-based flight height estimates, derived by comparing the body length of birds observed on the surveys with baseline body length information obtained and analysed by HiDef from surveys conducted across multiple sites. The baseline data, containing what is referred to hereafter as known height body lengths, have been measured from birds that show reflection on the sea surface, which calculation has shown to comprise only birds within 3 m of the sea surface.

The body lengths of birds recorded during the surveys were measured in the same way as the reflection data have been processed, with the maximum bird length (across multiple frames) used as the value for that record. For each maximum body length, a range of possible heights is calculated using the upper and lower 95% body lengths of the known height birds.

The minimum height of each record is calculated using the equation:

$$\text{Bird height} = \text{Aeroplane height} \times (1 - (l_{r\ min}/l_{s\ max})$$

Where:

$l_{r\ min}$ = lower 95% CI of birds with reflection; and,

$l_{s\ max}$ = maximum length of the bird from available frames.

The maximum height of each record is calculated using the equation:

$$\text{Bird height} = \text{Aeroplane height} \times (1 - (l_{r\ max}/l_{s\ max})$$

Where:

$l_{r\ max}$ = upper 95% CI of birds with reflection

This provides a minimum and maximum height value for each individual. In some cases, for birds recorded close to the sea surface, this calculation results in an estimate of height less than sea level, due to uncertainties in the body length measurements. These birds were assigned a height of zero, on the basis that they were definitely below rotor height but could not be assigned a reliable estimate. While inclusion of these in estimates of flight height would clearly bias the results, they could be included in estimates of the proportions at and below rotor height. Thus, height was analysed as a binomial response variable with respect to the lower rotor tip height (32.7

m; below/above), using the maximum estimated value (including the zero values as noted above in the below category). Data were filtered on distance from shore (selecting birds the same distance offshore as the wind farm) with inside/outside the wind farm as an explanatory variable.

It should be stressed however that estimates of bird flight height calculated from aerial imagery in the manner described include a large degree of uncertainty, due to several sources of potential error (e.g. the orientation of the bird relative to the camera, the comparatively small size of the bird image) and this is evidenced by negative height estimates (i.e. below sea level). Thus, the height data should be considered to provide a guide rather than definitive estimates.

3 RESULTS

3.1 Surveys

The survey design was based on 2 surveys in each of May, June and July. However, in both 2015 and 2019 it was only possible to undertake one survey in May. In 2015 an additional one was conducted in the first week of August (in agreement with MFRAG-O) and in 2019 an extra survey was completed in June (i.e. there were three surveys in that month). Thus, six surveys were successfully completed in both years, covering a very similar range of dates.

The six 2019 surveys were conducted between 28th May and 25th July 2019, spaced at approximately equal intervals through asthe period (as weather permitted). Each survey was conducted within a single day in good visibility (Table 3-1). The pre-construction surveys, conducted in 2015, covered the same period (30th May to 5th August).

Table 3-1. Survey dates, start and end times, and weather conditions.

Survey no.	Date (all 2019)	Start time	End time
1	28/05	10:49	12:22
2	10/06	11:09	12:27
3	22/06	10:52	12:13
4	29/06	10:25	11:48
5	19/07	08:16	09:49
6	25/07	11:55	13:26

As can be seen in Table 3-1, surveys were conducted between 8am and 1.30pm. Breeding seabird activity levels may vary through the day, and it is therefore possible that these survey times omitted peaks in activity (e.g. if these occur around dawn and dusk). However, not all seabirds appear to exhibit marked variations during the day (e.g. Furness et al. 2018 reported relatively constant levels of gannet activity throughout the day) and indeed recording average levels (e.g. during the middle of the day) could be considered more appropriate for characterizing usage levels. There was also considerable between survey variation in seabird abundance, despite the surveys having been flown at similar times, suggesting that factors other than time of day are also important in determining activity levels. In addition, given the remote location of the wind farm it must also be acknowledged that it was necessary to conduct surveys within periods of suitable weather and in accordance with safe flying practices, and these also impose limits on when surveys can be undertaken.

3.2 Spatial modelling and design based analysis of birds on the water

To estimate each species' abundance using the spatial models the data for each survey were analysed independently in order to avoid outputs being constrained by the need to fit to varying distributions between surveys. The 2015 data were reanalysed in order that the same methods were applied to both datasets (the original 2015 outputs are provided in ANNEX A for comparison).

The predicted density surfaces from the best-fit spatial models for each species on each survey are plotted across the total survey area in Figure 3-1 to Figure 3-7, with the location of observations overlaid. Models could not be fitted successfully to all combinations of species and survey (e.g. due to small numbers of observations on some surveys). In these cases, just the observations are presented without the underlying density surface. The predicted population abundances from the best-fit models are provided in Table 3-2 and for comparison the design-based population estimates are provided in Table 3-3. It should be noted that the model based estimates for each survey for gannet and razorbill were obtained from the before-after model which did not include the survey term, therefore these are monthly predictions from the averaged distribution (in other words, the plotted distribution is the same in each case, but the cell values vary). It was necessary to use these model outputs due to a failure to obtain model convergence for these species. The monthly estimates for guillemot, puffin and kittiwake were obtained from models which omitted the impact term but included survey (1-12) and the spatial interaction. These models therefore produced both different abundances and different distributions for each survey.

Table 3-2. Model derived population abundance estimates in the total survey area (shaded) and within the Wind Farm boundary for each species in each survey in 2015 and 2019. Entries marked with '-' indicate instances when small sample sizes prevented model fitting or unreliable estimates were obtained due to edge effects. Values for 2015 were re-estimated using the same methods as the 2019 data for consistency (the original estimates from Table 4 of the pre-construction monitoring report[1] are provided in Appendix 1). Note that model fitting was unsuccessful for the 2015 great black-backed gull and herring gull observations.

Species	Year	Region	Population abundance on each survey					
			1	2	3	4	5	6
Gannet	2015	Total survey area	174.14 (68.71-560.07)	461 (144.71-1663.8)	708.6 (253.68-2304.54)	182.64 (53.55-735.05)	17.51 (3.95-88.81)	8.89 (1.2-99.67)
		Wind Farm	56.38 (25.69-135.59)	149.26 (58.55-382.35)	229.43 (77.31-697.2)	59.13 (20.3-169.8)	5.67 (1.38-25.41)	2.88 (0.42-23.03)
	2019	Total survey area	48.96 (11.89-231.49)	397.49 (116.4-2146.68)	19.88 (4.29-90.52)	20.02 (3.8-128.9)	49.89 (15.48-190.94)	159.31 (45.04-713.7)
		Wind Farm	15.85 (4.22-54.54)	128.7 (46.51-428.35)	6.44 (1.4-23.03)	6.48 (1.26-32.73)	16.15 (5.54-51.56)	51.58 (16.33-179.91)
Guillemot	2015	Total survey area	39760.1 (20689.08-79196.5)	36561 (20289.51-67384)	15487.51 (7806.23-33179.9)	51036.88 (18376.31-181745.75)	7642.67 (2917.32-22387.06)	4063.53 (2531.28-6572.26)
		Wind Farm	5819.89 (3862.15-8494.54)	1421.16 (726.86-3277.18)	2060.09 (671.12-5699.66)	7015.87 (2874.09-18580.78)	1452.03 (597.6-4140.03)	902.15 (571.45-1371.54)
	2019	Total survey area	25525.3 (13044.34-55685.87)	86819.89 (51048.47-154260.6)	54556.22 (26481.73-124613.04)	41419.22 (27175.88-65578.77)	25857.29 (14639.11-51179.33)	9845.04 (4331.96-28441.8)
		Wind Farm	987.59 (378.26-3829.03)	10858.98 (6526.95-19028.2)	4129.67 (2560.53-7088.94)	2768 (1754.02-5172.78)	1306.54 (824.1-2301.73)	456.83 (206.08-1152.56)
Kittiwake	2015	Total survey area	1443.36 (240.58-Inf.)	3639.09 (1006.21-18202.84)	3375.96 (1287.41-42182.78)	3707.1 (1300.72-14844.79)	1666.87 (665.66-Inf.)	352.24 (119.93-2094.11)
		Wind Farm	37.74 (4.71-Inf.)	246.75 (41.85-1796.32)	62.47 (17.46-1291.96)	1290.7 (468.62-5478.88)	174.02 (49.15-532.56)	63.05 (22.28-273.71)
	2019	Total survey area	716.66 (224.81-3084.67)	4610.17 (1247.47-25631.62)	3394.08 (1572.48-9227.65)	3910.28 (1590.86-12892.57)	2176.33 (573.72-10062.28)	1440.09 (456.07-11148.52)
		Wind Farm	15.02 (2.33-108.29)	1648.42 (454.96-6363.4)	1005.38 (498.03-2368.57)	304.6 (76.64-1224.42)	353.41 (91.65-1729.73)	148.33 (46.72-476.5)

Species	Year	Region	Population abundance on each survey					
			1	2	3	4	5	6
Puffin	2015	Total survey area	1959.97 (1045.33-3909.2)	1409.81 (709.41-2834.88)	479.25 (274.2-894.54)	532.23 (307.77-1506.8)	213.98 (68.68-2470.41)	3133.13 (1847.2-5478.68)
		Wind Farm	193.19 (92.48-390.67)	72.91 (23.81-176.21)	19.75 (6.48-69.78)	2.66 (0.15-135.22)	2.62 (0.08-1017.92)	1027.46 (677.12-1489.49)
	2019	Total survey area	335.73 (132.41-975.68)	1170.59 (703.2-2115.31)	523.34 (252.3-1166.97)	520.57 (274.39-971.1)	310.5 (128.27-826.87)	509.74 (279.06 – Inf.)
		Wind Farm	16.82 (5.56-64.18)	38.7 (16.87-95.03)	15.63 (4.32-57.16)	2.77 (0.53-15.6)	9.9 (2.32-51.52)	0.07 (0 – Inf.)
Razorbill	2015	Total survey area	817.78 (378.69-1807.06)	2034.53 (1068.39-3815.14)	3527.92 (2435.72-5279.48)	1674.76 (710.26-3628.75)	37.71 (15.33-94.75)	9.62 (1.57-80.87)
		Wind Farm	49.28 (20.56-107.91)	122.62 (62.46-222.07)	212.62 (146.22-295.28)	100.94 (44.21-219.91)	2.28 (0.92-5.68)	0.58 (0.11-4.88)
	2019	Total survey area	2047.98 (1167.72-3514.64)	10407.67 (6957.55-16843.05)	4197.71 (2887.65-6092.87)	11246.81 (8048.72-16336.36)	3631.78 (2419.68-5715.97)	1289.6 (568.93-3499.66)
		Wind Farm	123.43 (74.26-224.69)	627.26 (426.84-963.7)	253 (171.63-378.9)	677.83 (486.76-967.67)	218.88 (143.62-365.07)	77.72 (34.6-216.58)
Great black-backed gull	2019	Total survey area	-	-	-	127.5 (36.4 - 833)	-	-
		Wind Farm	-	-	-	1 (0.3 - 10.8)	-	-
Herring gull	2019	Total survey area	-	5072.8 (1338.8 - 19979.2)	804.8 (260.8 - 3554.7)	533 (207.9 - 2030.8)	-	-
		Wind Farm	-	1298.2 (383.7 - 4431.9)	39.4 (8.9 - 231.5)	12 (2.2 - 112.4)	-	-

Table 3-3. Design-based population abundance estimates (and 95% confidence intervals) in the total survey area and within the Wind Farm boundary for each species in each survey in 2015 and 2019 (shaded). Abundance across the total survey area was estimated using the standard intensity data, Wind Farm abundance was estimated using the high intensity data. Confidence intervals estimated using a bootstrap resampling method (see text for details).

Species	Year	Area	Population abundance on each survey					
			1	2	3	4	5	6
Gannet	2015	Total survey area	266.6 (110.6-492.5)	543.3 (180.9-1126.1)	810 (422.2-1286.9)	211.3 (90.5-371.9)	29.6 (0-60.6)	9.8 (0-30.2)
		Wind Farm	25.2 (5-50.3)	64.8 (10.1-130.8)	536.4 (266.3-834.4)	20.1 (5-40.2)	24.6 (5-50.4)	0 (0-0)
	2019	Total survey area	60.8 (20.1-110.6)	566.9 (281.2-924.8)	20.4 (0-50.3)	30.2 (0-70.4)	50 (9.8-110.6)	177.2 (60.3-351.8)
		Wind Farm	0 (0-0)	0 (0-0)	0 (0-0)	0 (0-0)	5.3 (0-15.1)	0 (0-0)
Guillemot	2015	Total survey area	67486.7 (48838.3-93543.4)	68431.6 (49699.1-90366.4)	24508.3 (18886.8-30563.9)	77502 (47309.8-123530.3)	18220.9 (11111-27219.7)	5841.4 (4649.5-7187.4)
		Wind Farm	7794.9 (5620.2-10326.7)	2286.2 (1398.9-3345.3)	6243.9 (2168.9-12516.9)	9425.8 (5676.1-13833.7)	4750.2 (1485.9-8983.8)	971.2 (671.3-1318)
	2019	Total survey area	47705.2 (29811-71541.5)	143361.4 (106507.4-190991.8)	79641.7 (50488.3-118429.8)	61415.9 (51848.6-72706)	40754.1 (29792-52734.6)	12900.5 (8517.2-18166.9)
		Wind Farm	1258.8 (578.2-2406.4)	24570.4 (19214.9-30459.3)	6720.9 (4686.5-9314.1)	1986.6 (1454.7-2592.7)	1091.8 (652.8-1647.7)	232.5 (105.5-404.1)
Kittiwake	2015	Total survey area	1575.9 (210.8-4165)	3791.2 (1336.9-7498.8)	3451.5 (1407-5941)	3806.4 (1868.9-6192)	3759.2 (1557.3-6605.2)	424.3 (130.4-814.2)
		Wind Farm	70.4 (30.2-120.6)	25.2 (0-75.4)	384.8 (5-1106)	2334.7 (643.3-4986.8)	556.7 (140.7-1141)	78.9 (0-201)
	2019	Total survey area	571.3 (130.4-1176.6)	7918.5 (3445.8-13510.4)	3841.7 (2090.3-5941.2)	5204.2 (1999.6-9651.2)	2350.1 (995.1-4081.6)	1376.7 (532.8-2392.6)
		Wind Farm	10 (0-25.1)	4072.9 (2090.7-6654.7)	1862.6 (713.6-3181.7)	1167.9 (45.2-2825.5)	64.7 (0-160.8)	72.4 (0-216.1)
Puffin	2015	Total survey area	2614 (2053.4-3213.9)	2206.8 (1534.5-3032.7)	738.4 (483.3-1002.8)	1236.6 (374.6-2888)	377.8 (145-664.8)	4112.4 (3346.9-4917.6)

Species	Year	Area	Population abundance on each survey					
			1	2	3	4	5	6
		Wind Farm	247.4 (108.7-453.1)	77.9 (24.2-138.9)	61.1 (18.1-120.8)	36.9 (6-78.5)	11.7 (0-30.2)	1543.5 (1135.6-2017.8)
	2019	Total survey area	459.4 (290-664.5)	1600.4 (1014.9-2319.8)	721.5 (495.4-966.6)	698.4 (447.1-978.7)	397.6 (229.6-567.9)	875.8 (422.6-1426.3)
		Wind Farm	6.2 (0-18.1)	156.7 (90.6-223.5)	54.8 (18.1-102.7)	18.2 (0-48.3)	6 (0-18.1)	0 (0-0)
Razorbill	2015	Total survey area	1034.2 (519.2-1829.2)	2635 (1746.3-3799.9)	4457.7 (3209.9-5853.6)	2140.6 (1132.9-3622.9)	83.2 (23.6-153.4)	11.9 (0-35.4)
		Wind Farm	47.5 (17.7-88.5)	17.6 (0-47.2)	278.1 (76.7-525.1)	153.9 (23.6-336.5)	18.5 (0-53.1)	11.6 (0-29.5)
	2019	Total survey area	2680.1 (1793.8-3729.1)	12542.8 (9157.3-16605.5)	4668.5 (3658.3-5841.5)	12938.5 (10785.6-15542)	4026.3 (3020.5-5240)	1305.5 (672.4-2077)
		Wind Farm	71.1 (17.7-141.6)	1344.3 (1002.9-1705.3)	475.5 (283.2-690.4)	447.3 (277.3-619.7)	222.6 (47.2-477.9)	47.5 (11.8-94.4)
Great black-backed gull	2015	Total survey area	19.2 (0-50.3)	30.2 (0-70.4)	29.7 (0-70.6)	51.4 (10.1-110.6)	28.9 (0-80.4)	10.5 (0-30.2)
		Wind Farm	0 (0-0)	4.9 (0-15.1)	0 (0-0)	15.1 (0-45.2)	5.4 (0-15.1)	0 (0-0)
	2019	Total survey area	0 (0-0)	141.4 (0-321.7)	9.5 (0-30.2)	171.4 (60.3-321.9)	319.4 (0-954.9)	41.4 (0-110.6)
		Wind Farm	0 (0-0)	41.4 (0-115.6)	0 (0-0)	4.9 (0-15.1)	0 (0-0)	0 (0-0)
Herring gull	2015	Total survey area	70.2 (10.1-170.9)	70.7 (10.1-160.8)	10.6 (0-40.2)	414.4 (0-1176.1)	125.6 (0-371.9)	20.5 (0-50.3)
		Wind Farm	0 (0-0)	5 (0-15.1)	0 (0-0)	0 (0-0)	0 (0-0)	0 (0-0)
	2019	Total survey area	49.9 (10.1-90.7)	5370.6 (623-12022.7)	1040 (351.8-1920.2)	778.1 (291.5-1367.6)	0 (0-0)	743.6 (10.1-2221.7)
		Wind Farm	0 (0-0)	1578.4 (25.1-4161.5)	525 (50.1-1332)	0 (0-0)	0 (0-0)	0 (0-0)

3.3 Results of 2019 surveys and comparison with 2015

In both 2015 and 2019 the most abundant species recorded was guillemot. In 2015 the peak model abundance was estimated as 51,000 individuals within the total survey area (late July), while in 2019 the peak model abundance estimate was 87,000 (early June). Within the wind farm, the 2015 model peak was 7,000 (in July) and the 2019 peak was 11,000 (June). Including a correction factor of 1.237 (derived from Thaxter *et al*. 2010) to account for birds underwater at the time of the survey, the 2015 maximum number across the total survey area rises to just over 63,000 individuals and in 2019 to 107,000.

The main guillemot concentrations in both years were along the Caithness coast, although as can be seen from the survey plots (Figure 3-3), this species was recorded throughout the survey area.

In 2015 the Kittiwake abundance peaked at around 4,000 in the total survey area in June and July and 1,200 in the Wind Farm in July. Very similar levels were recorded in 2019 (Figure 3-7), with a peak abundance in the total area of 4,700 in June and a wind farm peak of 1,650.

In 2015, puffin abundance peaked in August at 3,100 in the total survey area and 1,000 in the Wind Farm. The August 2015 survey (which was outside the intended survey window, as noted above) was considered likely to have recorded the beginning of post-breeding dispersal and since no surveys were conducted in August in 2019 it may not be reliable to use the August 2015 for comparison. The June and July surveys recorded similar numbers in both years with around 200-2,000 in 2015 and 300-1200 in 2019 across the whole area and 3-200 in the wind farm in 2015 and 3-40 in 2019 (Figure 3-5).

In 2015, razorbill was present in highest numbers in early July with a peak abundance of nearly 3,600 in the total survey area and around 200 in the Wind Farm (4,140 and 235 respectively when individuals underwater are accounted for, correction factor 1.174, Thaxter *et al.* 2010). Numbers were overall higher in 2019, with up to 11,250 in total and 680 in the wind farm (13,200 and 800 respectively when individuals underwater are accounted for; Figure 3-6).

In 2015 the peak gannet estimate was 700 in the total survey area in early July, of which 230 were estimated to be present within the Wind Farm. In 2019 numbers recorded were generally lower, evidenced by the fact that models could only be fitted to two of the surveys (Figure 3-1). The model estimate for the early June 2019 survey was 400 in the total area and 130 in the wind farm.

Herring gulls were present in much lower numbers in 2015, and no models were successfully fitted to the 2015 data. Comparison of the design-based estimates indicates much higher numbers present in the survey area and wind farm in 2019 (Table 3-3), with a peak population of 5,500 and a wind farm peak of 3,000 (although the equivalent modelled wind farm peak was much lower at 1,300).

The peak estimate in 2015 was 50 great black-backed gulls across the total survey area in July, which compares with over 300 in 2019 (Table 3-3). In 2015 numbers on the wind farm peaked at 27 which compared with 90 in 2019, although lower numbers were seen more frequently on the wind farm in 2015 than 2019.

Design based estimates (Table 3-3) were typically higher than model based ones (Table 3-2), with a median difference of 13% in 2015 and 17% in 2019. These differences are a reflection of the greater flexibility that the model-based approach allows in terms of spatial variations, compared with the relatively simplistic design-based method. This effect tends to be more pronounced for subsets of the total area, leading to the greater magnitude of differences obtained within the Wind Farm. When species are distributed evenly, the two methods will generate similar results. But as a distribution becomes increasingly uneven (e.g. with large, localised aggregations), the magnitude of difference between the two methods will increase. For species such as seabirds, which exhibit large variations in density, model based methods are therefore preferable, although it was not possible to fit models to all species in all months due to data sparseness.

Plots of the locations of birds recorded in flight in both 2015 and 2019 have been added in ANNEX B. As would be expected, the distributions of each species in flight are similar to those for birds on the water.

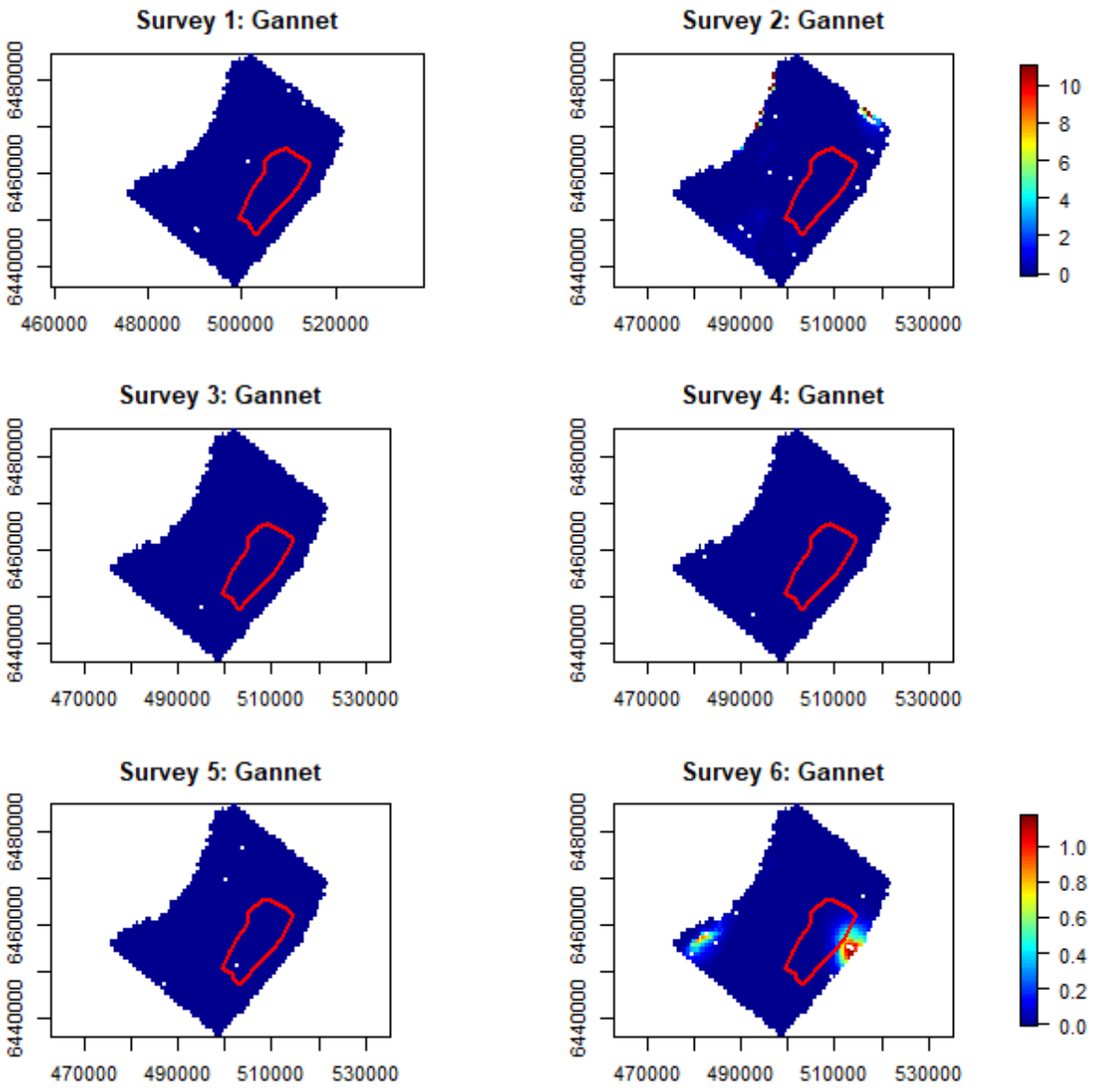

Figure 3-1. Gannet distributions in 2019 (scale bars indicate birds/km²). Density surfaces generated using the best fit spatial model for each survey (note the scale differs for each survey). White dots are birds recorded on the water (standard intensity data only). Note, too few birds were recorded to permit model fitting on surveys 1,3,4, and 5.

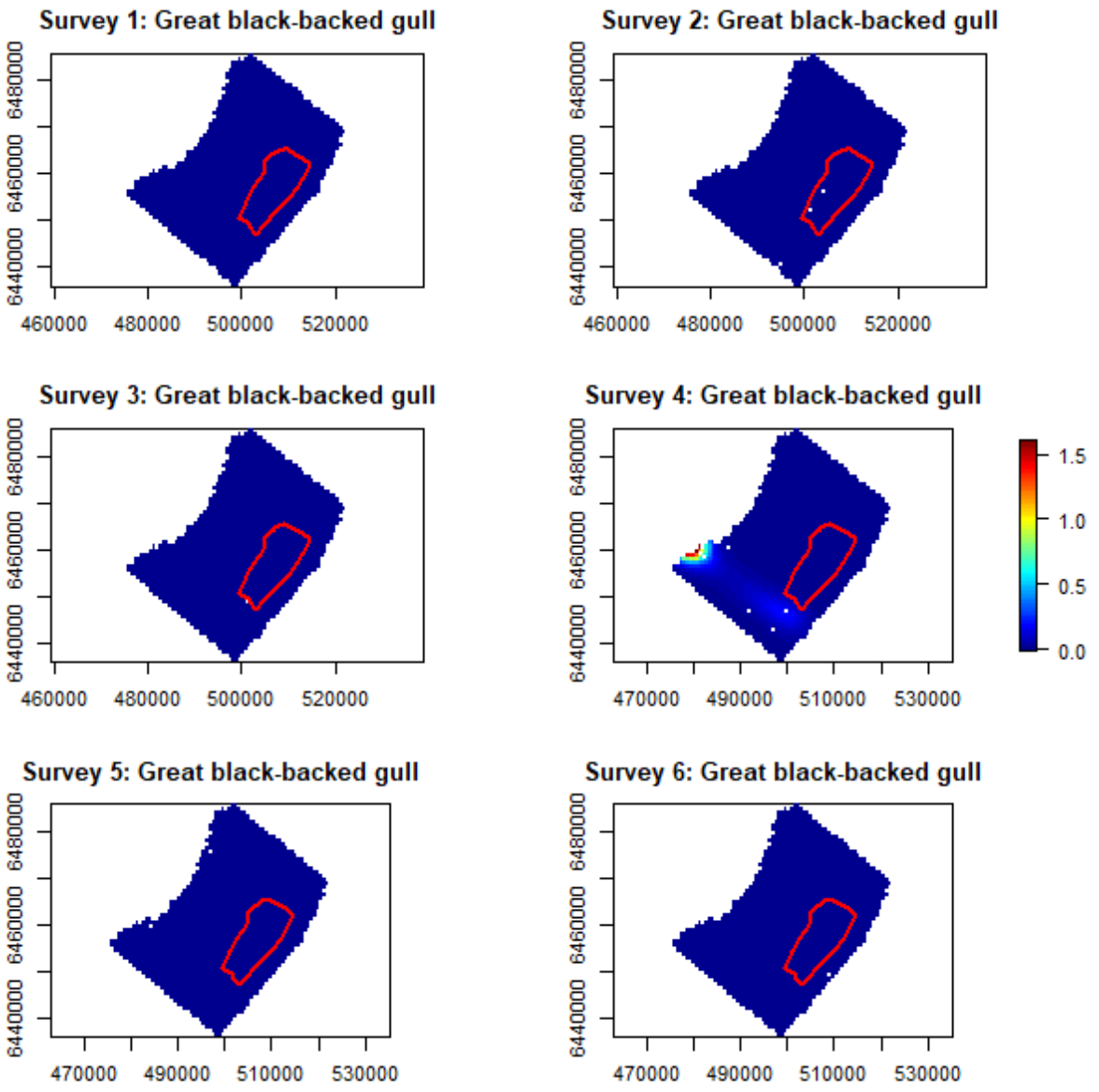

Figure 3-2. Great black-backed gull distributions in 2019 (scale bars indicate birds/km²). Density surfaces generated using the best fit spatial model for each survey (note the scale differs for each survey). White dots are birds recorded on the water (standard intensity data only). Note, too few birds were recorded to permit model fitting on surveys 1, 2, 3, 5, and 6.

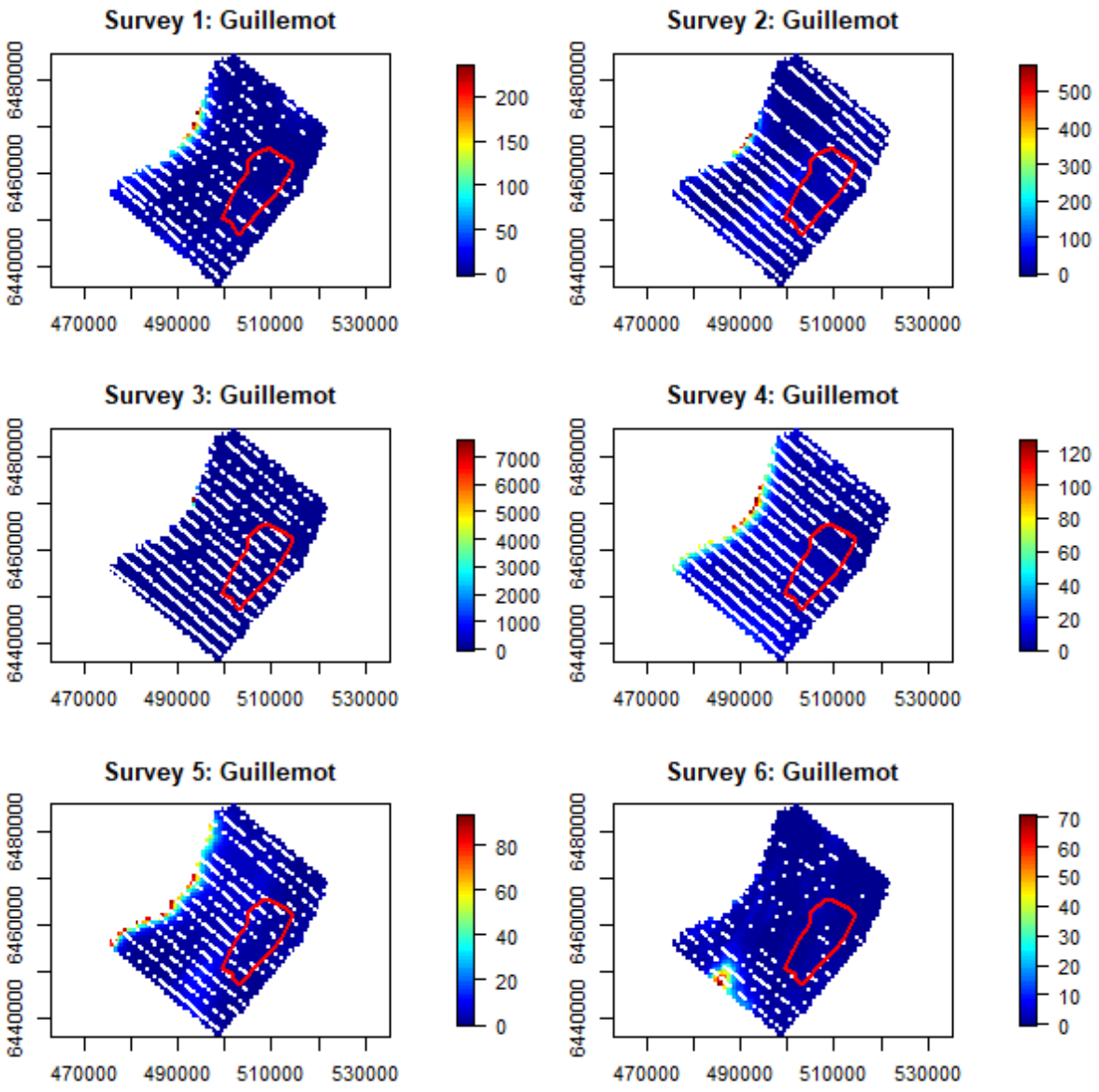

Figure 3-3. Guillemot distributions in 2019 (scale bars indicate birds/km²). Density surfaces generated using the best fit spatial model for each survey (note the scale differs for each survey). White dots are birds recorded on the water (standard intensity data only).

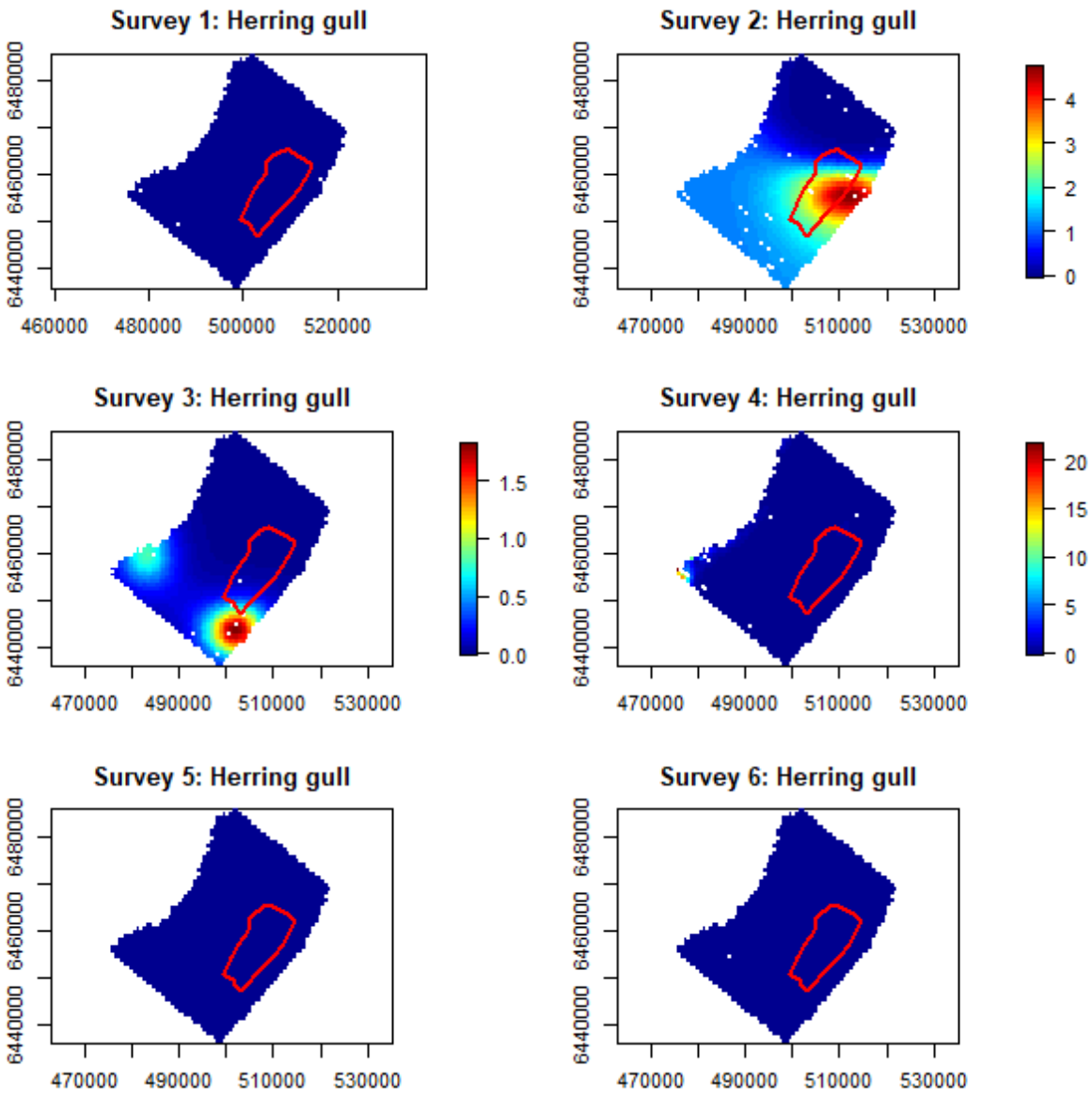

Figure 3-4. Herring gull distributions in 2019 (scale bars indicate birds/km²). Density surfaces generated using the best fit spatial model for each survey (note the scale differs for each survey). White dots are birds recorded on the water (standard intensity data only). Note, too few birds were recorded to permit model fitting on surveys 1, 5, and 6.

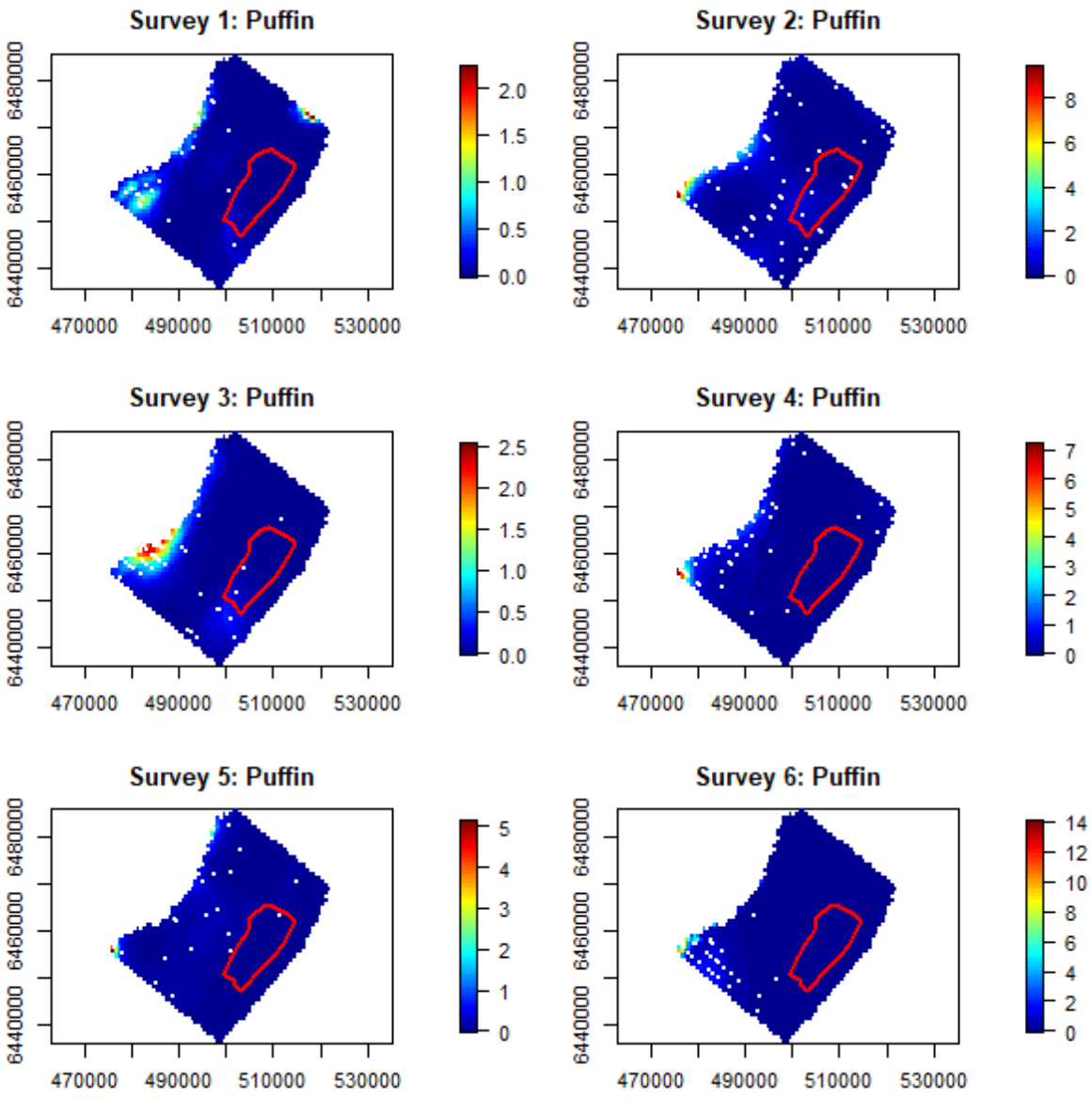

Figure 3-5. Puffin distributions in 2019 (scale bars indicate birds/km²). Density surfaces generated using the best fit spatial model for each survey (note the scale differs for each survey). White dots are birds recorded on the water (standard intensity data only).

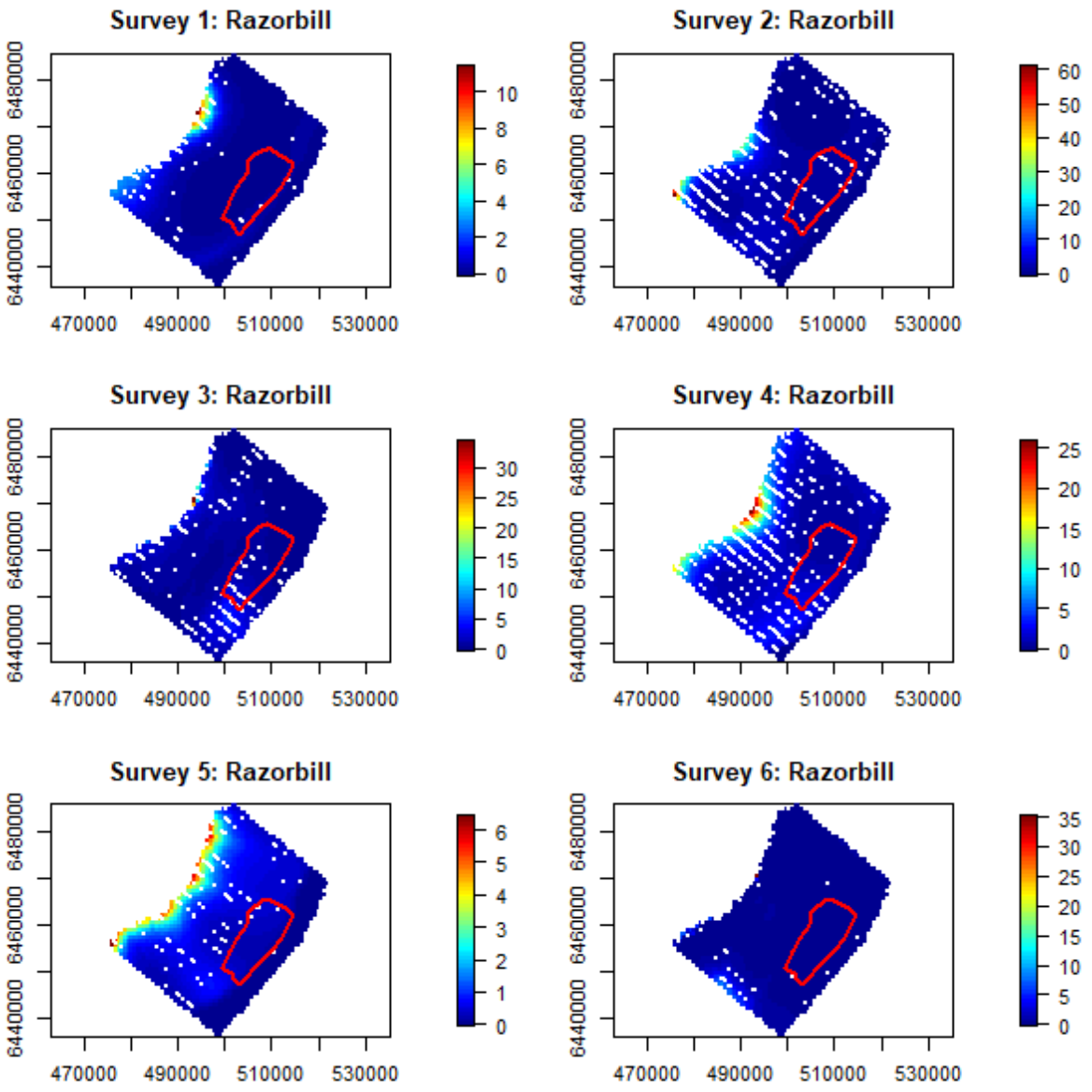

Figure 3-6. Razorbill distributions in 2019 (scale bars indicate birds/km²). Density surfaces generated using the best fit spatial model for each survey (note the scale differs for each survey). White dots are birds recorded on the water (standard intensity data only).

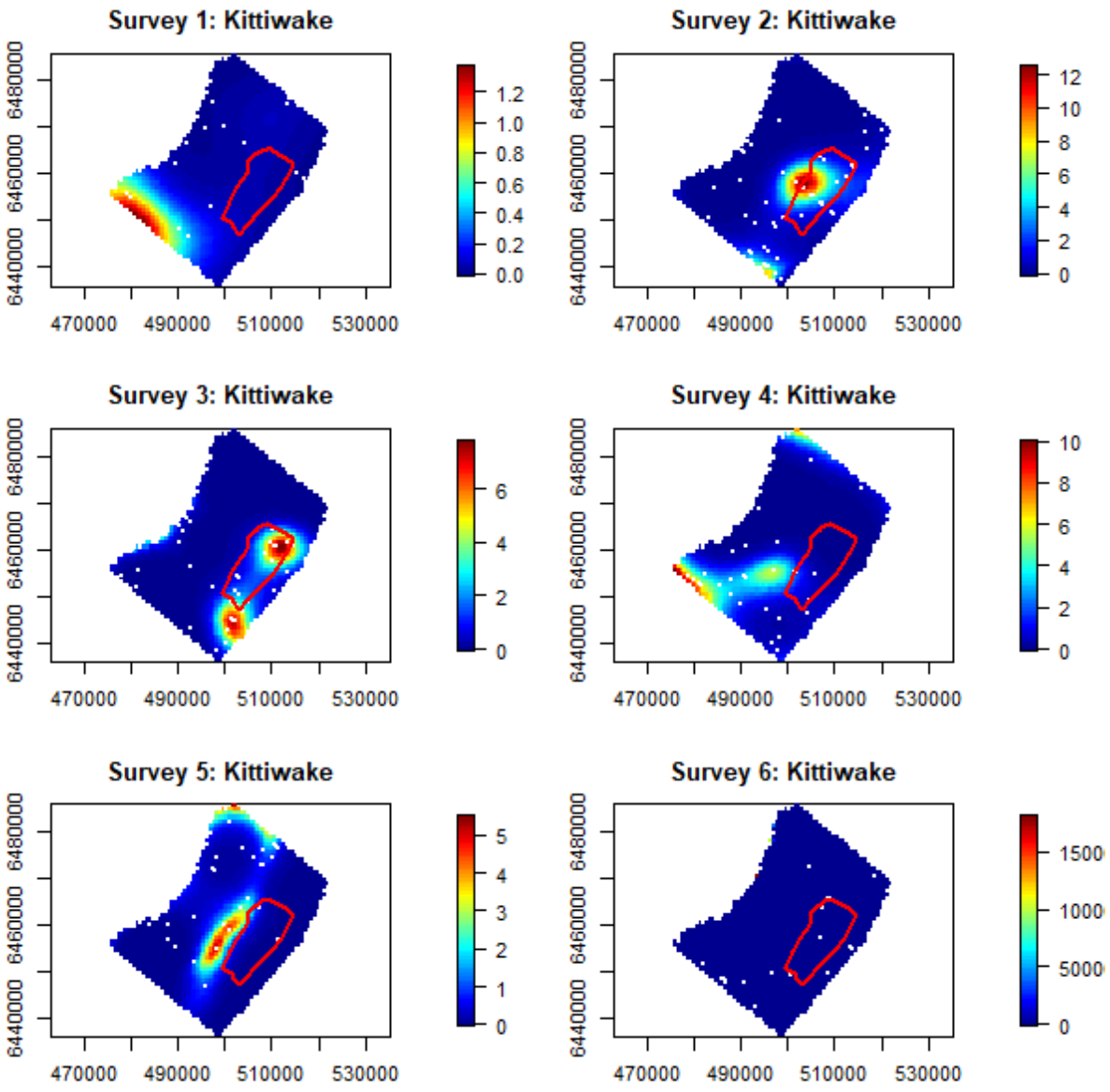

Figure 3-7. Kittiwake distributions in 2019 (scale bars indicate birds/km²). Density surfaces generated using the best fit spatial model for each survey (note the scale differs for each survey). White dots are birds recorded on the water (standard intensity data only). Note that the model fitting for survey 6 generated unreliable overall abundance estimates, driven by extreme values at the edges of the density surface.

3.4 Spatial modelling comparison of 2015 and 2019 distributions

Spatial models which included an 'impact' term to distinguish the 2015 and 2019 data were fitted for those species which were modelled in both years (gannet, guillemot, razorbill, kittiwake and puffin).

3.4.1 Gannet

There was no overall significant change in abundance from 2015 to 2019, with the estimated impact term having a value of 0.31 (robust S.E 0.78, p=0.39) but there was a significant interaction between impact and spatial smoother (p=0.03). Plotting of the spatially explicit differences

indicated a significant decrease centred on the wind farm and extending towards the coast with no areas of significant increase (Figure 3-8). Overall, beyond the region of decrease the density in the remainder of the survey area was almost identical between 2015 and 2019 (i.e. a value of ~0 in Figure 3-8).

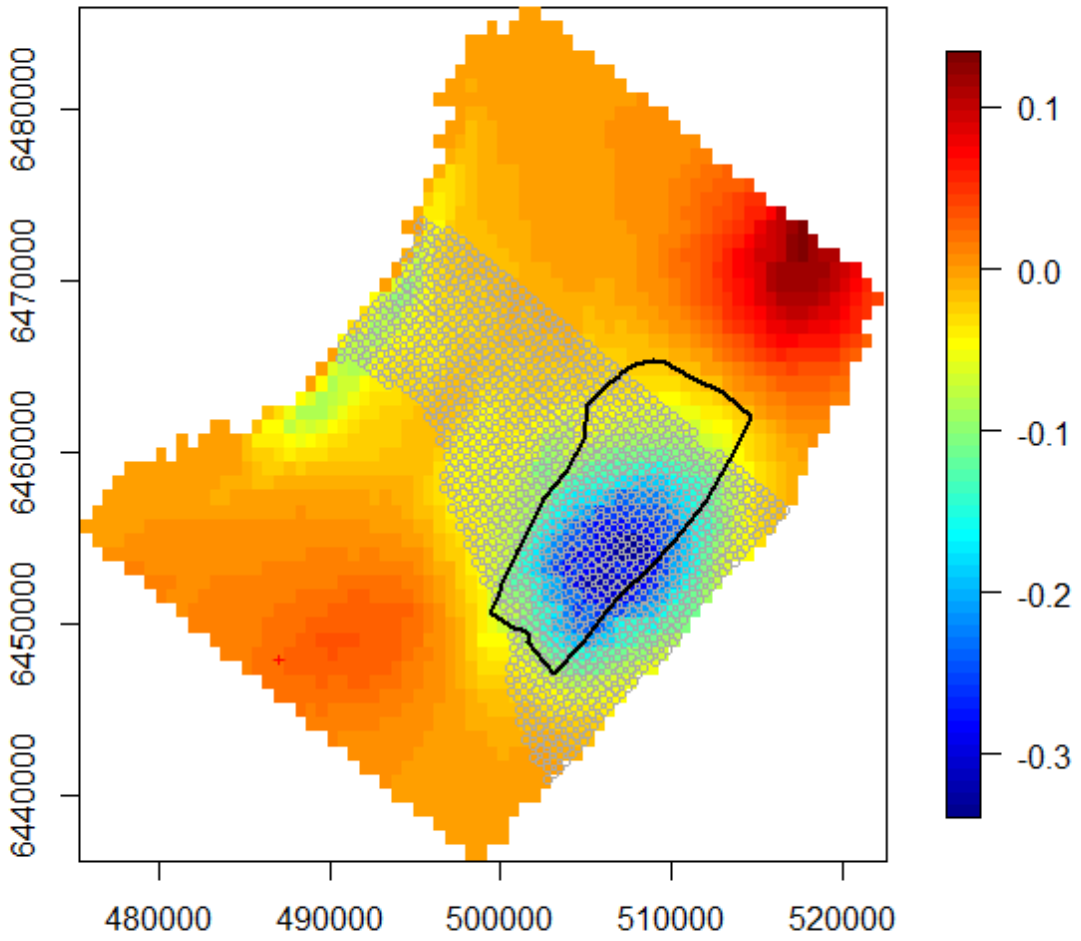

Figure 3-8. Gannet before-after difference surface derived from 100 bootstrap simulations. The surface is the difference in abundance, calculated as the 'after' value at each location minus the 'before' value. Significant positive differences (i.e. areas of higher abundance in the after survey) are marked with a red '+' and significant reductions by a grey 'o'.

3.4.2 Guillemot

There was an overall increase in abundance from 2015 to 2019, with the estimated impact term having a significant positive value of 4.7 (robust S.E 1.07, p<0.001) and a significant interaction between impact and spatial smoother (p=0.01). Plotting of the spatially explicit differences indicated a significant increase in the centre of the study region and extending to the southern edge, but no regions of significant decrease (Figure 3-9).

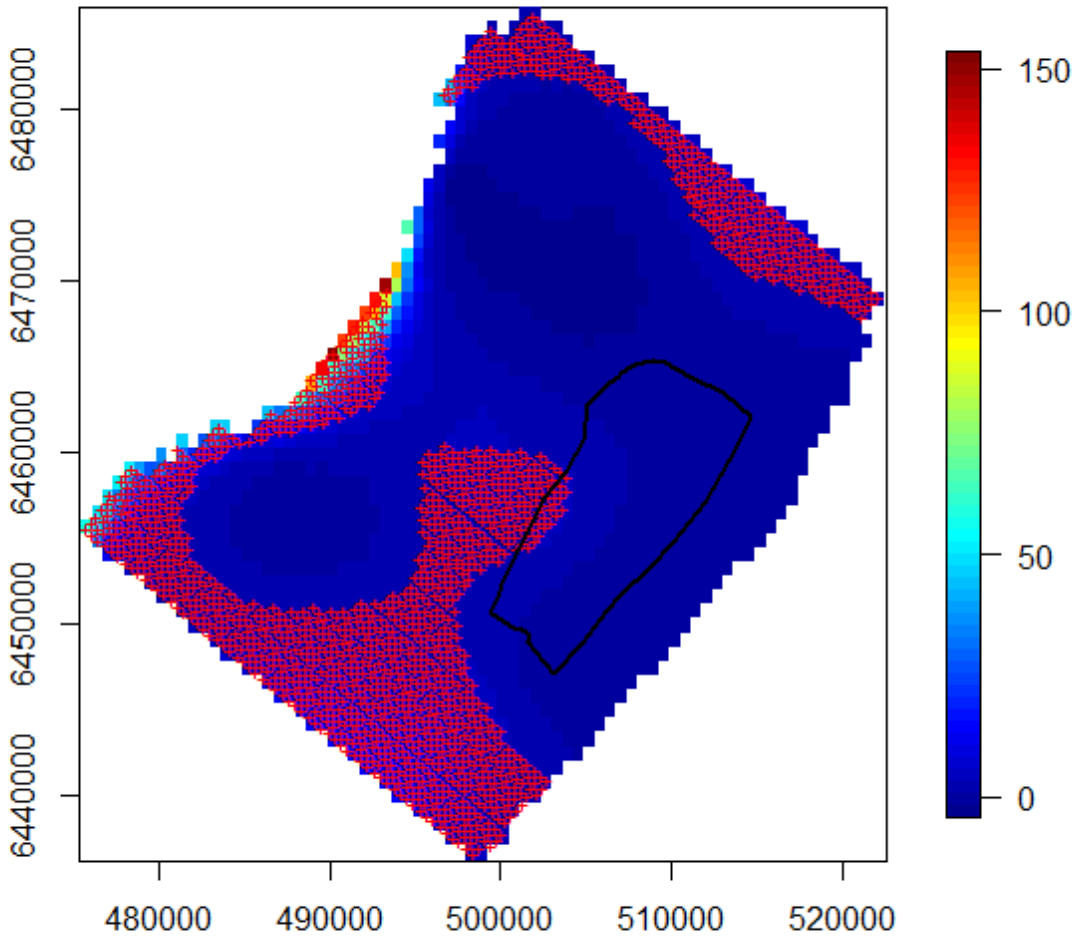

Figure 3-9. Guillemot before-after difference surface derived from 100 bootstrap simulations. The density is the difference in abundance, calculated as the 'after' value at each location minus the 'before' value. Significant positive differences (i.e. areas of higher abundance in the after survey) are marked with a red '+' and significant reductions by a grey 'o'.

3.4.3 Kittiwake

There was no overall significant change in abundance from 2015 to 2019, with the estimated impact term having a value of 0.23 (robust S.E 0.61, p=0.70) but there was a significant interaction

between impact and spatial smoother (p=0.001). Plotting of the spatially explicit differences indicated a significant increase offshore, centred just to the north of the wind farm extending into it, with a significant decrease in coastal waters (Figure 3-10).

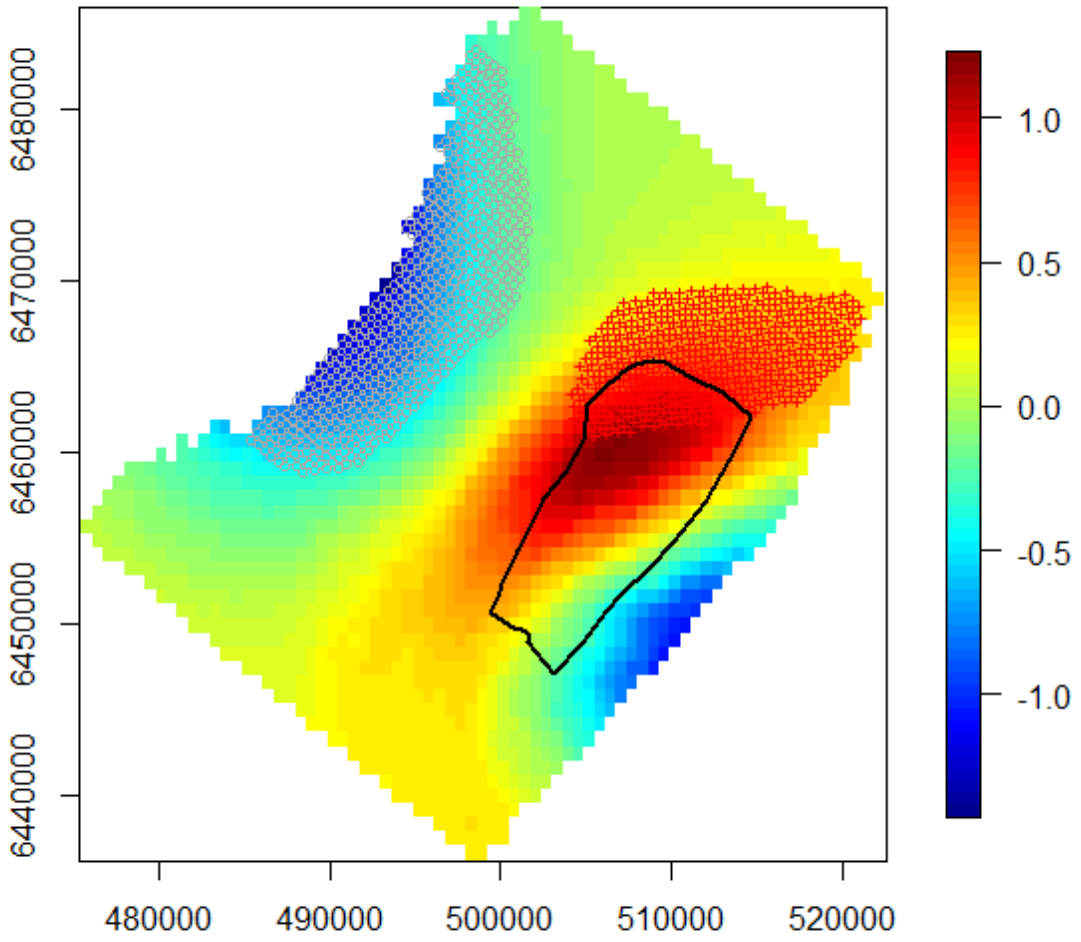

Figure 3-10. Kittiwake before-after difference surface derived from 100 bootstrap simulations. The density is the difference in abundance, calculated as the 'after' value at each location minus the 'before' value. Significant positive differences (i.e. areas of higher abundance in the after survey) are marked with a grey '+' and significant reductions by a grey 'o'.

3.4.4 Razorbill

There was a significant increase in abundance from 2015 to 2019, with the estimated impact term having a value of 1.9 (robust S.E 0.57, p<0.001) but the interaction between impact and spatial smoother was not significant (p=0.2). Plotting of the spatially explicit differences indicated an increase throughout most of the study area, with only the northern section having no significant change (Figure 3-11).

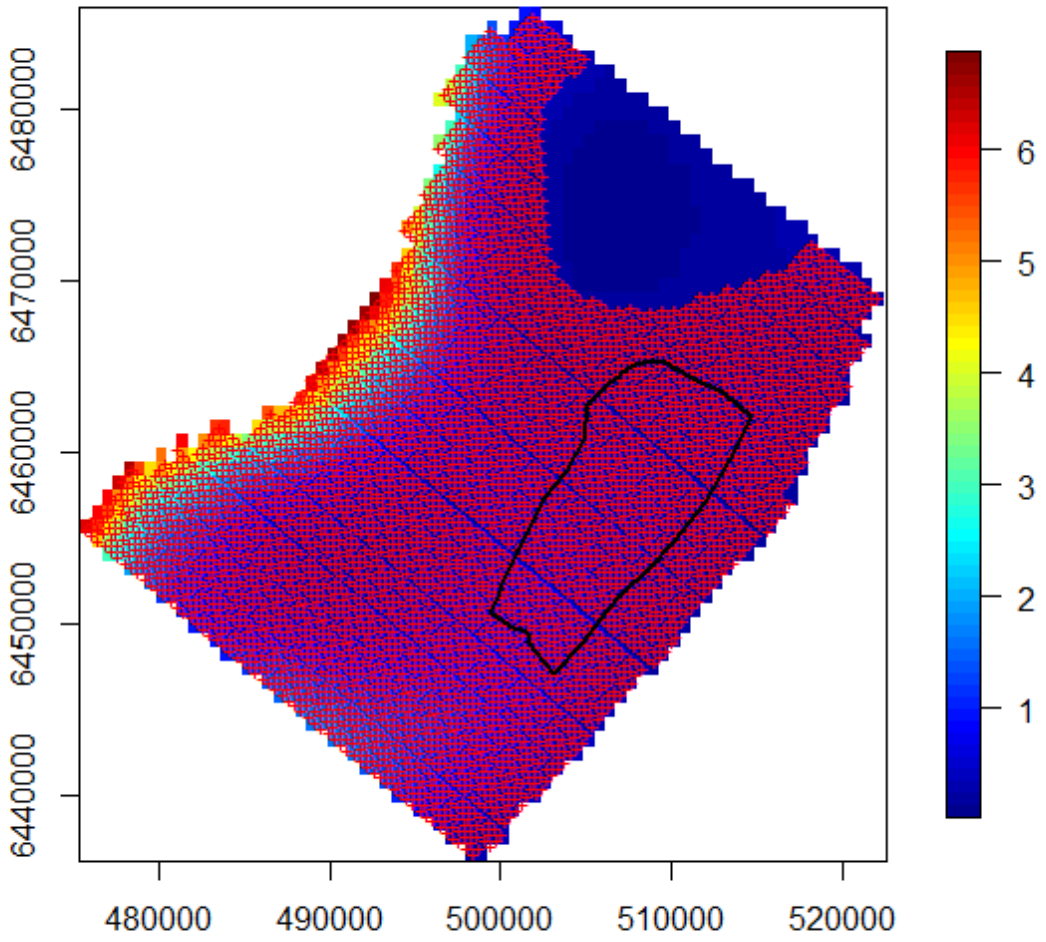

Figure 3-11. Razorbill before-after difference surface derived from 100 bootstrap simulations. The density is the difference in abundance, calculated as the 'after' value at each location minus the 'before' value. Significant positive differences (i.e. areas of higher abundance in the after survey) are marked with a grey '+' and significant reductions by a grey 'o'

3.4.5 Puffin

There was a significant overall decrease in abundance from 2015 to 2019, with the estimated impact term having a value of -1.81 (robust S.E 0.83, p=0.03) and a significant interaction between impact and spatial smoother (p<0.001). Plotting of the spatially explicit differences indicated a significant decrease in the northern and eastern half of the survey area, including the wind farm (Figure 3-12).

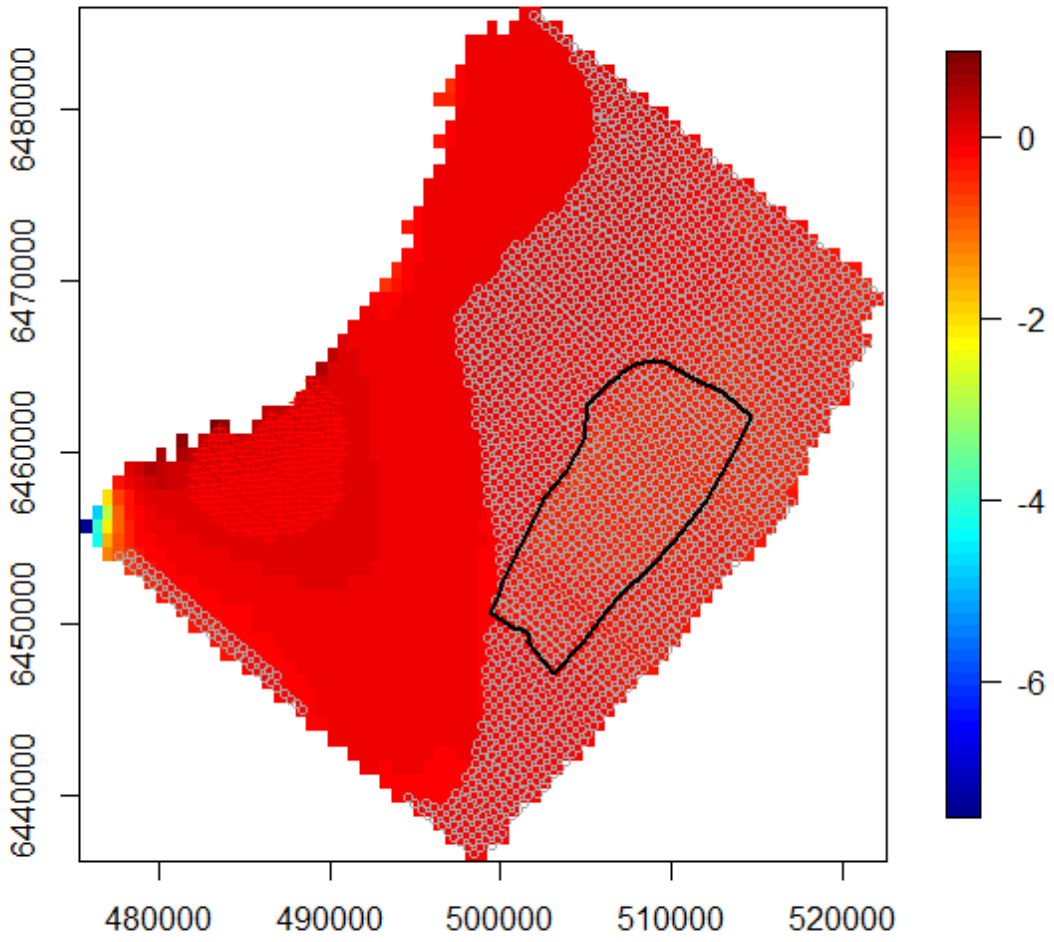

Figure 3-12. Puffin before-after difference surface derived from 100 bootstrap simulations. The density is the difference in abundance, calculated as the 'after' value at each location minus the 'before' value. Significant positive differences (i.e. areas of higher abundance in the after survey) are marked with a grey '+' and significant reductions by a grey 'o'

The potential for the spatial modelling results to be strongly influenced by individual surveys was tested using the *runInfluence* function in MRSea (see ANNEX D for results). This was considered at both the level of individual surveys (i.e. 1 – 12) and also individual transects within surveys (i.e. 1-192, 12 surveys x 16 transects). While these tests did indicate outliers in the data, since the values were calculated as quantiles, by definition there will be points outside the 95% confidence interval. However, these outliers were not a large distance outside the range of the remaining data, and the survey-transect level analysis revealed that outliers were recorded across multiple surveys in both 2015 (before) and 2019 (after). Therefore, these tests did not find evidence that the combined distributions as presented above were driven by particular surveys and the observed redistributions are considered robust.

3.5 Abundance of birds in flight

The abundance of birds recorded in flight across the total survey area and within the Wind Farm are presented in Table 3-4. Comparison of the design-based estimates for birds on the water (Table 3-3) and birds in flight (Table 3-4) across both years reveals a split between gannet and the gull species (kittiwake, herring gull and great black-backed gull) and the auks. When looked at across all the surveys, the former species were either recorded as often in flight as on the water (in-flight: gannet 45%, kittiwake 62%, great black-backed gull 60% and herring gull 56%), or much more often on the water (in flight: guillemot 9%, puffin 5% and razorbill 9%). These differences were consistent within each year with no apparent effect of the wind farm on this proportion. This presumably reflects differences in the species' foraging ecology, with gannets and gulls foraging on the wing, whereas auks forage from the sea surface and predominantly fly between foraging locations and the colony. Thus, gulls are equally likely to be recorded in flight as on the sea leading to a high degree of correlation, whereas auks are much more likely to be recorded on the sea surface than in flight and with no particular reason for the two estimates to be correlated.

Table 3-4. Design-based population abundance estimates of birds in flight in the total survey area and within the Wind Farm boundary for each species in each survey in 2015 and 2019 (shaded). Abundance across the total survey area was estimated using the standard intensity data, Wind Farm abundance was estimated using the high intensity data.

Species	Year	Area	Population abundance on each survey					
			1	2	3	4	5	6
Gannet	2015	Total survey area	764.4 (512.7-1015.5)	148.9 (70.4-231.2)	169.4 (90.5-261.4)	120.1 (50.3-191)	81 (20.1-150.8)	140.6 (60.3-251.3)
		Wind Farm	66.3 (20.1-130.7)	20.6 (0-45.2)	60.8 (25.1-100.5)	10.2 (0-25.1)	20 (0-50.3)	0 (0-0)
	2019	Total survey area	61 (20.1-110.6)	570.7 (140.7-1226.6)	20 (0-50.3)	81 (30.2-140.7)	19.1 (0-60.3)	49.8 (10.1-100.5)
		Wind Farm	0 (0-0)	0 (0-0)	0 (0-0)	0 (0-0)	0 (0-0)	4.9 (0-15.1)
Guillemot	2015	Total survey area	4903.1 (3759.2-6081.5)	5900.7 (4935.5-6956.2)	3802.6 (3025.7-4613.9)	2450.7 (1859.6-3137)	923.1 (442.3-1558.1)	19.9 (0-50.3)
		Wind Farm	182.1 (90.5-291.6)	814.1 (537.7-1146.1)	494 (276.4-789.2)	296.9 (170.9-422.3)	281.4 (55.3-623.2)	0 (0-0)
	2019	Total survey area	3635.5 (2724.1-4674.7)	5766.6 (4644-7026.3)	8175.7 (6614-10094)	6741.9 (5548.7-8011.4)	2420.5 (1809.4-3116.4)	510.6 (291.5-774)
		Wind Farm	153.1 (55.3-286.5)	329.8 (205.9-472.4)	535.9 (281.5-889.6)	445.5 (256.2-653.4)	232.4 (90.5-407.2)	5 (0-15.1)
Kittiwake	2015	Total survey area	3844.2 (2110.9-6021.9)	5014.8 (2934.9-7771.2)	5304.9 (4201.5-6604.7)	5117.2 (4111-6333)	6236.4 (4220.8-8826.7)	811.2 (552.9-1095.7)

Species	Year	Area	Population abundance on each survey					
			1	2	3	4	5	6
		Wind Farm	120.5 (75.4-175.9)	256.4 (130.7-392.2)	1032 (562.8-1613.7)	1253.8 (683.3-1915)	1090.2 (537.8-1814.8)	51 (20.1-85.4)
	2019	Total survey area	5194.9 (3155.8-8102.2)	10412.1 (7950.9-14329.4)	3472.6 (2864.8-4111.3)	4663.8 (3699.1-5719.6)	5848.7 (4533.2-7509.3)	4376.8 (2713.5-6504.1)
		Wind Farm	144.3 (45.2-301.6)	1793.3 (1241.3-2432.6)	556.2 (296.5-879.7)	491 (286.5-723.7)	407 (276.4-562.9)	414.6 (120.6-934.8)
Puffin	2015	Total survey area	0 (0-0)	193.8 (100.5-301.6)	112.3 (40.2-191)	29.3 (0-70.4)	30.8 (0-90.5)	0 (0-0)
		Wind Farm	0 (0-0)	5.1 (0-15.1)	36.1 (5-75.4)	0 (0-0)	0 (0-0)	0 (0-0)
	2019	Total survey area	20.1 (0-50.3)	159.8 (60.3-271.4)	61.2 (0-160.8)	9.9 (0-30.2)	10 (0-30.2)	19.7 (0-50.3)
		Wind Farm	4.9 (0-15.1)	15 (0-40.2)	5.1 (0-15.1)	0 (0-0)	0 (0-0)	0 (0-0)
Razorbill	2015	Total survey area	69 (20.1-120.6)	231.8 (120.6-351.8)	326.1 (180.9-502.6)	40 (10.1-80.4)	19.9 (0-50.3)	0 (0-0)
		Wind Farm	5.1 (0-15.1)	43.7 (9.9-95.5)	19.9 (5-40.2)	0 (0-0)	4.9 (0-15.1)	0 (0-0)
	2019	Total survey area	229.3 (110.6-361.9)	923.1 (613.2-1296.7)	1118.8 (814.2-1457.5)	1316 (965-1678.9)	151.9 (80.2-241.5)	0 (0-0)
		Wind Farm	0 (0-0)	39.9 (15.1-75.4)	35.6 (10.1-70.4)	89.5 (40.2-150.8)	15.1 (0-45.2)	0 (0-0)
Great black-backed gull	2015	Total survey area	79.2 (20.1-151)	70 (20.1-130.7)	50.7 (10.1-110.6)	20.1 (0-50.3)	80.3 (30.2-150.8)	60.8 (0-150.8)
		Wind Farm	0 (0-0)	0 (0-0)	0 (0-0)	0 (0-0)	0 (0-0)	10.2 (0-25.1)
	2019	Total survey area	91.3 (30.2-180.9)	91 (40.2-160.8)	70.8 (10.1-160.8)	110.8 (50.3-180.9)	19.9 (0-50.3)	51.1 (10.1-100.5)
		Wind Farm	0 (0-0)	15.5 (0-35.2)	5 (0-15.1)	5.1 (0-15.1)	0 (0-0)	0 (0-0)
Herring gull	2015	Total survey area	457.4 (180.9-834.3)	273.5 (150.8-442.3)	321.7 (100.5-663.7)	482.7 (251.3-774)	122.3 (20.1-271.4)	101.8 (20.1-221.1)
		Wind Farm	0 (0-0)	5.3 (0-15.1)	5 (0-15.1)	0 (0-0)	0 (0-0)	0 (0-0)
	2019	Total survey area	692.7 (251.3-1307)	1786.8 (1256.5-2422.8)	886.8 (572.7-1347)	709.1 (341.8-1316.8)	119.8 (30.2-231.2)	151.2 (0-442.3)

Species	Year	Area	Population abundance on each survey					
			1	2	3	4	5	6
		Wind Farm	0 (0-0)	669.2 (266.3-1181.1)	35.3 (10.1-65.3)	35.3 (10.1-70.4)	0 (0-0)	0 (0-0)

3.6 Seabird distributions in relation to turbine locations

The pooled densities of birds within circles of radius 100, 200, 300 and 400m around the turbine locations for each auk species are summarised in Table 3-5 and plotted in Figure 3-13 to Figure 3-17, together with a histogram of densities obtained for 1,000 randomly offset turbine layouts. Overall, the recorded density of birds (red lines) on the graphs for all the species was located within the middle of the bootstrapped distributions, indicating that the seabirds did not appear to be avoiding the turbines. If such avoidance behaviour was occurring the observed densities would be expected to be lower (the red line would lie to the left of the histogram peak) than those for the simulated turbine locations.

For guillemot, razorbill and puffin there were no clear trends in density with increasing distance from the turbines, although the observed razorbill densities were to the right of the histogram peaks, which could indicate attraction to the regions nearer to the turbines. For kittiwake and herring gull density increased with distance, which suggests there may have been some avoidance of regions closer to the turbines, although in neither species was the observed density clearly outside the peak of the histogram, so this may simply reflect chance variations rather than actual avoidance.

Table 3-5. Densities recorded within 400m of turbines.

Species	Observed density (birds/km²)				Sample size
	<100m	<200m	<300m	<400m	
Guillemot	59.5	55.3	56.3	52.2	6874
Puffin	0.38	0.19	0.42	0.40	44
Razorbill	5.7	5.2	4.0	3.4	551
Kittiwake	2.6	3.6	3.7	9.2	1733
Herring gull	0	2.0	13.7	7.8	465

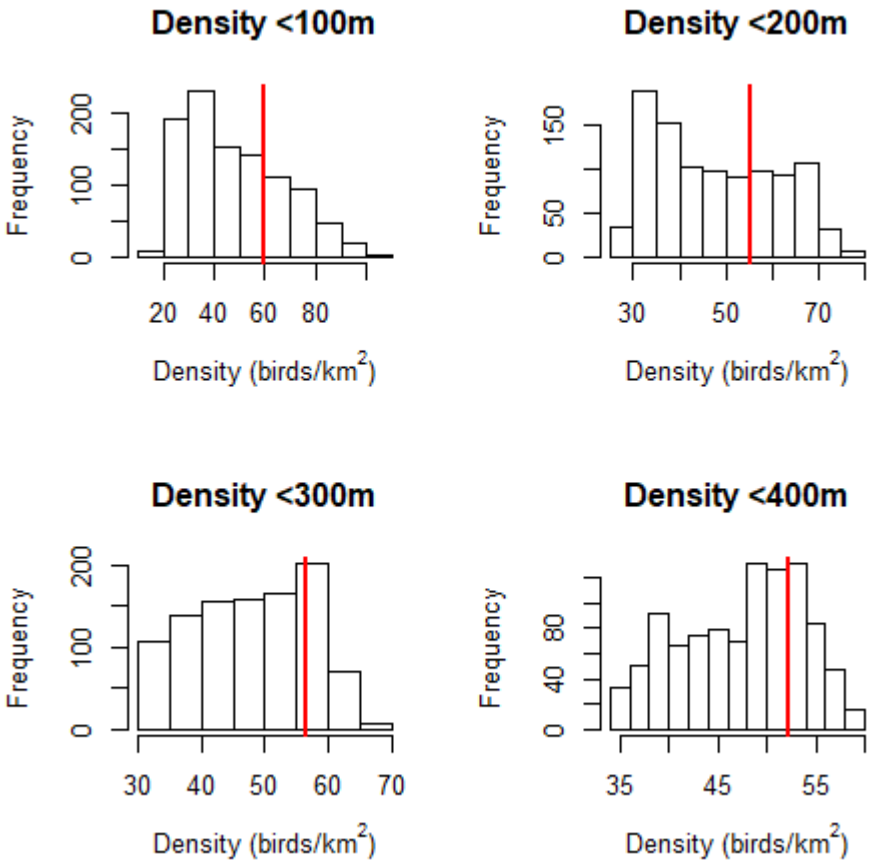

Figure 3-13. Guillemot densities within 100/200/300/400m of turbine locations (red lines) and distribution of densities estimated for 1,000 simulations with randomly re-positioned turbines (relative turbine positions maintained). Data combined across all six surveys.

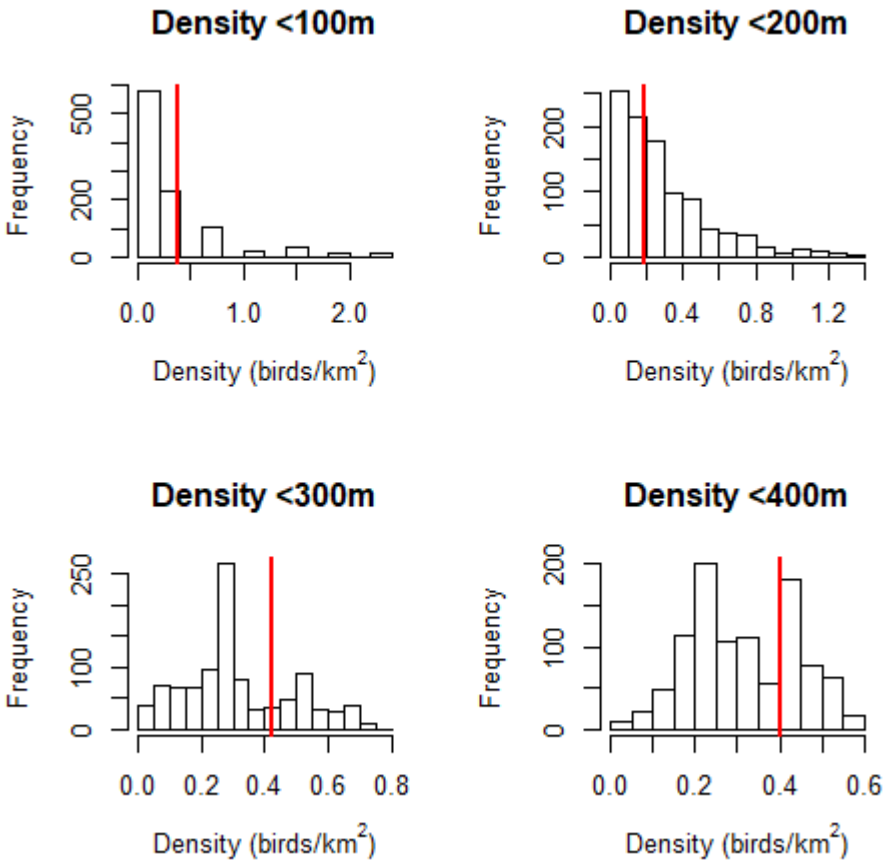

Figure 3-14. Puffin densities within 100/200/300/400m of turbine locations (red lines) and distribution of densities estimated for 1,000 simulations with randomly re-positioned turbines (relative turbine positions maintained). Data combined across all six surveys.

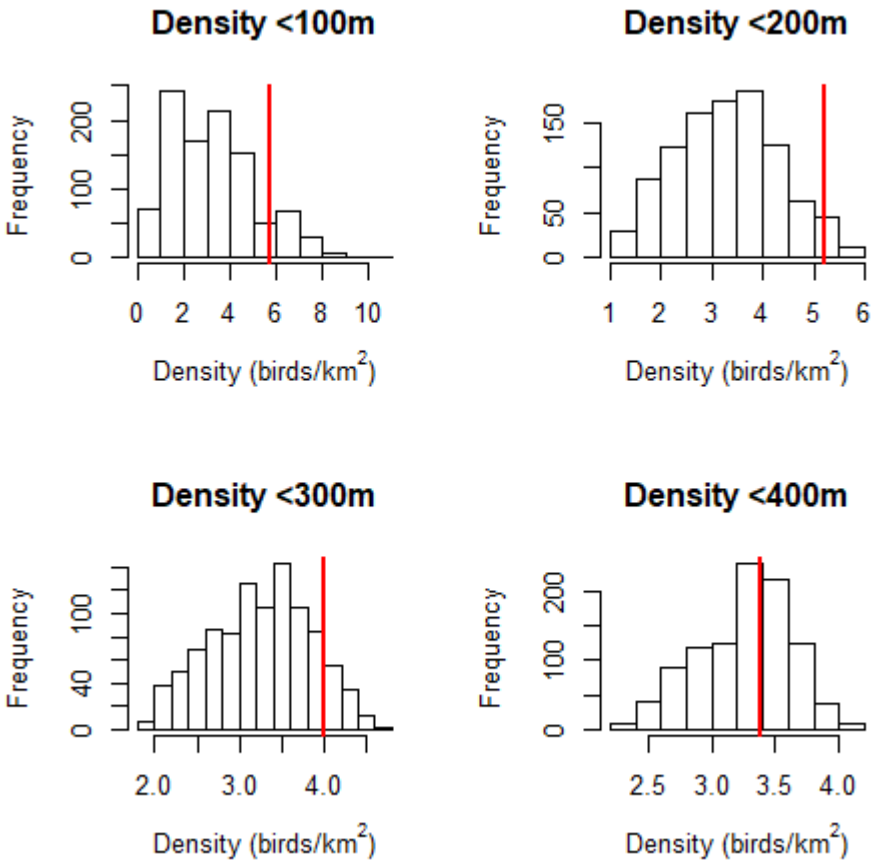

Figure 3-15. Razorbill densities within 100/200/300/400m of turbine locations (red lines) and distribution of densities estimated for 1,000 simulations with randomly re-positioned turbines (relative turbine positions maintained). Data combined across all six surveys.

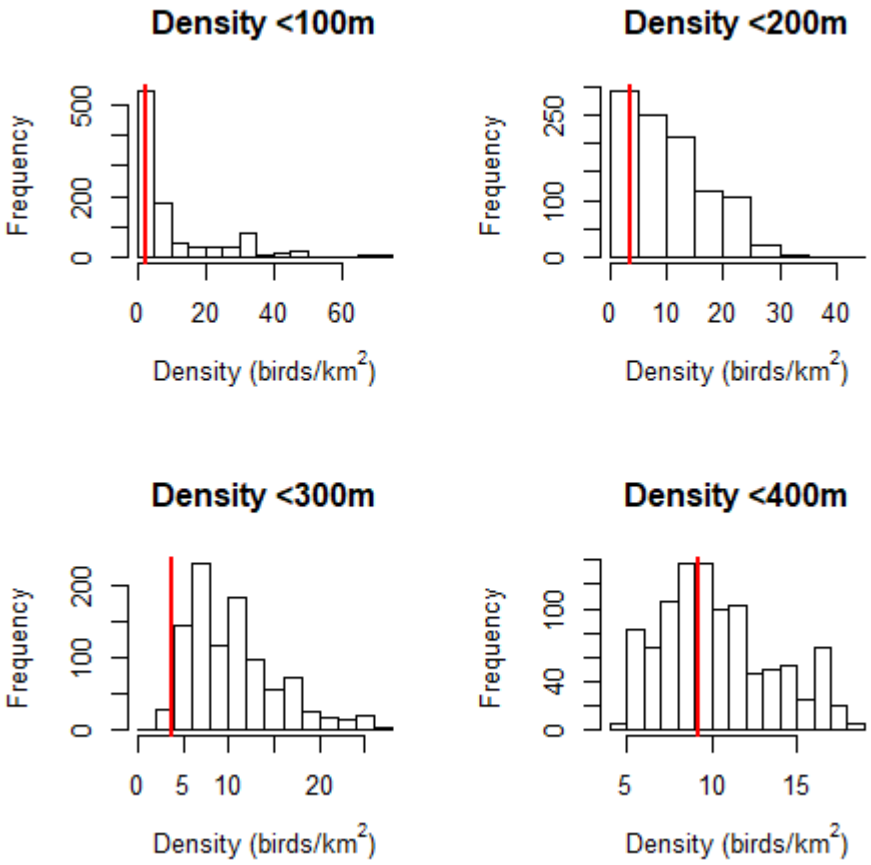

Figure 3-16. Kittiwake densities within 100/200/300/400m of turbine locations (red lines) and distribution of densities estimated for 1,000 simulations with randomly re-positioned turbines (relative turbine positions maintained). Data combined across all six surveys.

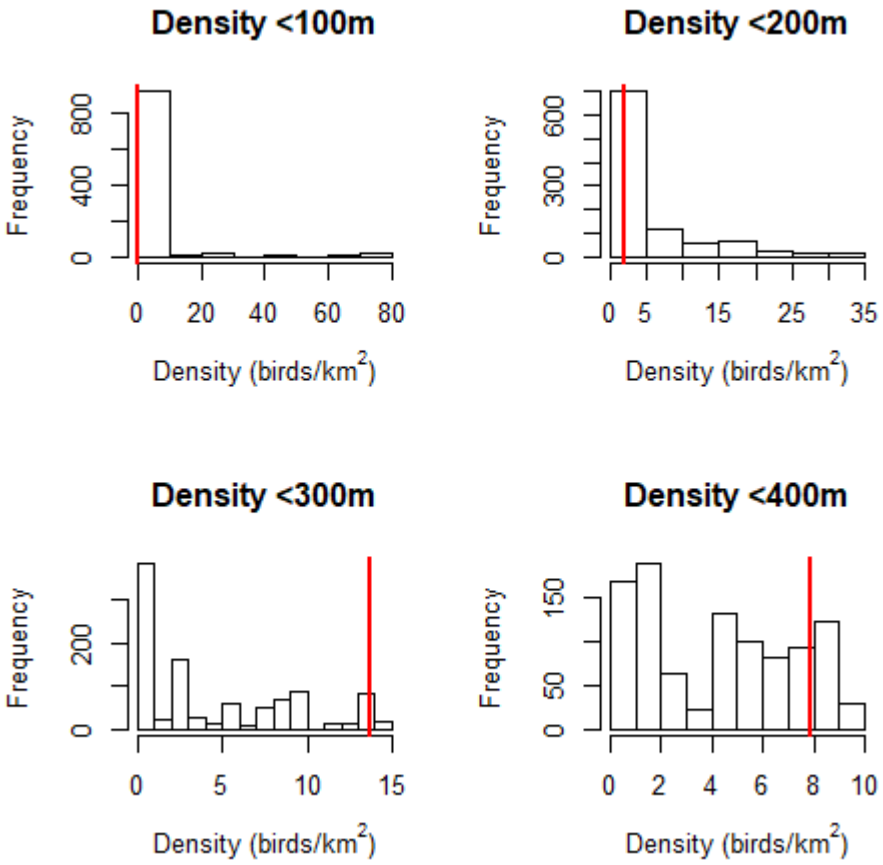

Figure 3-17. Herring gull densities within 100/200/300/400m of turbine locations (red lines) and distribution of densities estimated for 1,000 simulations with randomly re-positioned turbines (relative turbine positions maintained). Data combined across all six surveys.

To test if a real turbine avoidance effect, if present, would have been detected, birds within one of the turbine radii (i.e. 0-100, 0-200, 0-300 or 0-400 m) were removed from the dataset prior to running the bootstrap routine (i.e. simulating avoidance of turbines to that distance). Examples of the outputs for guillemot and puffin for simulated displacement of birds within 100 m (Figure 3-18 and Figure 3-19) and within 400 m (Figure 3-20 and Figure 3-21) indicated that following this imposed turbine avoidance the 'observed' densities (i.e. the real data but following removal of individual within 100 m or 400 m of turbines) are clearly lower than the resampled distributions, evidenced by the red lines moving to the left on the relevant histograms. For example, in Figure 3-18, with all birds within 100m of actual turbine locations removed, the recorded density, as expected, is zero (Figure 3-18, top-left panel), however the density with respect to the resampled turbines peaks at 30/km^2. However, the observed density within larger radii (Figure 3-18, top-right and lower panels) remains within the resampled range, indicating that the correct removal distance would be expected to be identified by this method.

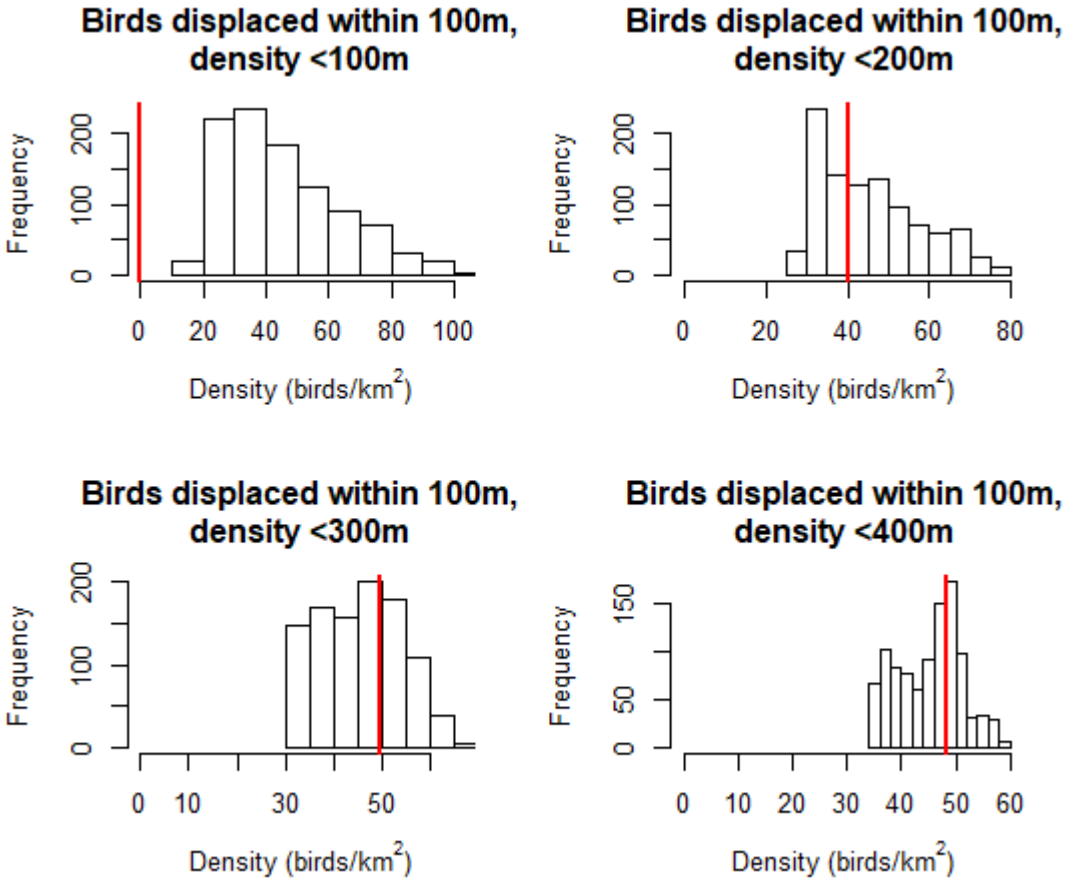

Figure 3-18. Guillemot densities within 100/200/300/400 m of randomly re-positioned turbine locations with removal of all birds within 100 m of planned turbine locations (relative turbine positions maintained). Red lines indicate actual densities within radial distances of turbine positions (including the removal as noted).

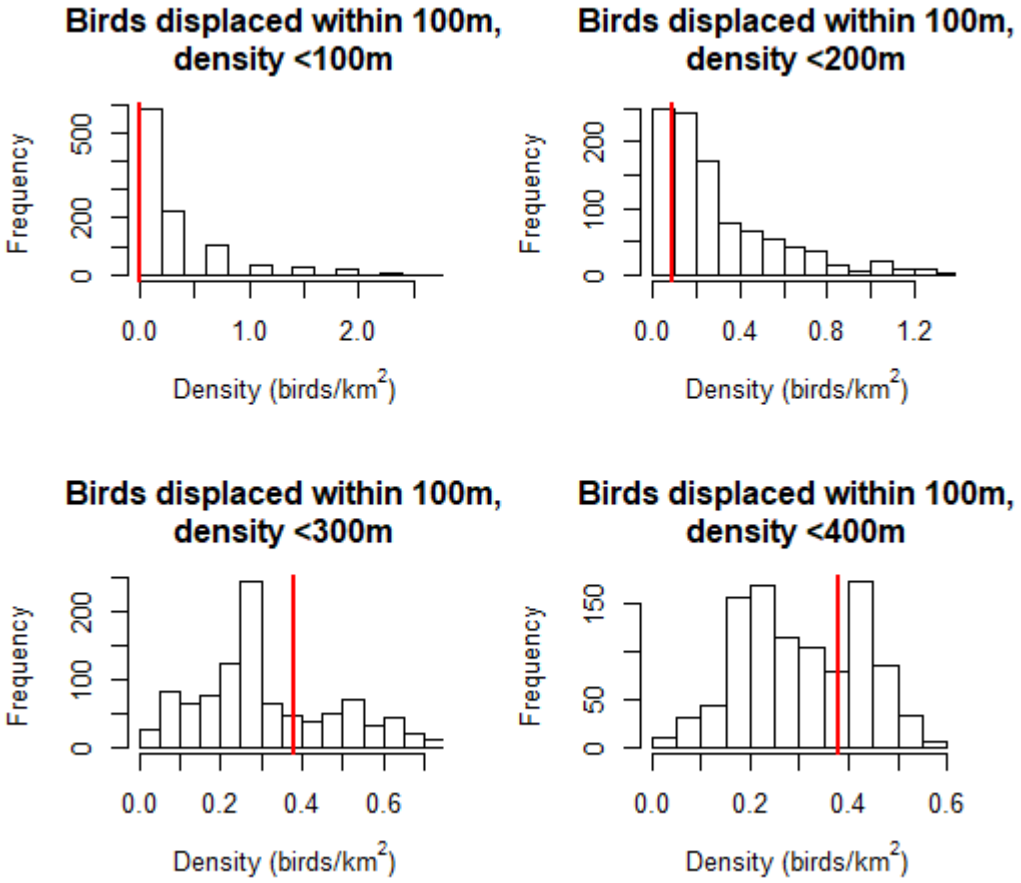

Figure 3-19. Puffin densities within 100/200/300/400 m of randomly re-positioned turbine locations with removal of all birds within 100m of planned turbine locations (relative turbine positions maintained). Red lines indicate actual densities within radial distances of turbine positions (including the removal as noted).

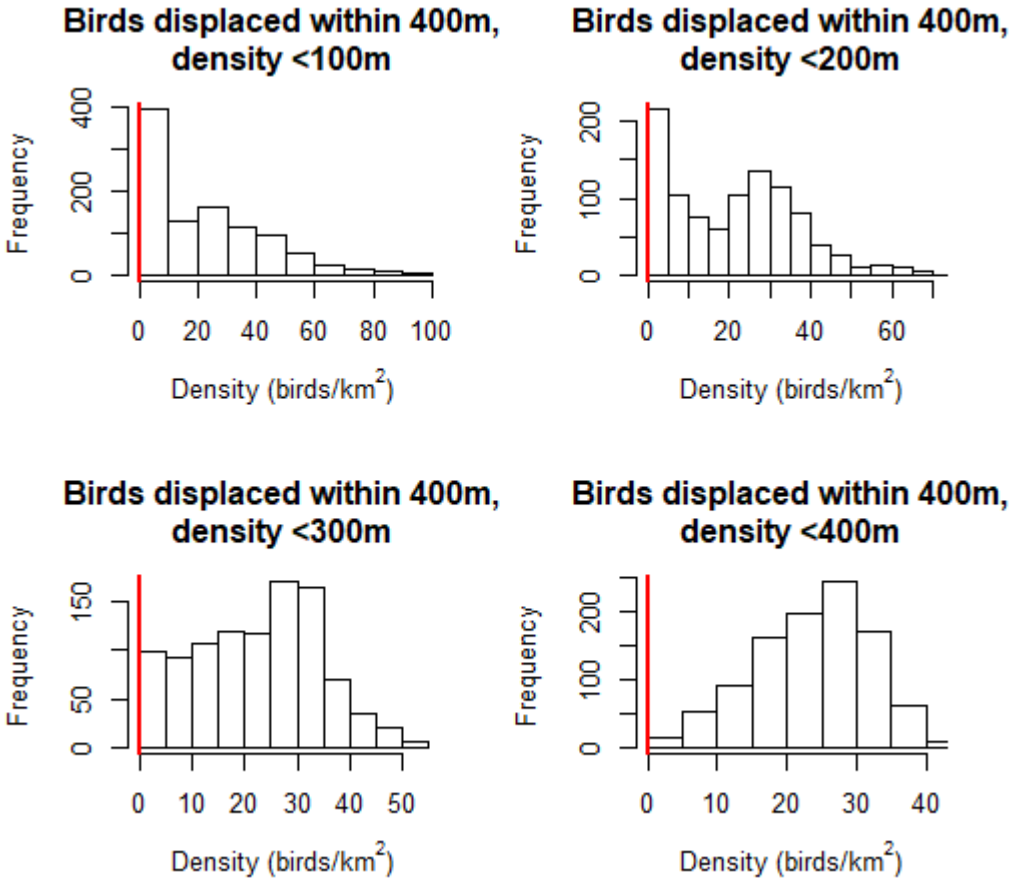

Figure 3-20. Guillemot densities within 100/200/300/400 m of randomly re-positioned turbine locations with removal of all birds within 400 m of planned turbine locations (relative turbine positions maintained). Red lines indicate actual densities within radial distances of turbine positions (including the removal as noted).

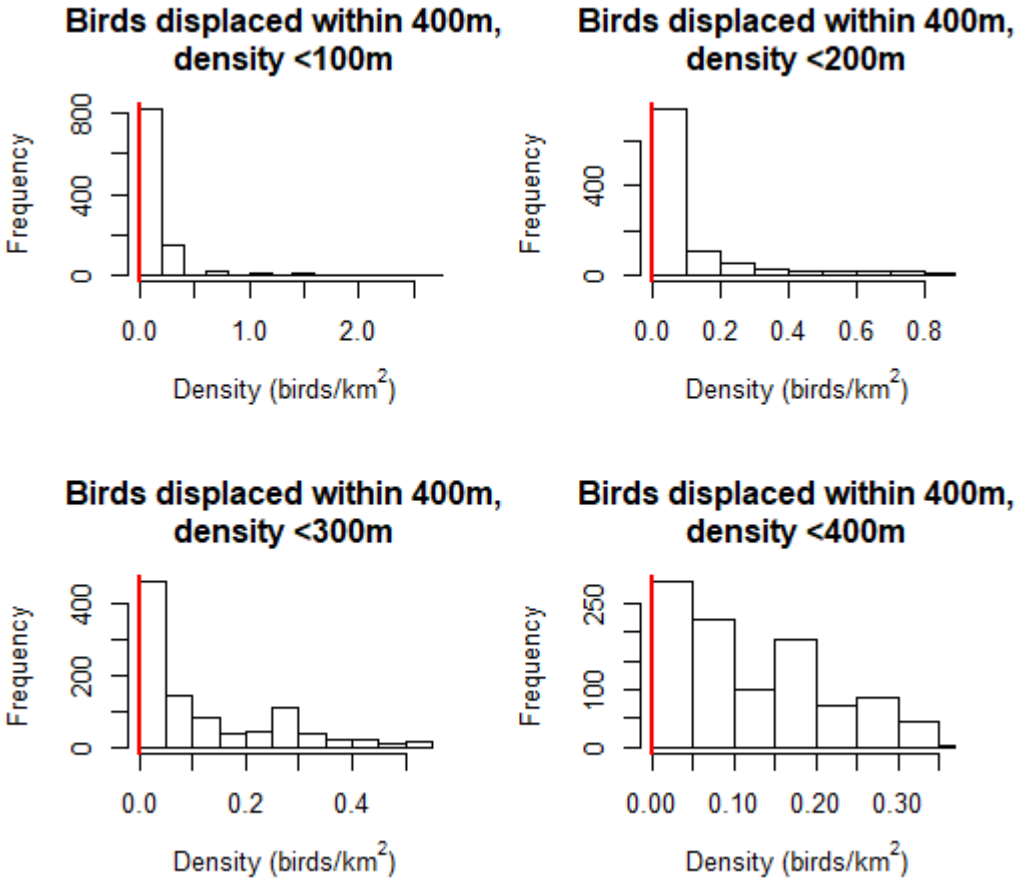

Figure 3-21. Puffin densities within 100/200/300/400 m of randomly re-positioned turbine locations with removal of all birds within 400 m of planned turbine locations (relative turbine positions maintained). Red lines indicate actual densities within radial distances of turbine positions (including the removal as noted).

A permutation test was used to calculate how likely it was that the shifts in the 'true' density relative to the simulated turbine locations would be obtained by chance. This probability of a chance effect was calculated as the proportion of random samples which had density estimates as small, or smaller, than the observed estimates (Table 3-6).

The results of the permutation tests for guillemot indicated that if birds avoided turbines by 100 m or more, the bootstrap simulation method was expected to identify the correct displacement distance (this can be seen by the presence of the lowest probabilities in the shaded cells of Table 3-6). For example, if birds were displaced by 300 m around actual turbine locations (Table 3-6 column 3), in none of the simulated turbine layouts (out of 1,000) was a lower density obtained, although for all displacement distances there would be a risk of identifying the effect as a smaller one (i.e. the values above the shaded cells were also low, although not as low as the shaded cell values).

Table 3-6. Guillemot permutation test results. Values are the probability that the difference between density estimates around actual turbine locations and around randomly relocated turbine positions would be observed by chance rather than due to displacement. Shaded cells indicate the probabilities of detecting the 'correct' displacement magnitudes (i.e. that turbine avoidance up to *x* m is correctly identified and not ascribed to a different avoidance distance). Probability values are considered significant (i.e. unlikely to be due to chance) if less than 0.05.

Probability that lower density around actual turbine locations (within *y* m) is due to chance rather than displacement	Distance (m)	Birds displaced within *x* m			
		100	200	300	400
	100	<0.001	0.033	0.147	0.305
	200	0.426	<0.001	0.031	0.145
	300	0.659	0.160	<0.001	0.029
	400	0.675	0.398	0.055	<0.001

For puffin, recorded in smaller numbers than guillemot, there was a lower probability of detecting the simulated effect, with only displacement from 400 m reaching a 5% significance threshold (Table 3-7). However, with the exception of displacement by only 100 m, the shaded cell values are much lower than the cells above and below. Thus, even though the test results fails to reach the 5% significance threshold, these outputs combined with the histogram plots (Figure 3-14, Figure 3-19 and Figure 3-21) provide a strong evidence base that if a displacement effect was present it would be indicated by this analysis, even in low abundance species.

Table 3-7. Puffin permutation test results. Values are the probability that the difference between density estimates around actual turbine locations and around randomly relocated turbine positions would be observed by chance rather than due to displacement. Shaded cells indicate the probabilities of detecting the 'correct' displacement magnitudes (i.e. that turbine avoidance up to *x* m is correctly identified and not ascribed to a different avoidance distance). Probability values are considered significant (i.e. unlikely to be due to chance) if less than 0.05.

Probability that lower density around actual turbine locations (within *y* m) is due to chance rather than displacement	Distance (m)	Birds displaced within *x* m			
		100	200	300	400
	100	0.582	0.602	0.717	0.820
	200	0.249	0.141	0.331	0.493
	300	0.732	0.698	0.069	0.201
	400	0.702	0.686	0.499	0.026

Thus, for each of the key bird species recorded within the wind farm, there was no indication of turbine avoidance when assessed across all the survey data combined.

3.6.1 Turbine avoidance in relation to turbine RPM

To investigate whether the density of birds around turbines was related to their operational status the data were split into subsets using the average RPM of the closest turbine when each bird observation was recorded. Five RPM samples were analysed, 0-2, 2-4, 4-6, 6-8 and 8+. The graphed outputs for each species and RPM subset are provided in ANNEX F, and a summary table is provided below. To provide context, it is useful to consider how frequently a rotor blade will

approach the sea surface at these RPM values: 2 RPM = 1 every 10 seconds; 4 RPM = 1 every 5 secs; 6 RPM = 1 every 3.33 secs; 8 RPM = 1 every 2.5 secs.

Table 3-8. Summary of turbine avoidance outputs analysed for subsets of turbine RPM. Sample sizes are provided in brackets. The turbine response is presented as 4 characters representing indications for attraction (+) or avoidance (-) or neither (0) in sequential 100 m bands around the turbines (0-100 m, 100-200 m, 200-300 m, 300-400 m). For example, '-/-/0/+ (50)' would indicate avoidance in the 0-100 m and 100-200 m bands, neither attraction nor avoidance in the 200-300 m band and attraction in the 300-400 m band, with a sample size of 50. Attraction or avoidance were assigned if the observed density was higher or lower (respectively) than the peak of the resampled densities. NA = not applicable.

Species	RPM (sample size)					
	0-2	2-4	4-6	6-8	8+	all RPM
Guillemot	0/-/0/0 (2187)	0/+/+/+ (2308)	0/+/+/+ (1609)	+/+/+/+ (599)	-/+/+/+ (171)	+/+/+/+ (6874)
Puffin	+/+/+/+ (11)	-/-/0/0 (16)	-/0/+/+ (14)	-/-/-/- (3)	NA(0)	0/0/0/0 (44)
Razorbill	+/+/+/+ (96)	+/0/0/0 (192)	+/+/+/+ (154)	-/+/0/0 (95)	-/-/0/0 (14)	+/+/+/0 (551)
Kittiwake	0/0/0/0 (615)	-/-/-/0 (430)	-/0/-/+ (439)	-/-/-/0 (186)	-/-/-/0 (63)	0/0/-/0 (1733)
Herring gull	-/-/+/+ (255)	-/-/-/- (64)	-/+/+/+ (144)	NA (2)	NA (1)	-/0/+/+ (465)

Sample sizes varied across the RPM subsets and were very small for puffin across all subsets (range 0 to 16) and for herring gull at higher values for RPM. Among the species recorded in higher numbers (guillemot, razorbill and kittiwake) there were fewer recorded in the wind farm at higher RPM values (i.e. >=6).

If the species under consideration here avoid turbines by greater distances when the rotors are spinning faster, then it would be predicted that as the turbine RPM increased the observed densities in the radial bands around the turbines would decrease when compared with the densities expected by chance. On the basis of the preliminary results above, the species appear to have varied in their responses.

The most numerous species, guillemot, were present at either the same or higher densities around turbines than would be expected by chance, largely irrespective of RPM, with only the density within 100m for RPM values of 8 and higher being lower than the value expected by chance. There is therefore little evidence that turbine operation affected guillemot distributions.

There was a weak indication of avoidance in razorbill at RPM values above 6 and at distances <200m from the turbines, but the small sample sizes at higher RPM values means little confidence can be placed on this result.

The density of kittiwakes around turbines at low RPM values (<2) was the same as that expected by chance (i.e. no apparent response), but above 6 RPM lower densities than expected were found at distances up to 300m.

Puffin were observed in insufficient numbers for the results of the RPM analysis to be considered reliable, while herring gull were only present at lower RPM values (<6) and had densities in the

RPM subsets which were consistent with varying levels of both attraction and avoidance with no trend apparent.

3.7 Flight height

The proportion of birds flying below rotor height (defined as 32.7 m above MSL) was compared between birds recorded inside the wind farm and those outside, having first filtered by distance to obtain a subset of birds recorded between 15 km and 22 km offshore (i.e. the same distance as the wind farm). A binomial GLM was fitted to the data with the response variable (below/above lower rotor height) modelled in relation to birds recorded inside or outside the wind farm. Bird heights were estimated with uncertainty with a mean, minimum and maximum value (see HiDef methods), therefore the maximum height estimate was used in the models to ensure the outputs were precautionary. In addition, for some individuals no height was estimated but the individual was categorized as flying at less than 22 m from the sea surface (in Table 3-9 this included the right-most three columns: birds with a reflection but no height, birds with a maximum height below PCH and birds with a height estimate below sea level). These individuals were included in the 'below rotor height' group in the modelling. Summary data are provided in Table 3-9.

Table 3-9. Summary of flight height data. Birds with a reflection but no height estimate were defined as flying at <=3m. If the bird length was less than that estimated from bird with reflections a negative (<sea level) height was estimated. Both categories were included as 'below PCH' in the analysis. Some birds had only a maximum height estimate, in all cases below PCH.

Species	Total	No. with a height estimate		No. with a reflection but no height estimate (<3m)	No. with a max height estimate only (all below PCH)	No. estimated to be below sea level
		Height estimate > PCH	Height estimate < PCH			
Gannet	46	6	4	28	4	4
Kittiwake	3158	462	668	339	119	1570
Great black-backed gull	19	16	1	0	1	1
Herring gull	355	151	69	5	37	93

For gannet, kittiwake and great black-backed gull there were no significant differences in the proportion recorded above/below rotor height inside or outside the wind farm (gannet p = 0.99; kittiwake p=0.38; great black-backed gull p=0.99). A significant difference was obtained for herring gull (p<0.001), with the percentage at rotor height estimated to be much lower in the wind farm (24.1%, n=141) than outside (54.7%, n=214), indicating that a higher proportion of individuals of this species flew lower when in proximity to the turbines. For gannet the overall proportion at rotor height was estimated as 6.7% (n=46), for kittiwake as 14.9% (n=3,158) and for great black-backed gull as 89.3% (n=19).

4 DISCUSSION

4.1 Evidence for broad scale wind farm effects on seabird distributions and abundance

On the basis of the design-based population estimates, the post-construction surveys found broadly similar overall abundance (within the total study area) for all species. Within the wind farm, five species were (on average) more abundant in 2019 than 2015: guillemot, razorbill, kittiwake, great black-backed gull and herring gull and two were less abundant: gannet and puffin. Of the latter, gannet had the most marked difference, with only two individuals recorded within the wind farm boundary across all six surveys in 2019. Gannets are generally considered to exhibit a high degree of wind turbine avoidance, and the 2019 results appear to support this observation. Puffin, while present in lower numbers in 2019, were still recorded within the wind farm, and the lower abundance appears to relate to lower overall recorded numbers. It is also important to note that the peak in 2015 was recorded on the late survey conducted in August, which probably reflected post-breeding dispersal, and that the last 2019 survey was almost two weeks earlier (25th July, compared with 5th August).

The other five species all had higher average abundance in the wind farm in 2019, although there was considerable variation between surveys. While large gulls are considered to show little response to wind farms, auks are typically thought to be displaced by offshore turbines. However, for guillemot and razorbill at least, the design-based data do not indicate the presence of displacement.

However, a more robust assessment of an overall wind farm effect can be obtained from the spatial models fitted to the before (2015) and after (2019) construction data. These models were fitted following the guidance for the MRSea package (Scott-Hayward *et al.*, 2013), with an initial model-fitting process to identify the most appropriate structure to model explanatory covariates (depth, distance to coast and spatial smoother) before fitting the before/after categorical variable with an interaction term (with the spatial smoother).

The model results therefore indicated if there was the presence of both an overall change ('impact') and also if there was spatial component to those changes.

For gannet, the spatial model found no evidence for an overall change in abundance, but a very strong and significant spatial effect, with a decline centred on the wind farm, backing up the more simplistic observations of gannet avoiding the wind farm derived from the design-based estimates.

Similarly, the puffin abundance was not found to have changed in the study area, but again there was a significant interaction between impact and spatial smoother. However, while the area of reduced abundance included the wind farm, the reduction covered a much larger area and was centred to the east of the site boundary. While it might be considered that the peak recorded on the August 2015 survey could have influenced the overall result, examination of the *runInfluence* results (ANNEX D) reveals no evidence that this survey was exerting an influence on the results. Thus, this result does not appear to have been due to the inclusion of the (probable) post-breeding dispersal in 2015.

There was a significant increase in the overall guillemot abundance, but the spatial component of this relationship was not significant at the 5% level (or 10% level). No regions of the study area were found to have significant reductions, but the southern half had significant increases.

Kittiwake showed a significant redistribution effect, but no overall change in abundance. There was a significant decrease in abundance in coastal waters, and a significant increase centred on the northern edge of the wind farm, with a significant decrease in coastal waters. The reasons for this are not apparent, although this species is not noted for its aversion to wind farms and therefore it is plausible that this represented a change in relation to prey distributions.

Razorbill had both a significant increase in overall abundance and a significant interaction between impact and spatial smoother. Abundance increased across almost all of the survey area, including the Wind Farm.

It was not possible to fit spatial models to the great black-backed gull and herring gull data so no further exploration of these species in relation to wind farm avoidance was conducted.

Consideration was given to the potential that construction activity at the adjacent Moray East Wind Farm could have influenced the distribution of birds. ANNEX E provides a plot of the locations where piling activity occurred during the survey period (May 28th to 25th July, inclusive). Piling only occurred on the same day as one of the surveys (survey 6 on 25th July), at a single location approximately 15km from the Beatrice site boundary. At five other locations piling occurred on the day before the survey, however none of these was within the Beatrice 4km buffer and therefore the likelihood that any of these piling events will have had a detectable effect on the seabird distributions is considered to be very small.

4.2 Evidence for fine scale turbine effects on seabird distributions and abundance

The 2015 pre-construction and 2019 post-construction data were collected using a survey which was designed to obtain high resolution bird location data to investigate within wind farm distributions in relation to turbine locations. In 2015 there were no structures for the birds to respond to, therefore the data were manipulated to simulate avoidance of turbines within radii of 100 m to 400 m. The pre-construction analysis indicated that if turbine avoidance occurred it would be detected by the analysis method developed for these data. The 2019 post-construction monitoring provided the first test of this method using survey data collected within an operational wind farm.

The method repeatedly randomizes the turbine locations (collectively) and estimates the density of birds in relation to each random iteration to build up a distribution of densities for other possible turbine locations, albeit these are only offset from the real locations by up to approximately 500 m.

The null hypothesis for this analysis is that, under conditions of no turbine avoidance, the observed (i.e. real) density of birds within the 100-400m radii of the turbines will coincide with the peak range of the random distribution. This is most readily interpreted by plotting the randomized densities as a histogram and overlaying the observed value. As well as generating a prediction of the result under the null situation (of no avoidance or attraction) the method can also indicate the direction of deviations from this situation: if the observed density is lower than the randomised peak (i.e. the red line is to the left of the histogram) this indicates avoidance, while a higher density (red line to the right) indicates attraction.

For all species tested (i.e. those with sufficient observations; guillemot, razorbill, puffin, kittiwake and herring gull), the pooled analysis found no indication of systematic turbine avoidance, although this conclusion is slightly less robust for herring gull due to the smaller sample size.

Furthermore, for guillemot there is an indication that the observed densities within 100 m and 200 m of the turbines are higher than the randomized peak, suggesting attraction to turbines. This was also observed in razorbill, up to 300 m and possibly also puffin, although the smaller sample size for this species reduces confidence in this conclusion.

To further test the reliability of the method, simulated turbine avoidance was applied to the guillemot and puffin data in the same manner as used for the pre-construction analysis. As with the pre-construction results, this indicated that the method would identify avoidance if it was present, with the manipulated 'observed' densities offset from the peak densities of the randomized distributions as expected in each case. This was backed up by the permutation results which for guillemot correctly identified the actual manipulation in each case, although the results for puffin were less apparent, a difference due to the relative sample sizes available for the two species.

Consideration of whether the observed densities around the turbines was related to their operational status, assessed using the mean turbine RPM during the survey periods, indicated there may be differences between species. For guillemot there was little indication of a difference in densities at different RPM, while for razorbill and kittiwake there was an indication of weak avoidance at the higher RPM values. Too few data were available to draw conclusions on puffin and herring gull. Overall fewer birds were recorded in the wind farm when the turbines had higher RPM, thus it could be concluded that birds were less inclined to enter the wind farm when the turbines were rotating faster. However, since RPM is positively related to wind speed, it is also possible that the conditions may have been less favourable for foraging in the wind farm during these periods. Furthermore, other factors such as wind direction and tide state may also play an important role in determining foraging distributions, and with only six surveys it may also simply be a chance effect. Future monitoring will provide further information on this.

The 2019 survey data reported on here were collected during the first year of wind farm operation. There will be two further years of data collection using the same methods which will be combined with the 2019 data for analysis. The spatial modelling will be undertaken in a similar manner to that presented here, ideally with all years of data included (i.e. pre-construction and multiple post-construction) to further explore large scale distributions. The turbine avoidance analysis will be undertaken following the same methods as presented in the current report and options for how to combine the current (year 1) monitoring data with that collected during the subsequent monitoring will also be explored. However, it is important to note that the turbine avoidance method was deliberately designed to avoid between year comparisons and the potential for background inter-annual variations to confound results, so this analysis is intended to be effectively stand-alone.

4.3 Synthesis of wind farm and turbine responses

A key aspect of the Beatrice ornithology monitoring is the collection of data to permit analysis designed to detect both large scale and fine scale responses to the wind farm. The driver for adopting this approach was to be able to derive a mechanistic understanding of seabird responses

to wind farms. Armed with the better understanding obtained from such a study, the goal is to be able to make predictions for how seabirds will respond at other wind farms which may have different design characteristics (e.g. closer or more widely spaced turbines). The results of the 2019 post-construction surveys provide a range of spatial scales at which to make such predictions.

4.3.1 Gannet

Gannet has been found to exhibit high levels of wind farm avoidance in other studies (e.g. APEM 2014, Dierschke *et al*. 2016, Leopold *et al*. 2013, Vanermen *et al*. 2013, Vanermen *et al*. 2016, Garthe *et al*. 2017a,b). The results of the current study are in agreement with these previous studies and provide a clear indication that gannets avoid wind farms. This overall avoidance was sufficiently marked that it was not possible to consider turbine avoidance as virtually no gannets were recorded within the wind farm. One conclusion of this growing evidence base is that displacement is perhaps a greater potential source of impact for this species than collision risk, with the former potentially needing to be assessed with higher rates of displacement than the current 60-80%. Conversely, the current collision avoidance rate of 98.9% may well be an underestimate of the level of avoidance this species performs.

4.3.2 Puffin

The spatial modelling indicated that there may have been some avoidance of the wind farm, although that conclusion is made with low confidence due to the fact the apparent avoidance only covered part of the wind farm site. However, of the birds which did enter the wind farm there was no indication that turbines were avoided. Taken together, there does not appear to be a notable response of puffin to the presence of the wind farm. The displacement rates currently applied for this species are 30-70%, and the current results would indicate that the lower end of this range is likely to be more appropriate for similar wind farms.

4.3.3 Guillemot

There was no indication from either the spatial modelling or the turbine avoidance analysis that guillemots have responded to the presence of the wind farm. Indeed, there was a suggestion of elevated densities in the immediate vicinity of turbines (up to approximately 200 m). No data on prey distributions are available, however underwater structures are known to aggregate fish, so it is possible that guillemots have been attracted to the enhanced foraging opportunities presented. It certainly would appear that the displacement rates of 30-70% currently used in assessment are considerably over-estimated, at least in the breeding season for similar wind farms.

4.3.4 Razorbill

The spatial modelling and turbine avoidance analysis lead to similar conclusions for razorbill as for guillemot, while the pooled analysis of turbine avoidance also found no indication of systematic avoidance of the wind farm or individual turbines, and some evidence of higher densities in proximity to the turbines. There was a weak indication of turbine avoidance when they were operating at higher RPM values, however the sample size was small so this should not be over-interpreted. Thus, overall it seems plausible that the current 30-70% displacement rates used in assessment are over-estimates for this species too, at least in the breeding season for similar wind farm designs.

4.3.5 Kittiwake

The results for kittiwake are more difficult to interpret than for some of the other species. The spatial modelling indicated that numbers had increased in an area centred to the north of the Wind Farm and extending into it. The turbine avoidance analysis, pooled across all surveys, found little evidence to suggest avoidance of turbines, albeit densities were generally lower closer to the turbines, however there was an indication that at higher turbine RPM values the birds may have given the turbines a wider berth (up to 300 m).

There was no indication that flight heights differed for kittiwakes recorded in the Wind Farm compared with those outside. However, the uncertainties in estimating flight heights from digital aerial survey imagery limits the degree of confidence in this result.

4.3.6 Great black-backed gull

Great black-backed gulls were recorded in low numbers in both the pre-construction and post-construction surveys, which is to be expected given the small size of the East Caithness population. Given these low numbers it is difficult to draw conclusions on how, if at all, the wind farm is affecting the species. The species was only recorded within the wind farm on one survey in 2019, compared with four in 2015, however, this may simply be a chance effect. Further understanding of this species' behaviour and possible wind farm interactions will be gained from the planned tracking studies to be conducted in future years (currently planned for 2022).

4.3.7 Herring gull

Herring gulls were recorded in considerably larger numbers in 2019, with a peak overall abundance more than 10 times that seen in 2015 and within the wind farm of over 124 times higher. It is not apparent why such an increase would have occurred, and it is difficult to draw conclusions on this result. The turbine avoidance analysis found no evidence for this species avoiding turbines although the relatively small sample size limits the degree of confidence in this result. However, this would correspond to previous observations that large gull species are not displaced to an appreciable extent by wind farms (Dierschke *et al*. 2016).

There was a significant apparent difference in flight heights for birds in the wind farm compared with those outside, with only 18% estimated to be at rotor height within the wind farm, compared with 53% outside the wind farm. However, the uncertainties in estimating flight heights from digital aerial survey imagery limits the degree of confidence that this is a robust finding.

5 REFERENCES

APEM (2014) Assessing northern gannet avoidance of offshore windfarms. APEM ref: 512775.

BOWL (2016) Pre-construction aerial survey report. http://marine.gov.scot/sites/default/files/bowl_pre-construction_aerial_surveys_report-redacted.pdf

Burton, N.H.K., Thaxter, C.B., Cook, A.S.C.P., Austin, G.E., Humphreys, E.M., Johnston, A., Morrison, C.A., & Wright, L.J. (2013). Ornithology Technical Report for the Proposed Dogger Bank Creyke Beck Offshore Wind Farm Projects. A report carried out by the British Trust for Ornithology under contract to Forewind Ltd BTO Research Report No. 630

Dierschke, V., Furness, R.W. and Garthe, S. (2016). Seabirds and offshore wind farms in European waters: Avoidance and attraction. Biological Conservation 202: 59-68.

Garthe, S., Peschko, V., Kubetzki, U. and Corman, A-M. (2017a) Seabirds as samplers of the marine environment – a case study of northern gannets. Ocean Science, 13, 337-347.

Garthe, S., Markones, N. and Corman, A.M. (2017b) Possible impacts of offshore wind farms on seabirds: a pilot study in northern gannets in the southern North Sea. Journal of Ornithology, 158, 345-349.

Leopold, M. F., van Bemmelen, R. S. A. and Zuur, A. (2013) Responses of local birds to the offshore wind farms PAWP and OWEZ off the Dutch mainland coast. Report C151/12, Imares, Texel.

Pistorius PA, Hindell MA, Tremblay Y,Rishworth GM (2015) Weathering a Dynamic Seascape: Influences of Wind and Rain on a Seabird's Year-Round Activity Budgets. PLoS ONE10(11): e0142623. doi:10.1371/journal.pone.0142623

Scott-Hayward, L.A.S., C.S. Oedekoven, M.L. Mackenzie, C.G. Walker, and E. Rexstad. (2013). User Guide for the Mrsea Package V0.1.2: Statistical Modelling of Bird and Cetacean Distributions in Offshore Renewables Development Areas. University of St. Andrews Contract for Marine Scotland; Sb9 (Cr/2012/05). University of St Andrews.

Thaxter, C. B., Wanless, S., Daunt, F., Harris, M.P., Benvenuti, S., Watanuki, Y., Grémillet, D. and Hamer, K.C. (2010). Influence of wing loading on the trade-off between pursuit-diving and flight in common guillemots and razorbills. The Journal of Experimental Biology, 213, 1018-1025.

Vanermen, N., Courtens, W., Van de walle, M., Verstraete, H. and Stienen, E.W.M. (2016) Seabird monitoring at offshore wind farms in the Belgian part of the North Sea: Updated results for the Bligh Bank and first results for Thorntonbank. Rapporten van het Instituut voor Natuur- en Bosonderzoek 2016 (INBO.R.2016.11861538). Instituut voor Natuur- en Bosonderzoek, Brussels.

Vanermen, N., Stienen, E.W.M., Courtens, W., Onkelinx, T., Van de walle, M. and Verstraete, H. (2013) Bird monitoring at offshore wind farms in the Belgian part of the North Sea - Assessing seabird displacement effects. Rapporten van het Instituut voor Natuur- en Bosonderzoek 2013 (INBO.R.2013.755887). Instituut voor Natuur- en Bosonderzoek, Brussels.

ANNEX A. COMPARISON OF MODEL BASED ESTIMATES FROM 2015 ANALYSIS AND 2019 ANALYSIS

Following the pre-construction surveys, BOWL (2016) presented abundance estimates obtained from spatial modelling. Following the 2019 post-construction surveys (reported here) the spatial models included both sets of survey data with the inclusion of a before/after categorical model term with the aim of identifying wind farm effects. In the period between the two analyses there were minor updates made to the spatial modelling method used (i.e. the MRSea packages was revised) and the spatial grid used for the model was slightly different (in order to accommodate both datasets). As a consequence the abundance estimates for the pre-construction surveys presented in the current report are slightly different from those in BOWL (2016). For clarity the two sets of abundance estimates are presented below.

Pre-construction results from BOWL (2016)

Table 4. *Model derived population abundance estimates in the total survey area and within the Wind Farm boundary for each species in each survey. Estimates were generated as predictions from the best-fit models identified in Table 3 using appropriate covariate values for the total survey area and within the Wind Farm boundary respectively. Entries marked with '-' indicate instances when small sample sizes prevented model fitting.*

Species	*Area*	*Population abundance on each survey*					
		1	*2*	*3*	*4*	*5*	*6*
Gannet	*Total survey area*	*198.3*	*520.6*	*816.6*	*206.1*	-	-
	Wind Farm	*21.9*	*207.9*	*458.5*	*4.1*	-	-
Guillemot	*Total survey area*	*48494.2*	*50252.9*	*20176.8*	*61625.6*	*8457.8*	*4501.4*
	Wind Farm	*5410.1*	*2720.5*	*6056.7*	*7630.5*	*680.5*	*803.1*
Kittiwake	*Total survey area*	*1689.6*	*3708.1*	*3415.1*	*3801.5*	*1683.2*	*377.9*
	Wind Farm	*13.3*	*196.6*	*62.0*	*1616.6*	*86.2*	*101.3*
Puffin	*Total survey area*	*1738.2*	*1315.5*	*566.5*	*930.9*	*261.6*	*3413.7*
	Wind Farm	*209.7*	*60.6*	*50.3*	*33.9*	*5.5*	*938.2*
Razorbill	*Total survey area*	*798.6*	*1686.7*	*3692.1*	*1750.2*	-	-
	Wind Farm	*68.3*	*122.5*	*177.0*	*229.4*	-	-

2015 spatial model abundance estimates re-calculated for this report.

Species	Area	Population abundance on each survey					
		1	2	3	4	5	6
Gannet	Total survey area	174.14	461	708.6	182.6	17.5	8.9
	Wind Farm	56.38	149.3	229.4	59.1	5.7	2.9
Guillemot	Total survey area	39760.1	36561.0	15487.5	51036.9	7642.7	4063.5
	Wind Farm	5819.9	1421.3	2060.1	7015.9	1452.0	902.1
Kittiwake	Total survey area	1443.4	3639.1	3375.9	3707.1	1666.9	352.2
	Wind Farm	37.7	246.7	62.5	1290.7	174.0	63.0
Puffin	Total survey area	1959.9	1409.8	479.2	532.2	214.0	3133.1
	Wind Farm	193.2	72.9	19.7	2.7	2.6	1027.5
Razorbill	Total survey area	817.8	2034.5	3527.9	1674.8	37.7	9.6
	Wind Farm	49.3	122.6	212.6	100.94	2.3	0.6

ANNEX B. DISTRIBUTION OF BIRDS IN FLIGHT IN 2015 AND 2019

The locations of birds recorded in flight on each survey in each year are plotted in figures B1 to B14 (note that the plots are provided for each species in turn, 2015 then 2019). These were not analysed using spatial models on the basis that physical covariates (e.g. depth and distance to coast) are unlikely to explain the observed distributions.

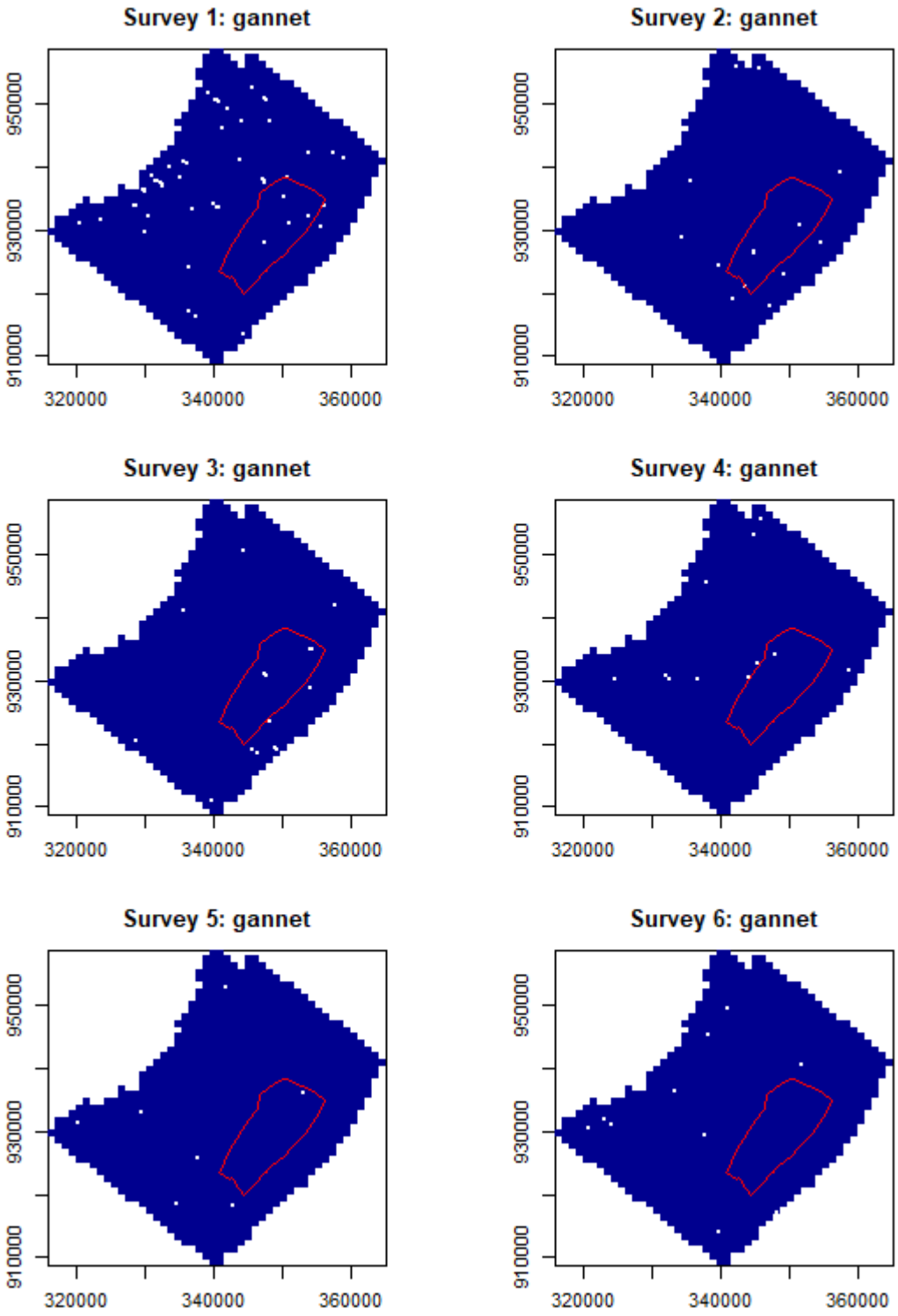

Figure B1. Locations of gannet recorded in flight during 2015 surveys.

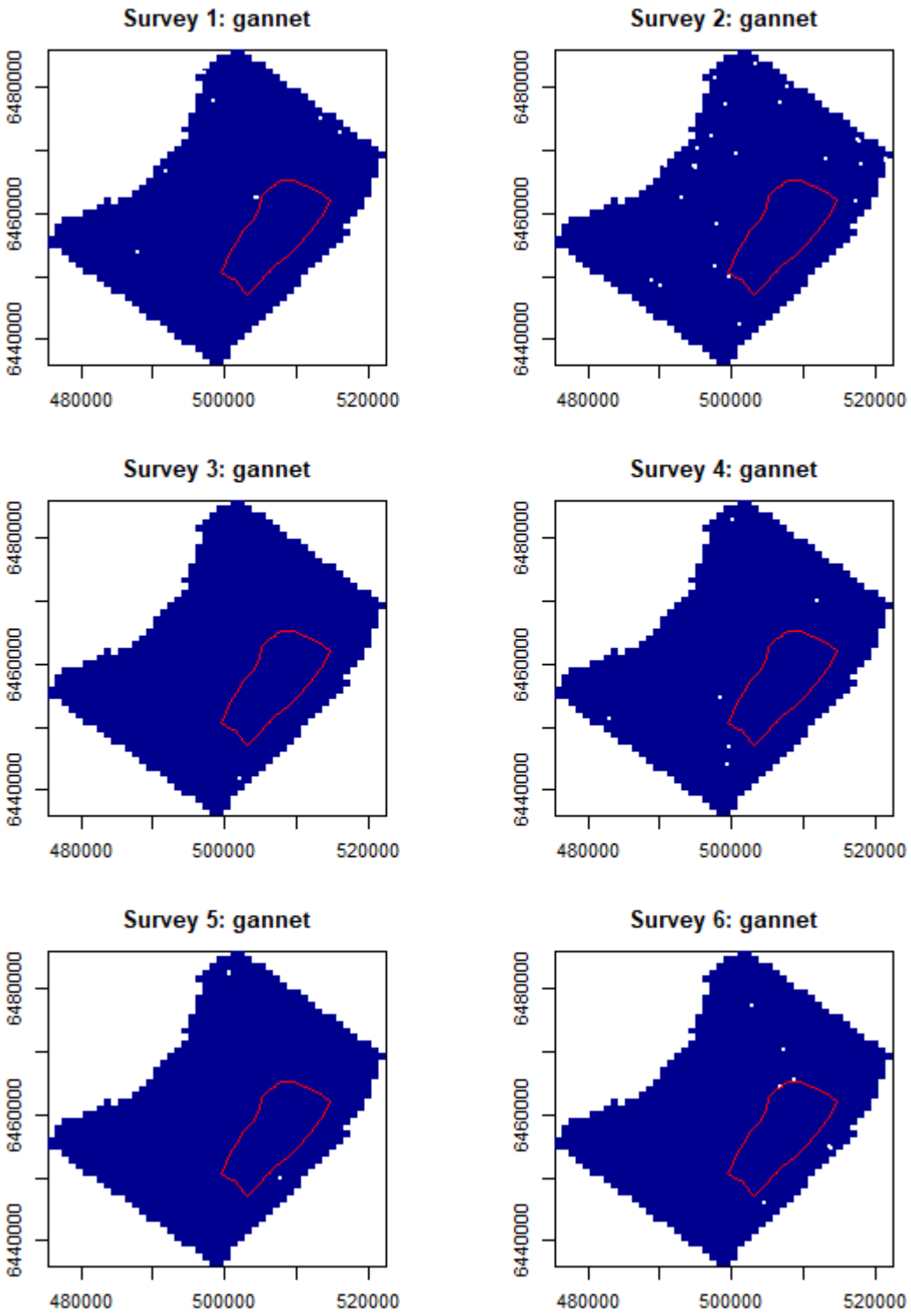

Figure B2. Locations of gannet recorded in flight during 2019 surveys.

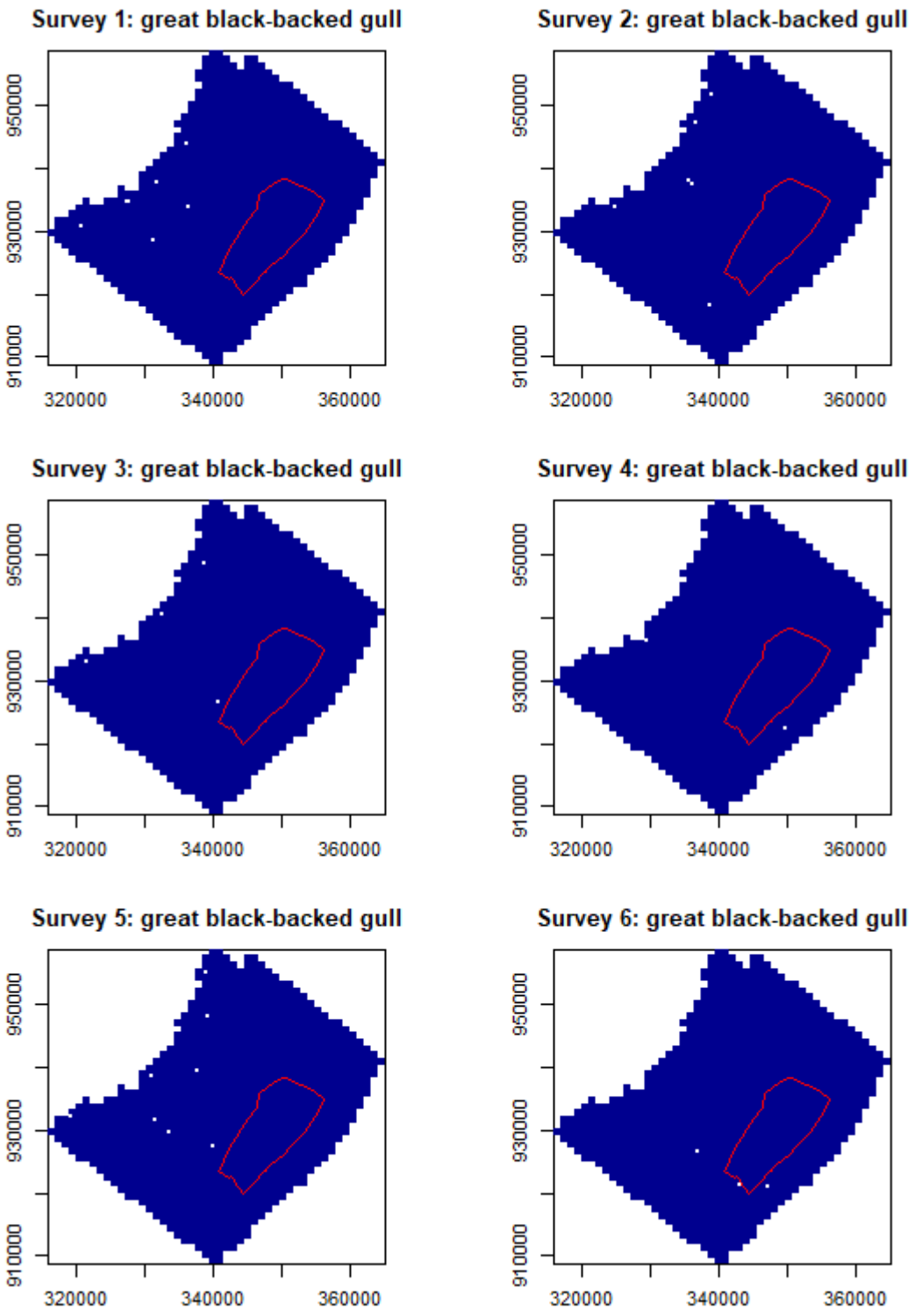

Figure B3. Locations of great black-backed gull recorded in flight during 2015 surveys.

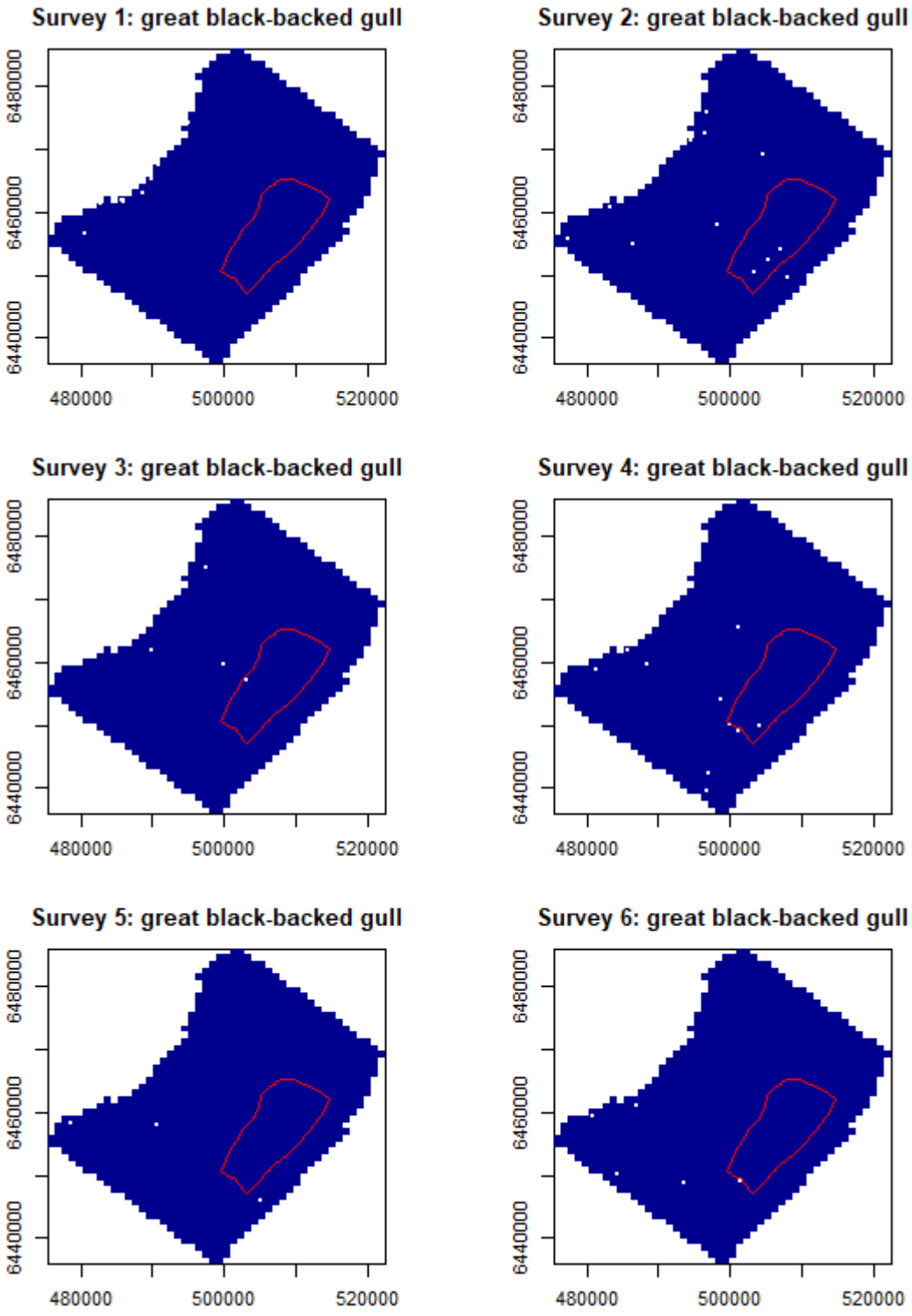

Figure B4. Locations of great black-backed gull recorded in flight during 2019 surveys.

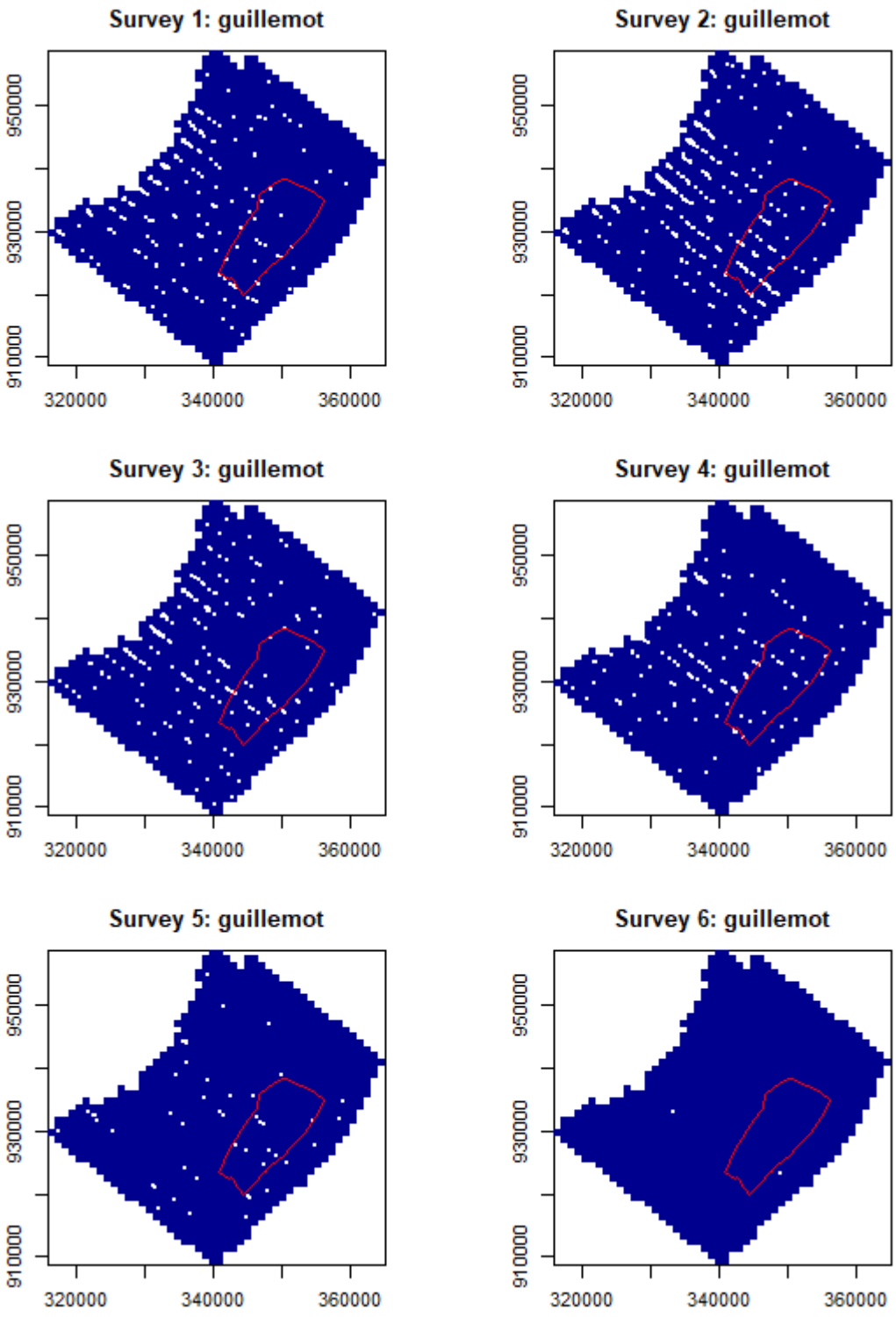

Figure B5. Locations of guillemot recorded in flight during 2015 surveys.

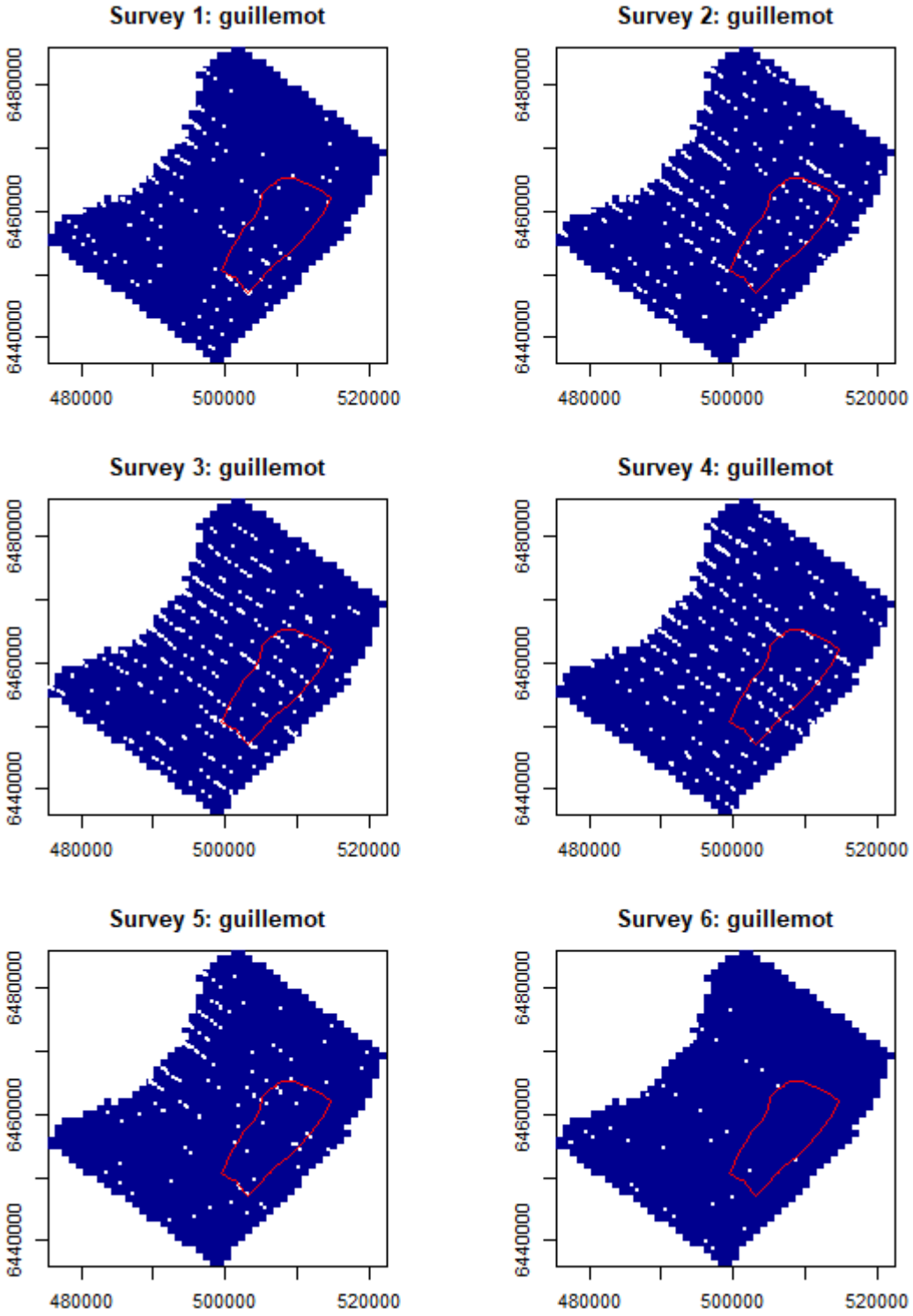

Figure B6. Locations of guillemot recorded in flight during 2019 surveys.

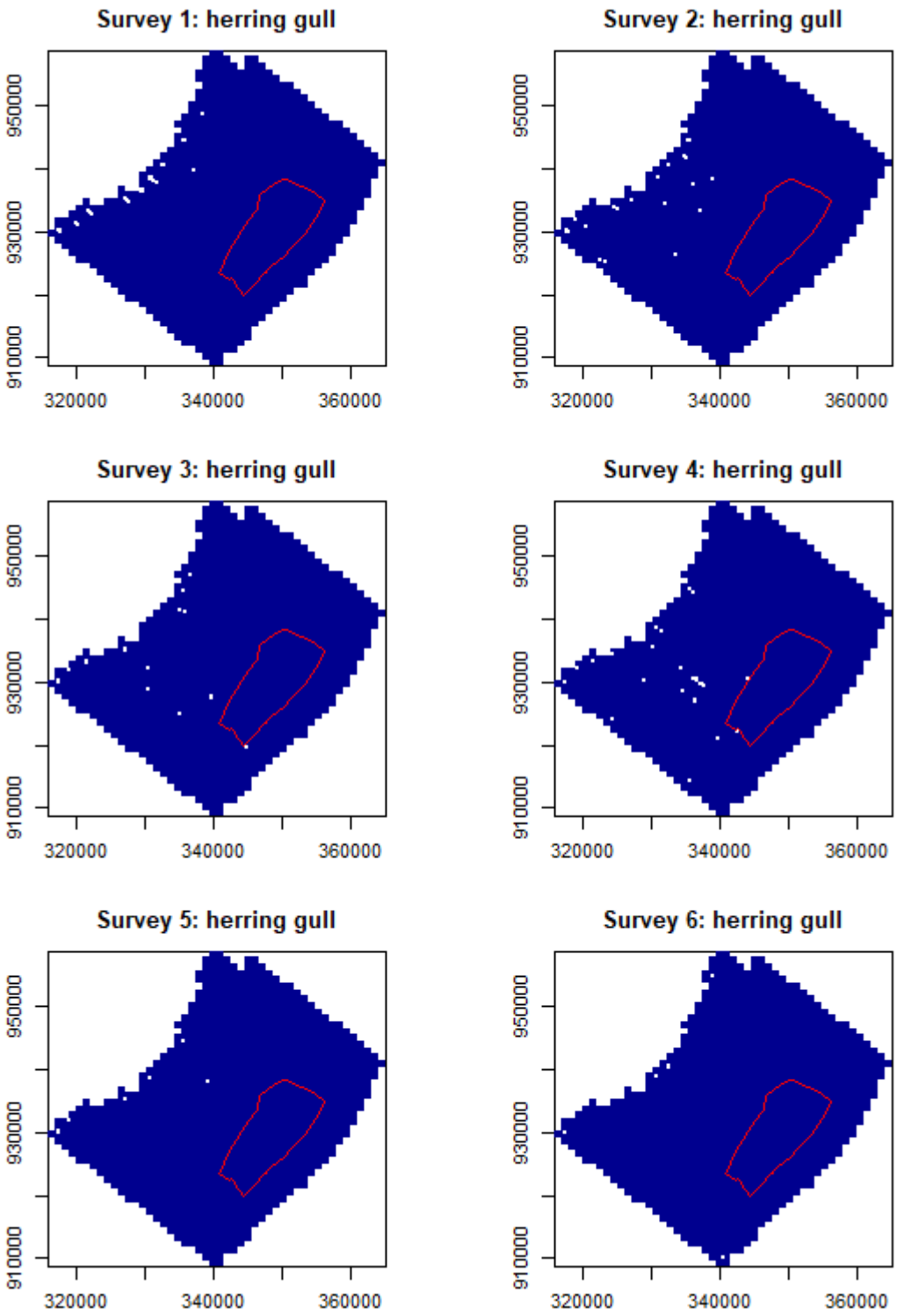

Figure B7. Locations of herring gull recorded in flight during 2015 surveys.

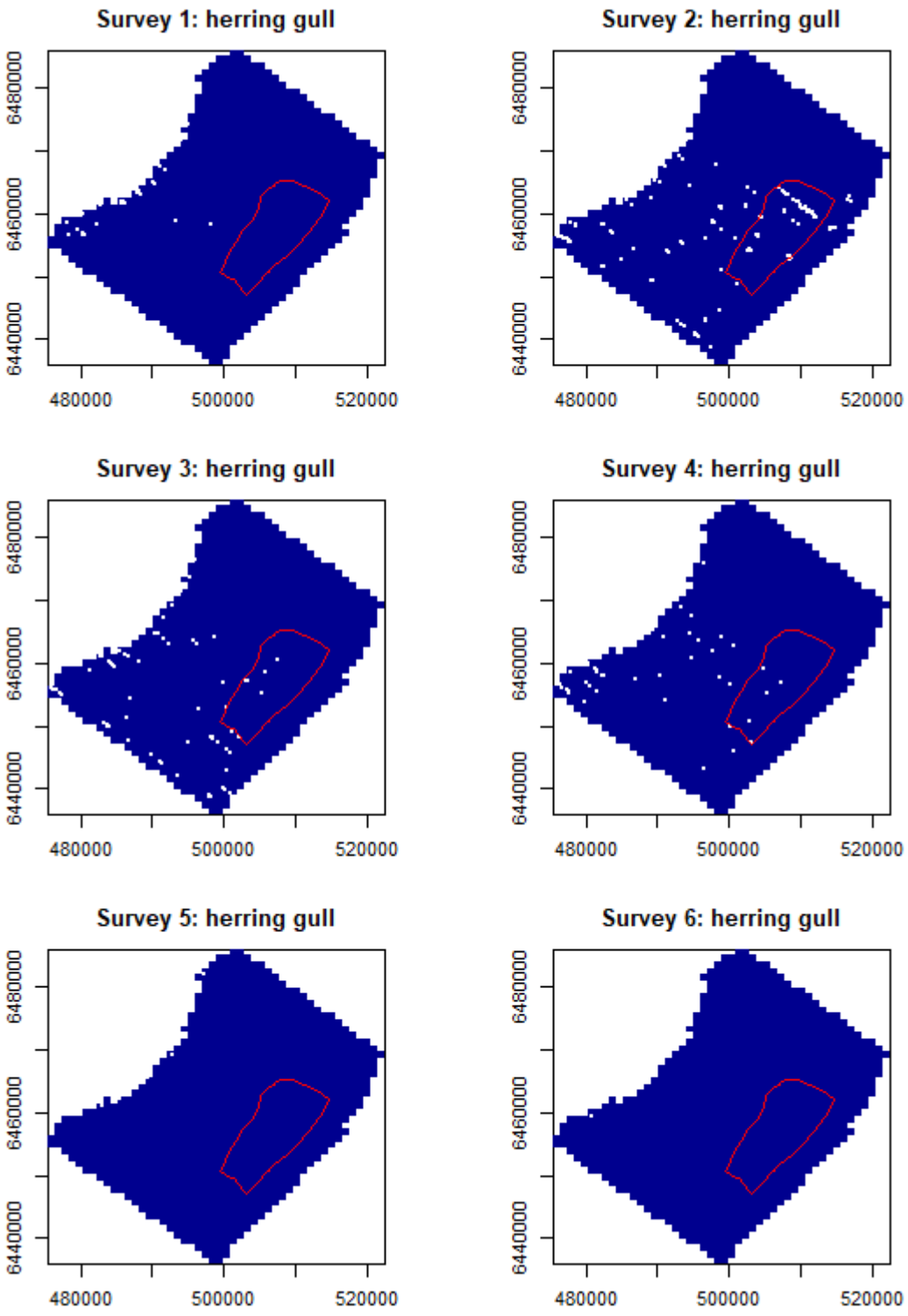

Figure B8. Locations of herring gull recorded in flight during 2019 surveys.

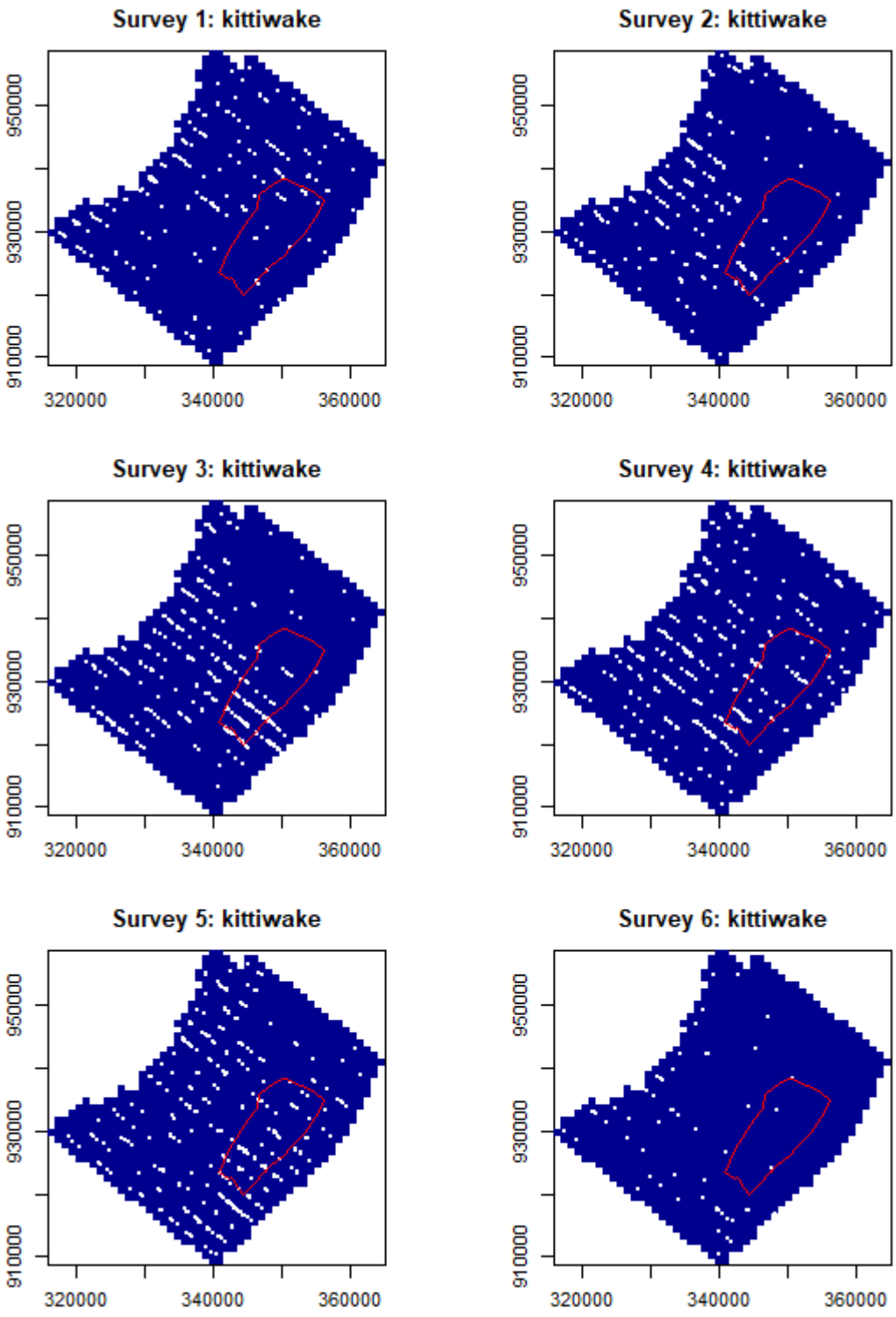

Figure B9. Locations of kittiwake recorded in flight during 2015 surveys.

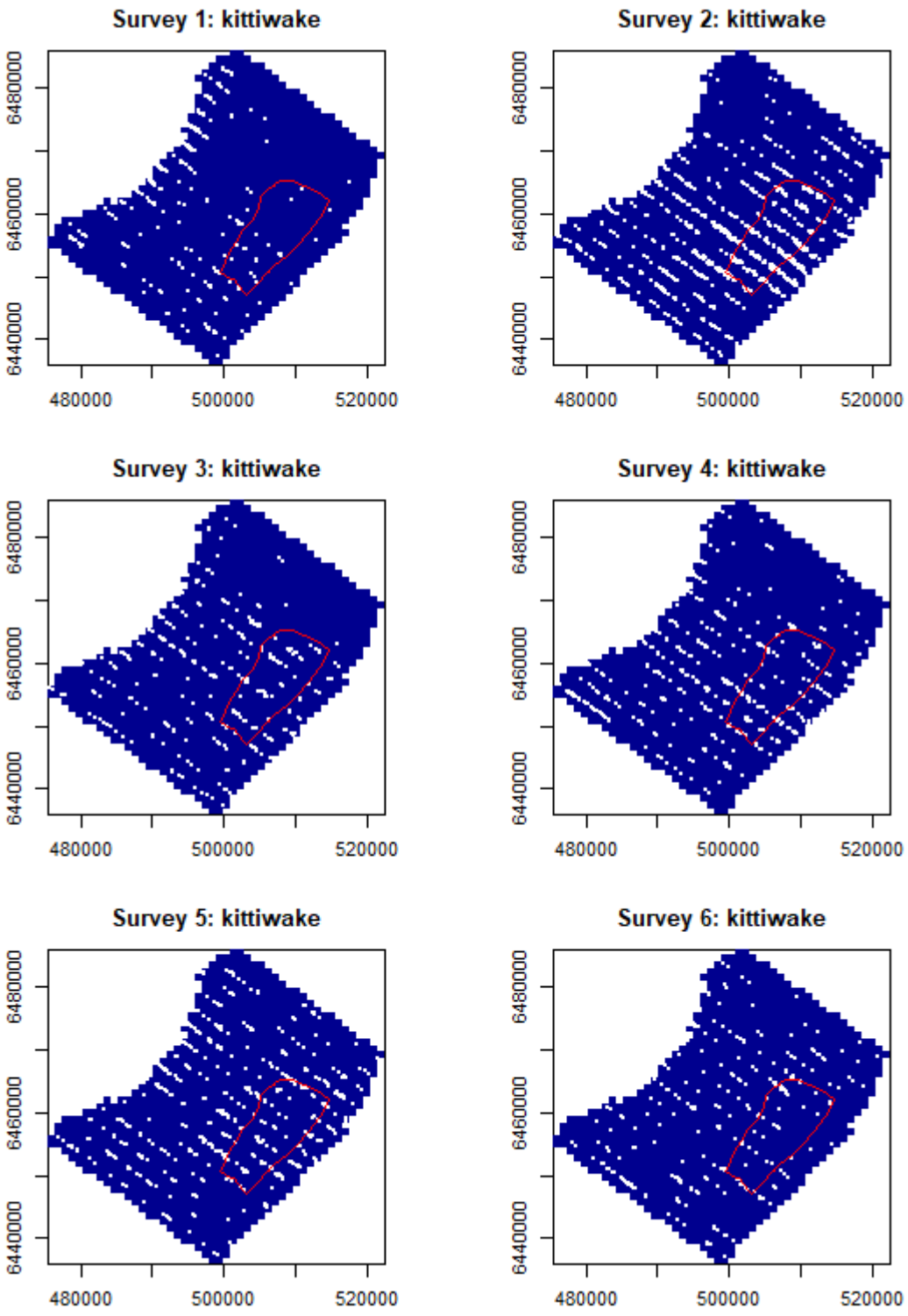

Figure B10. Locations of kittiwake recorded in flight during 2019 surveys.

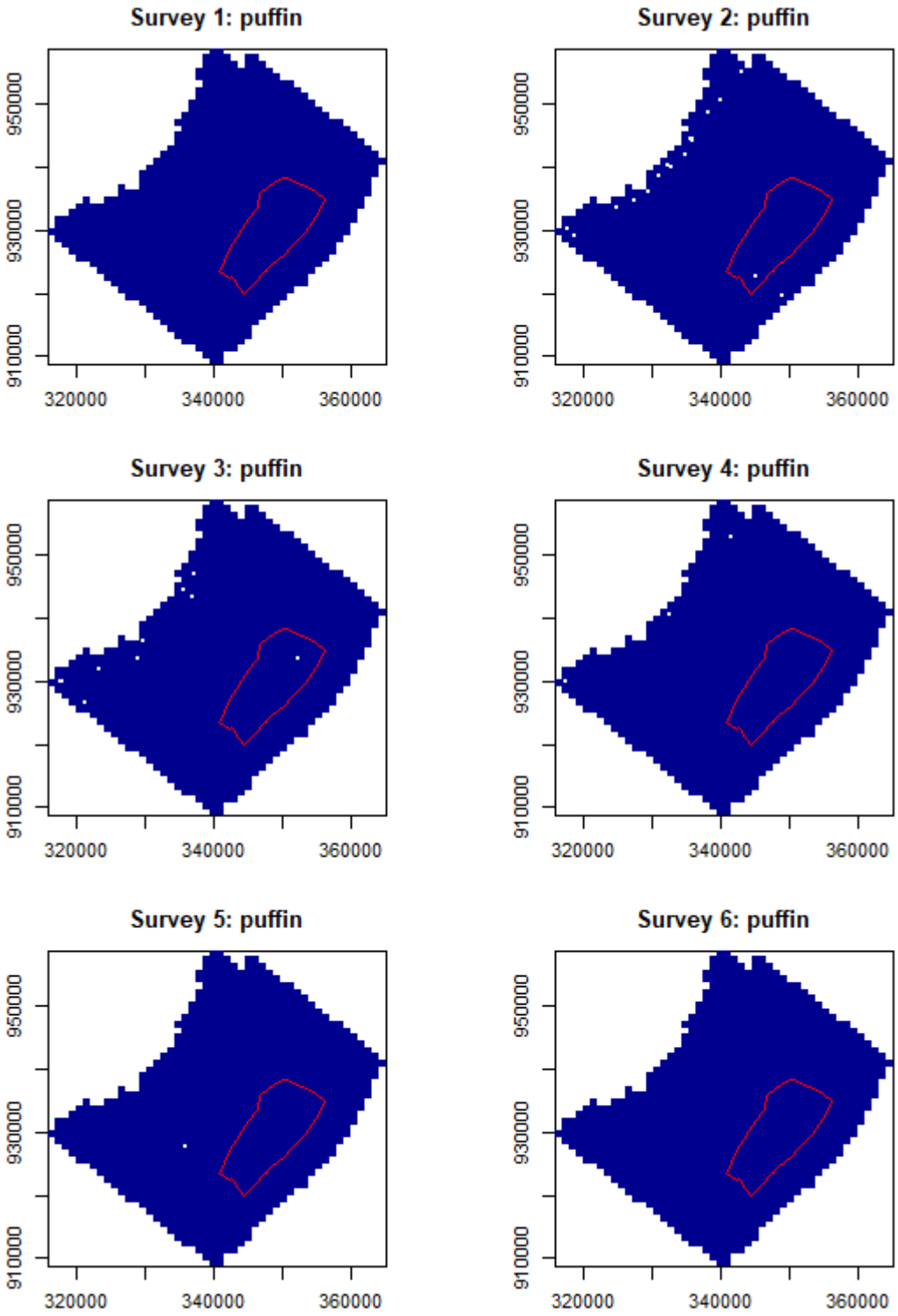

Figure B11. Locations of puffin recorded in flight during 2015 surveys.

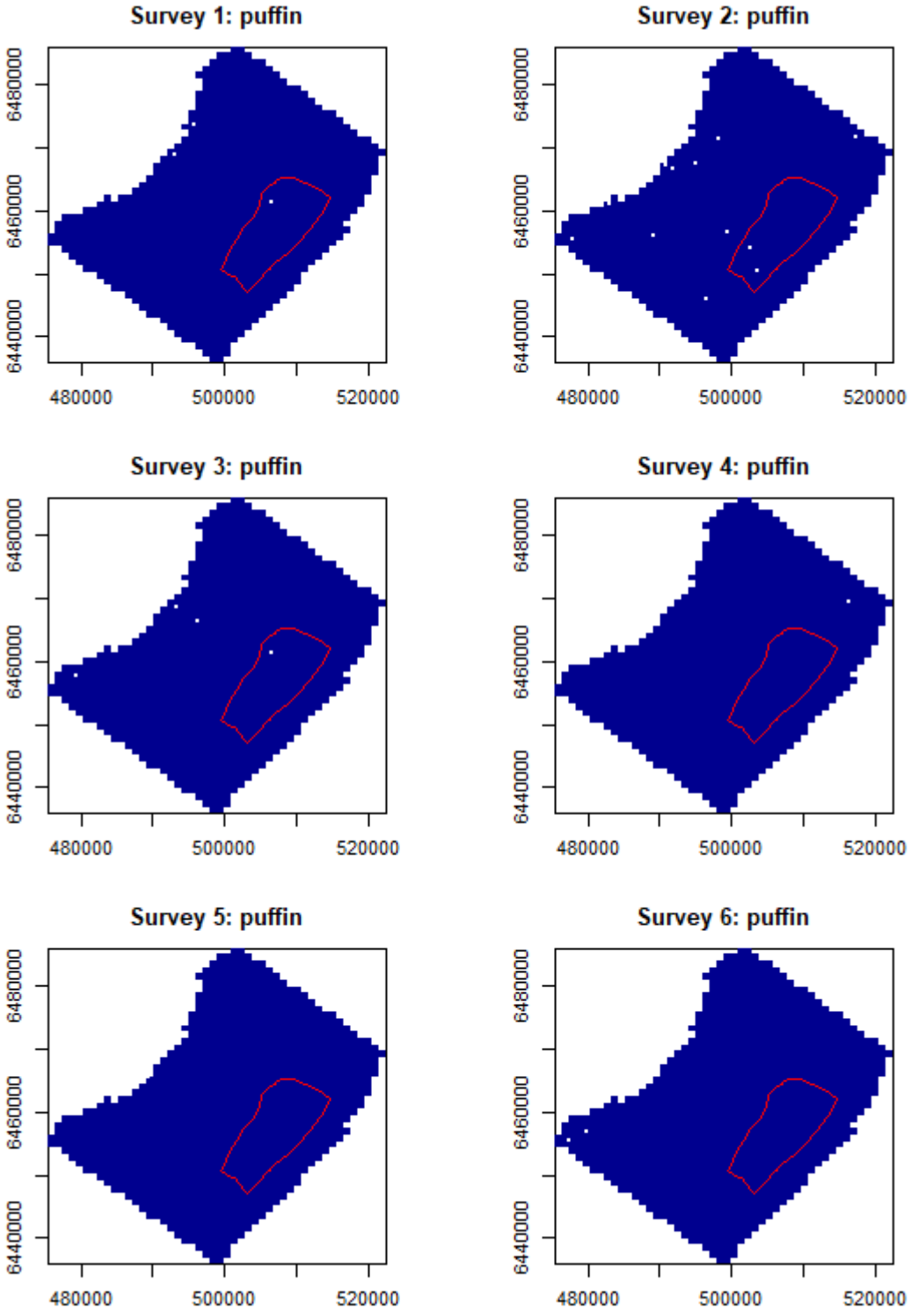

Figure B12. Locations of puffin recorded in flight during 2019 surveys.

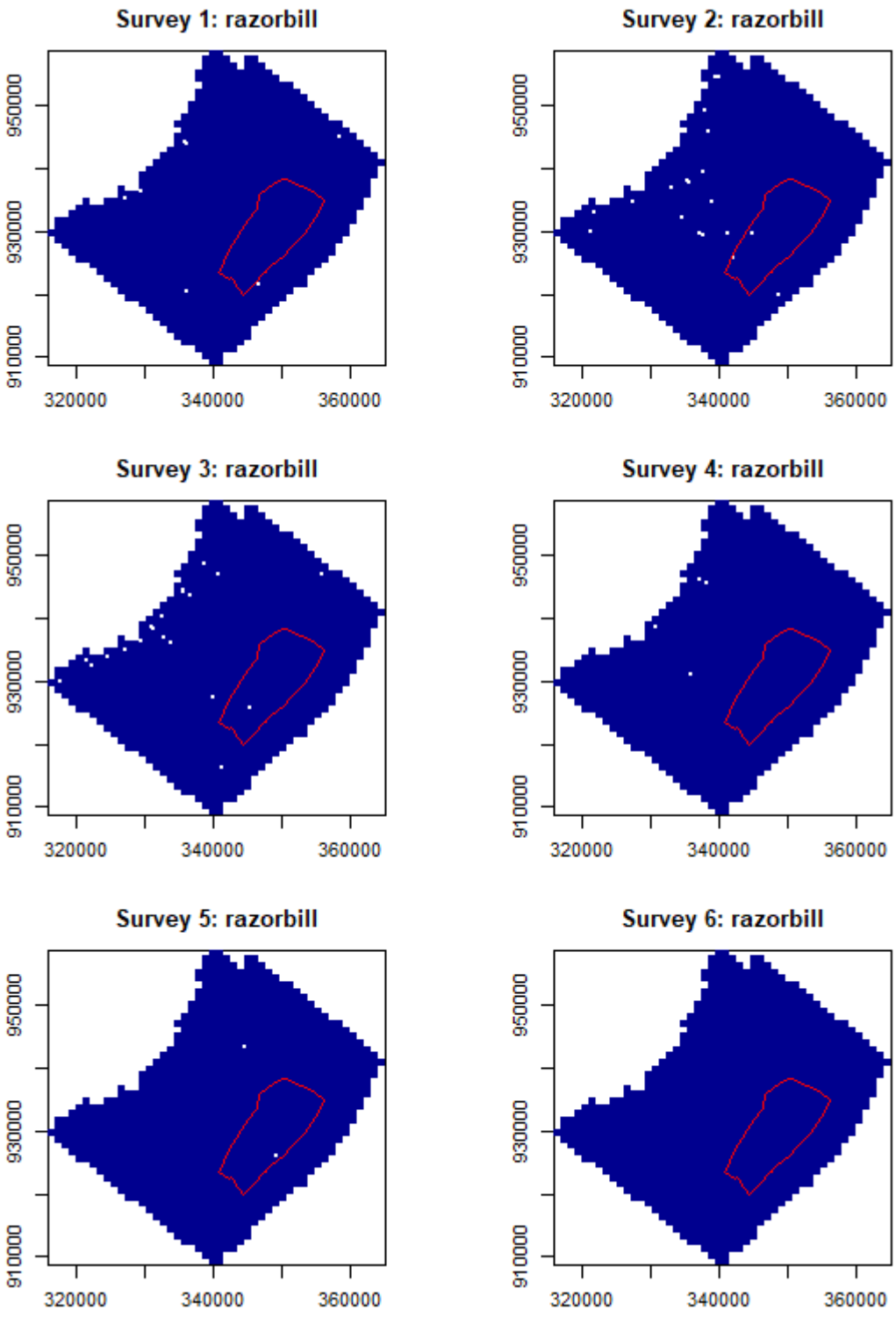

Figure B13. Locations of razorbill recorded in flight during 2015 surveys.

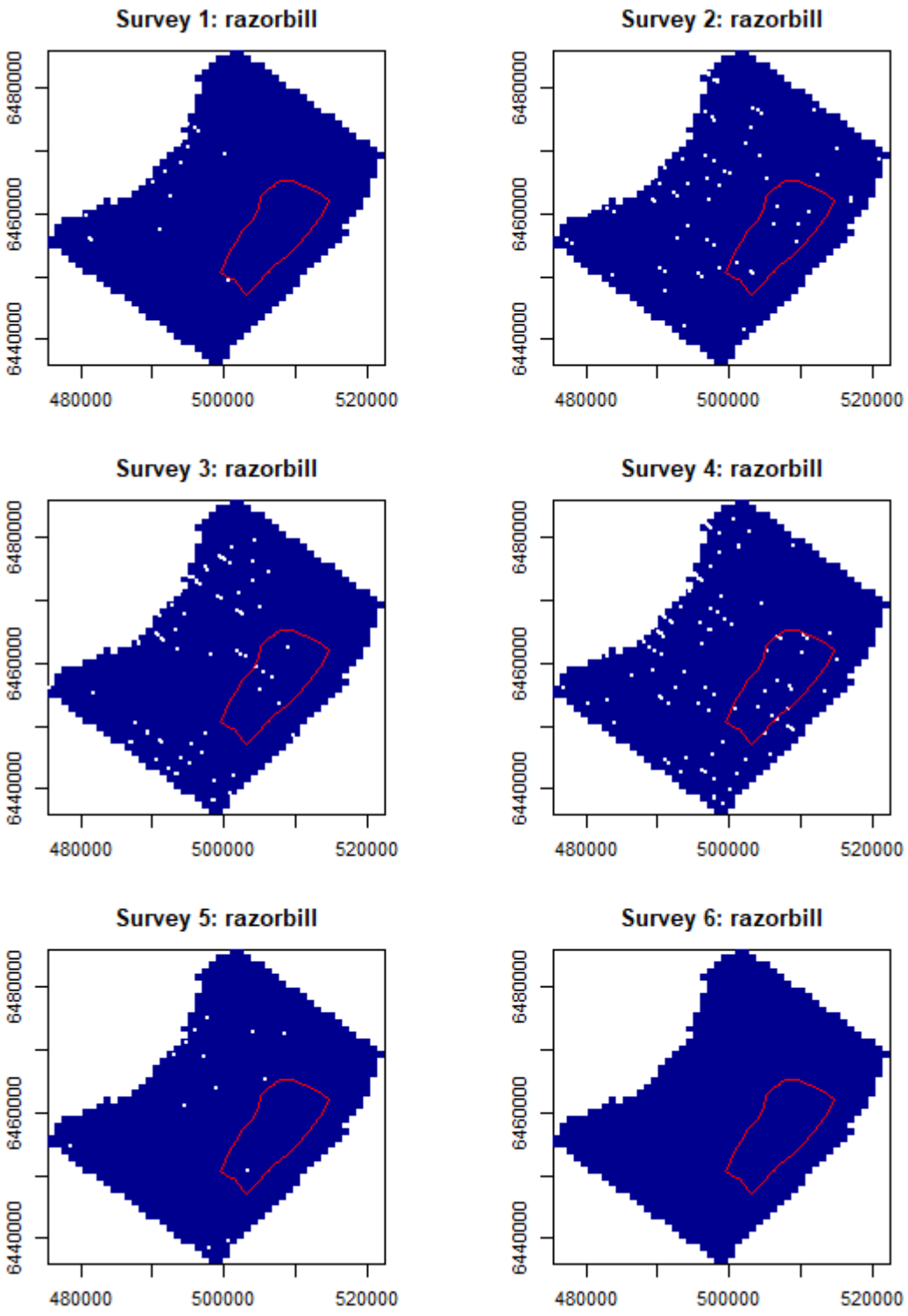

Figure B14. Locations of razorbill recorded in flight during 2019 surveys.

ANNEX C. BEFORE:AFTER MODEL PARTIAL PLOTS

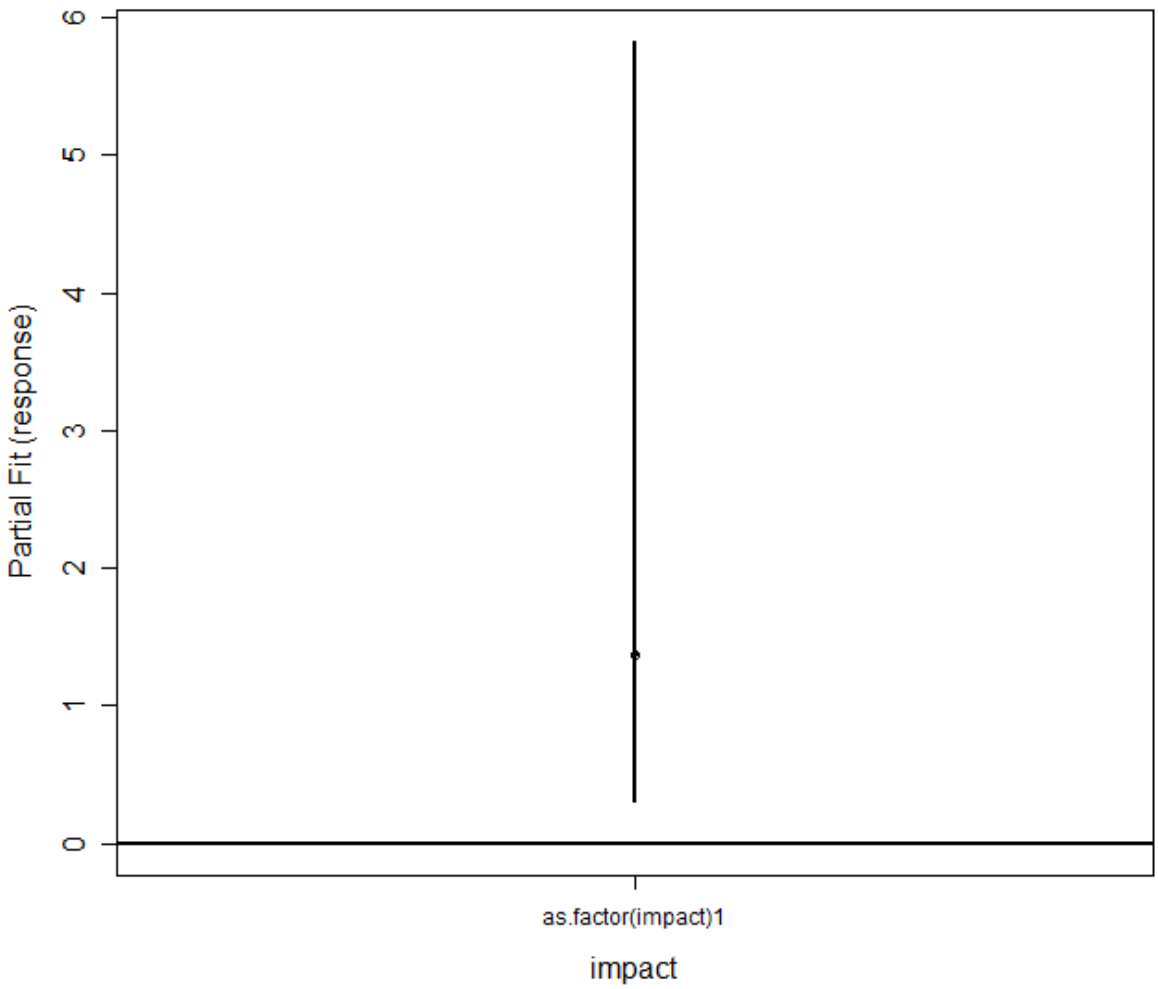

Figure C3.1 Gannet partial plot of impact

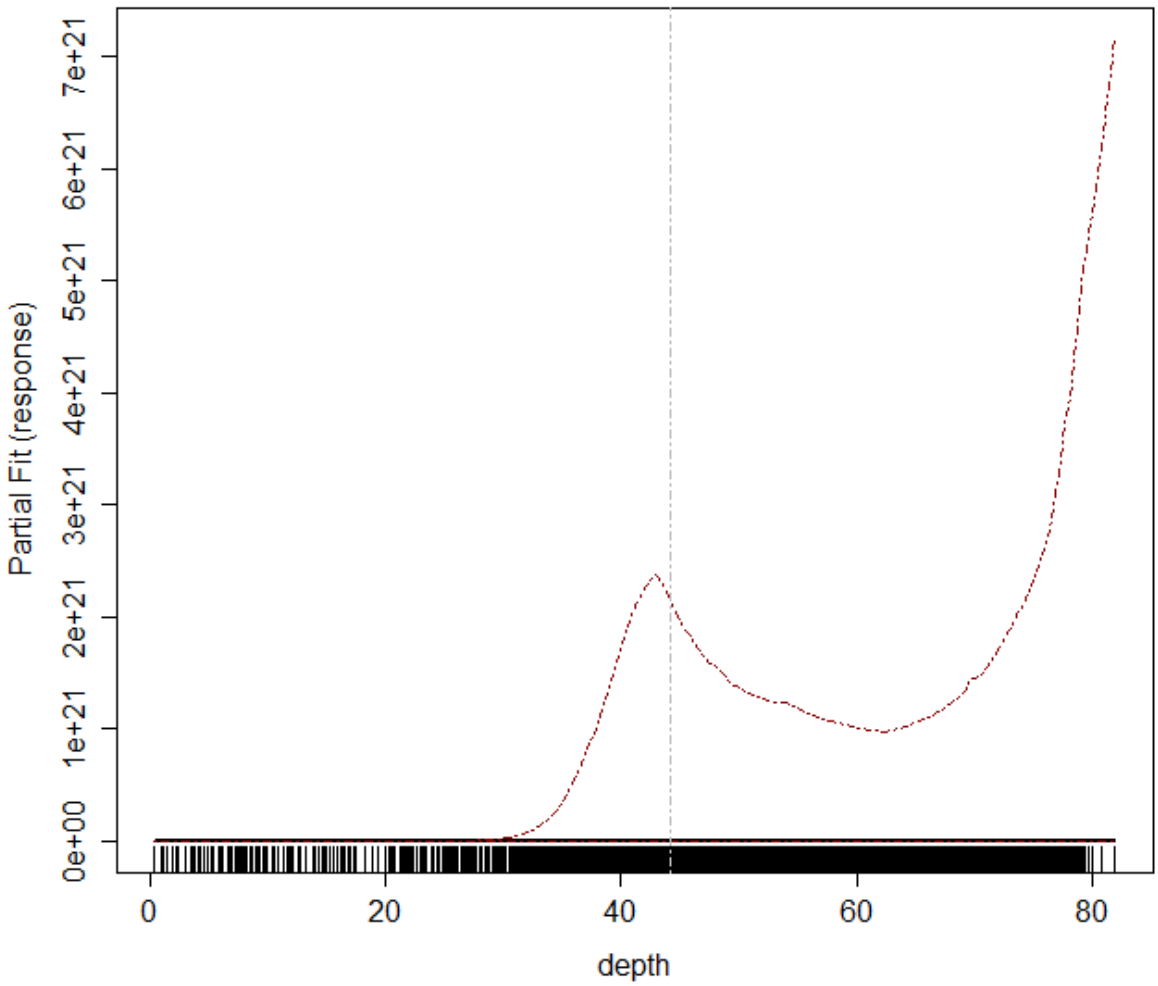

Figure C3.2 Gannet partial plot of depth

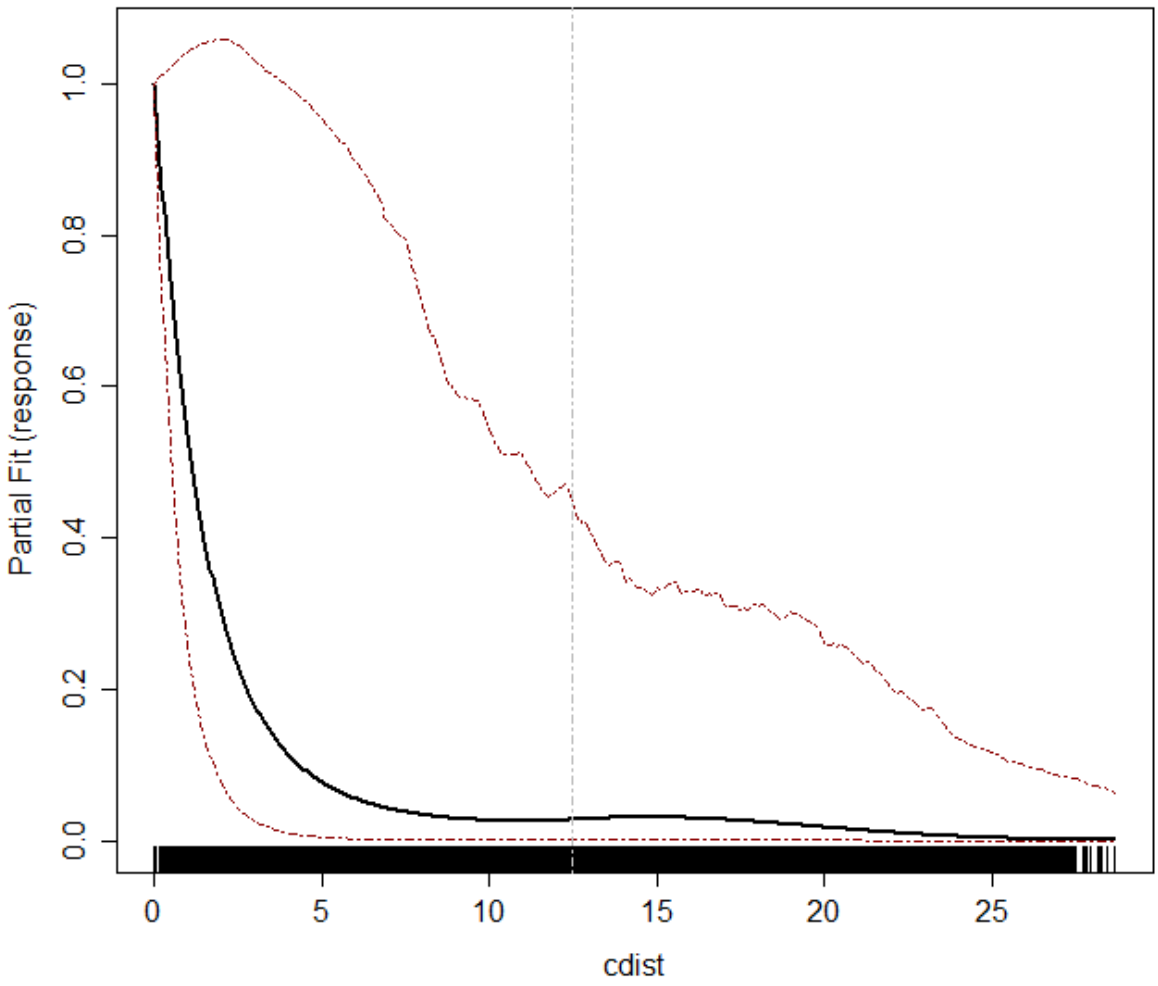

Figure C3.3. Gannet partial plot of distance to coast (cdist).

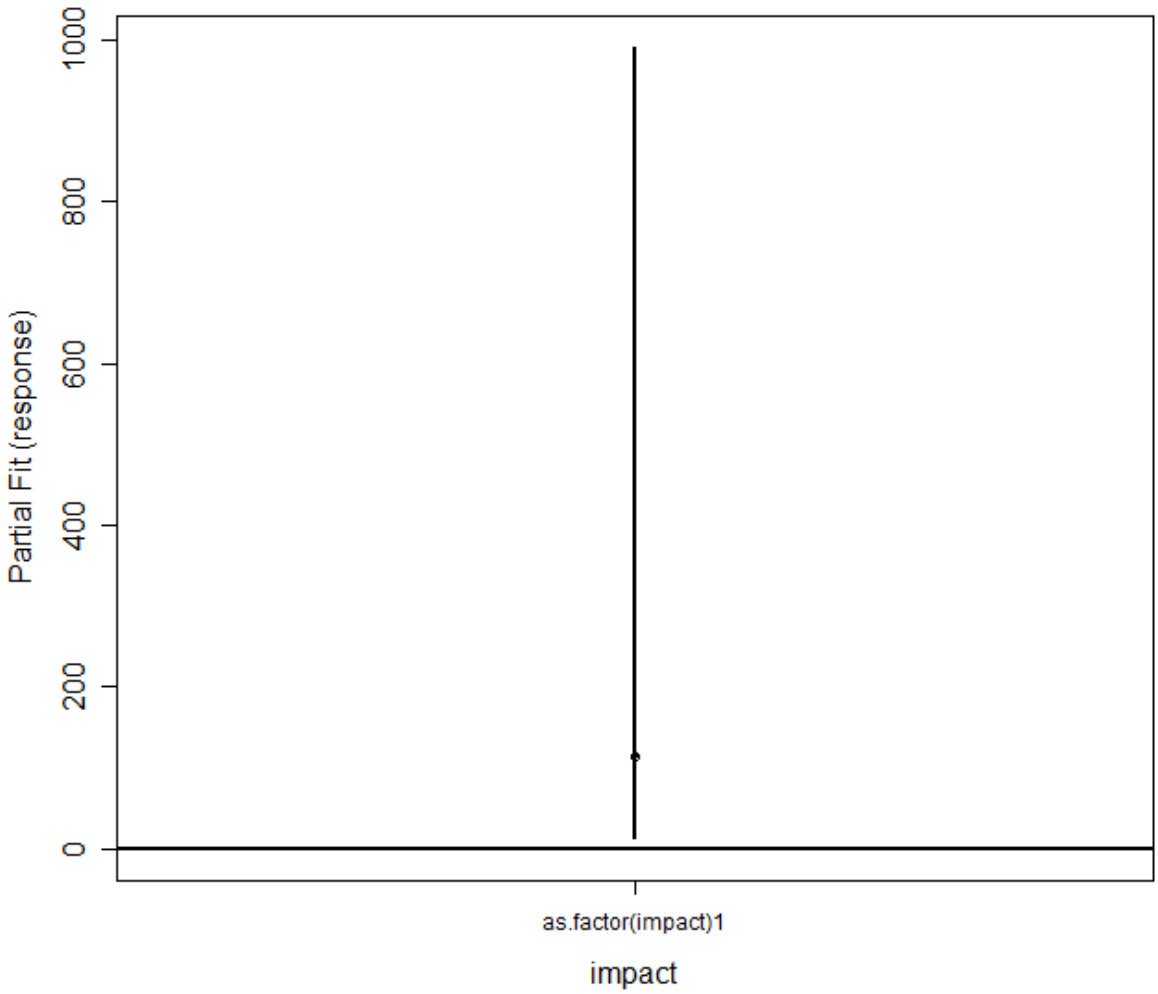

Figure C3.4. Guillemot partial plot of impact.

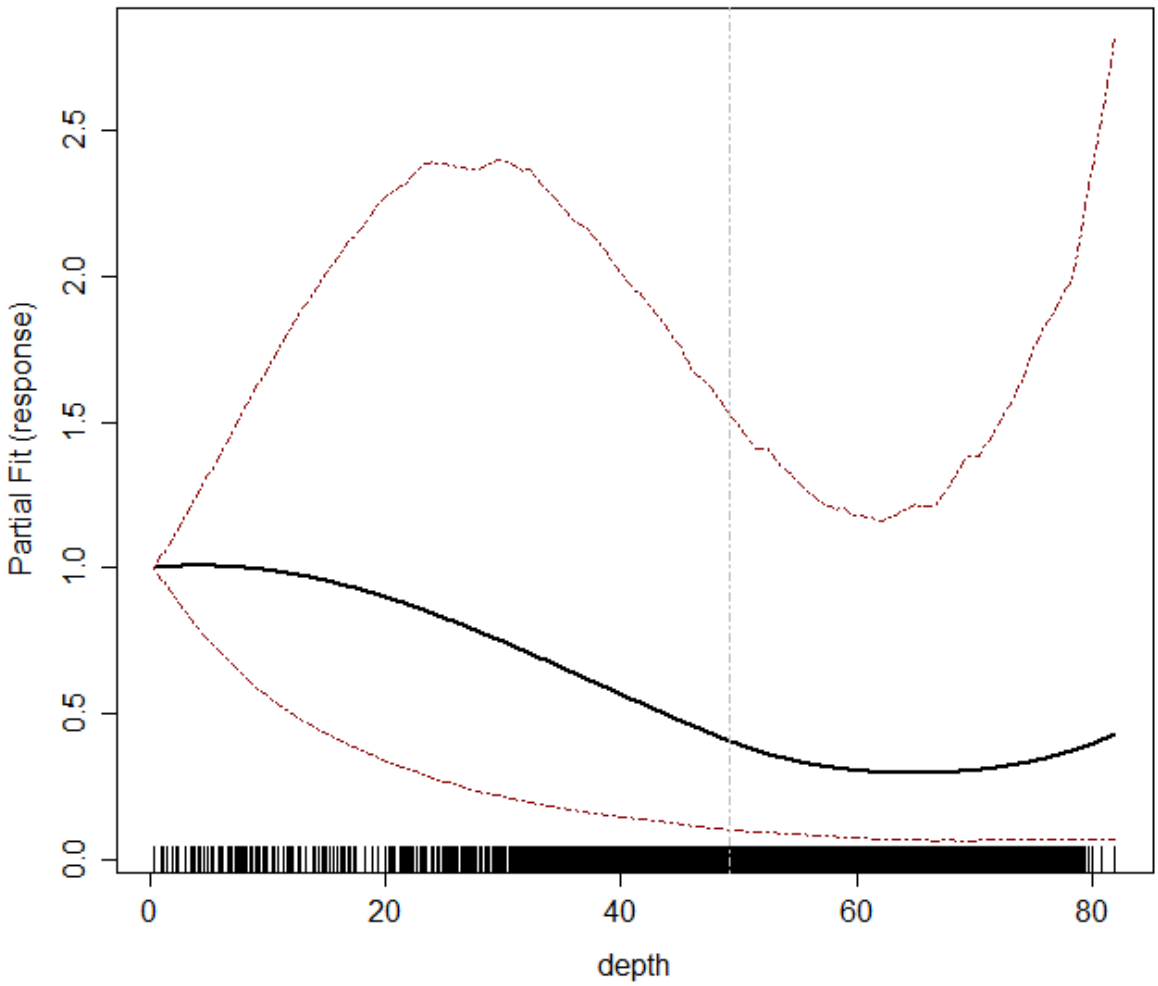

Figure C3.5. Guillemot partial plot of depth.

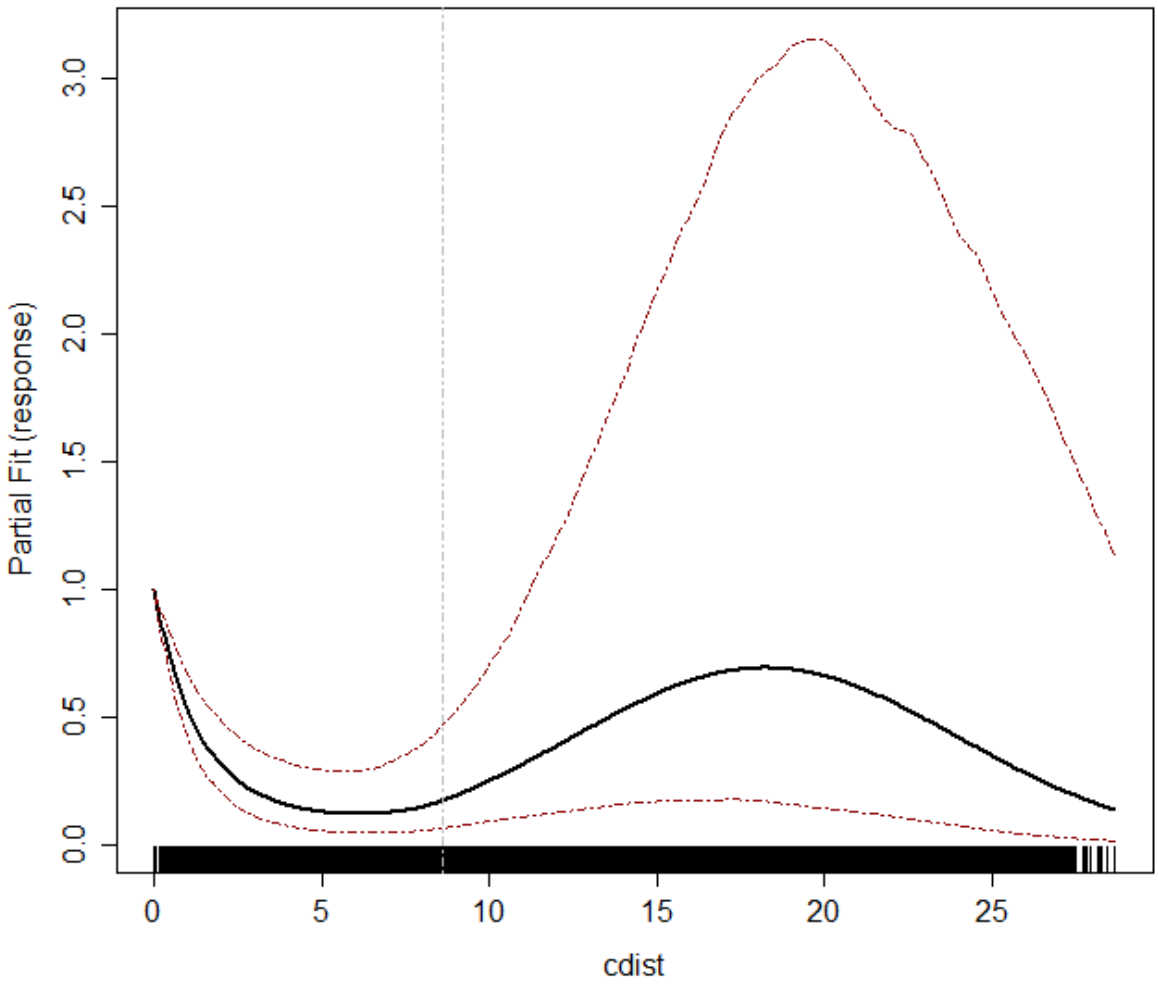

Figure C3.6. Guillemot partial plot of distance to coast (cdist).

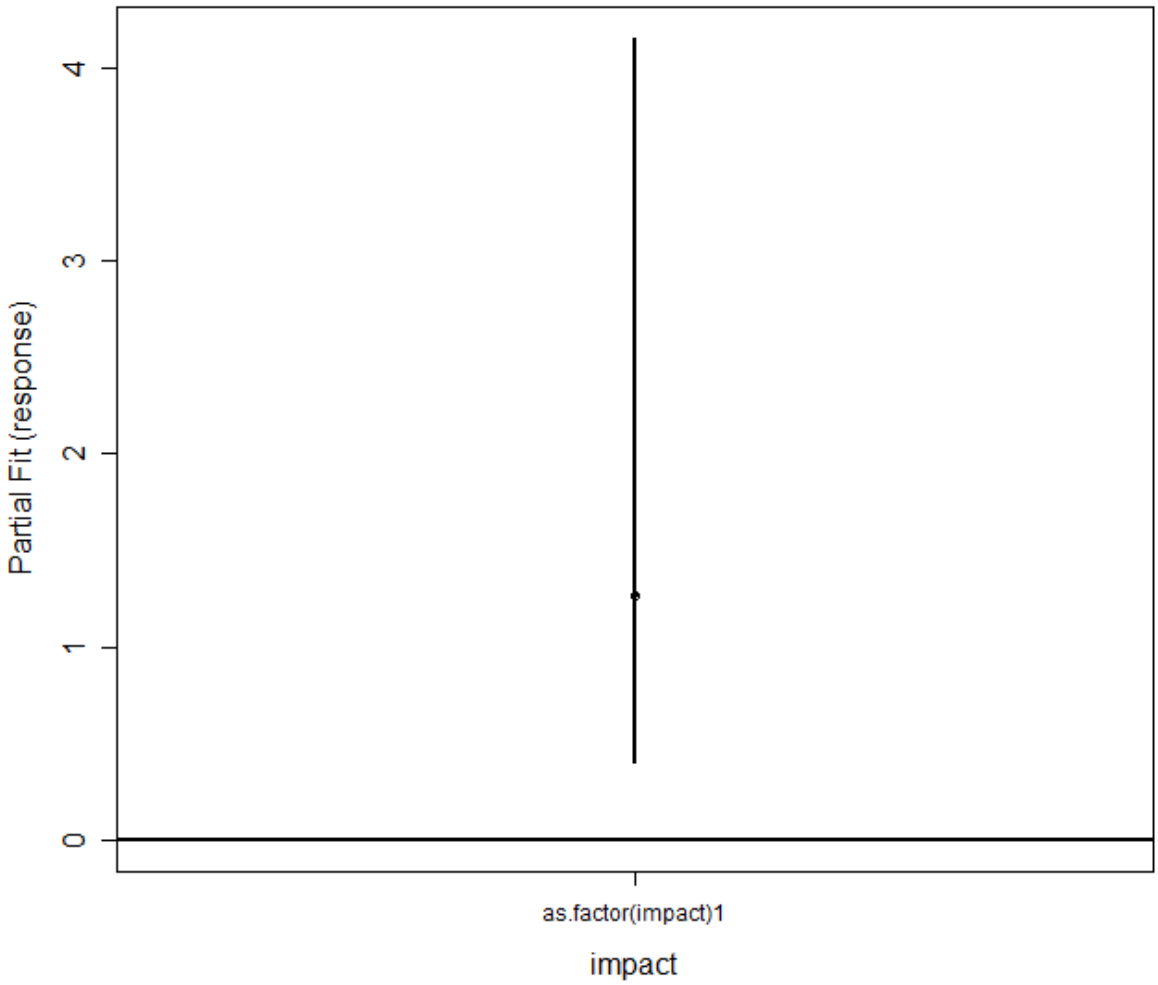

Figure C3.7 Kittiwake partial plot of impact.

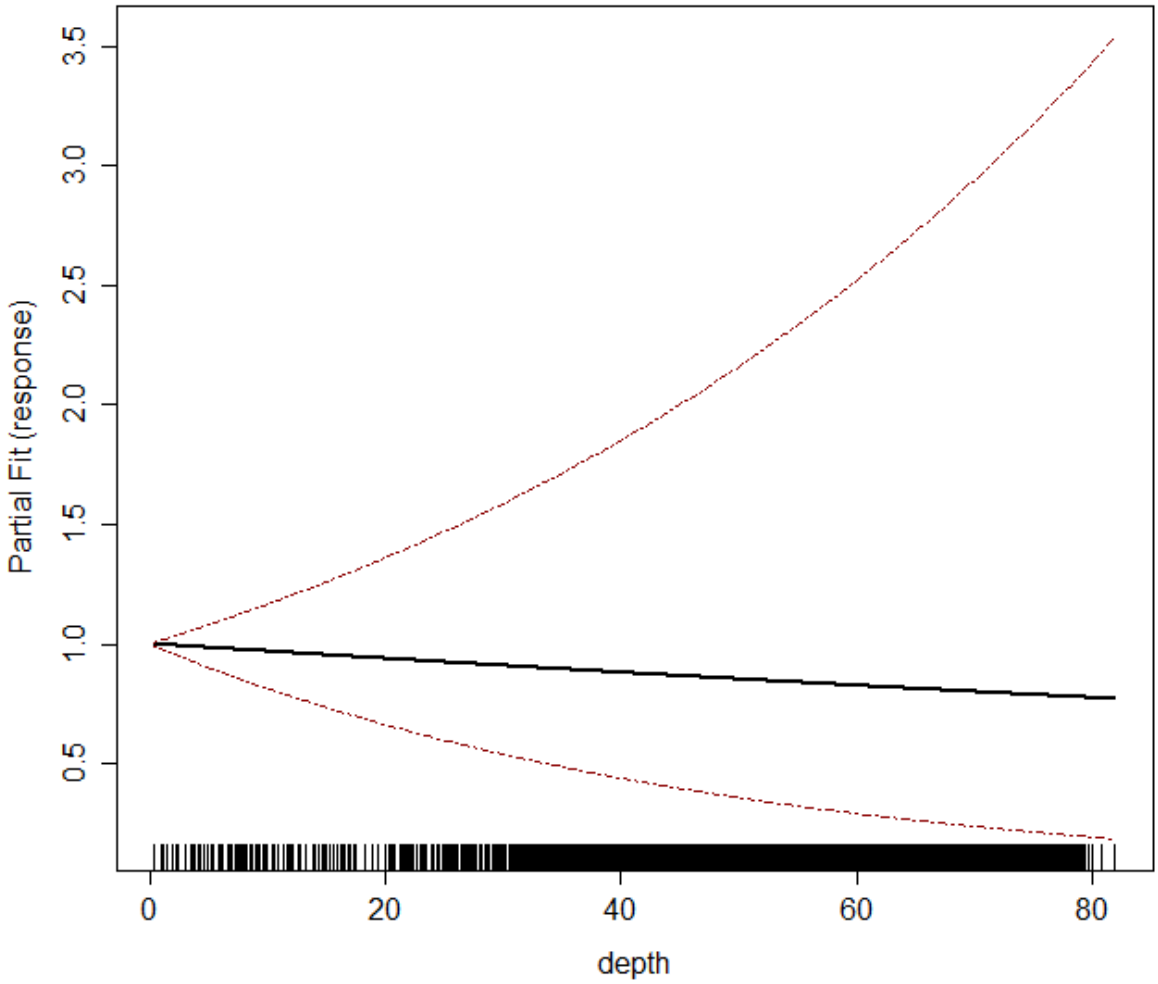

Figure C3.8. Kittiwake partial plot of depth.

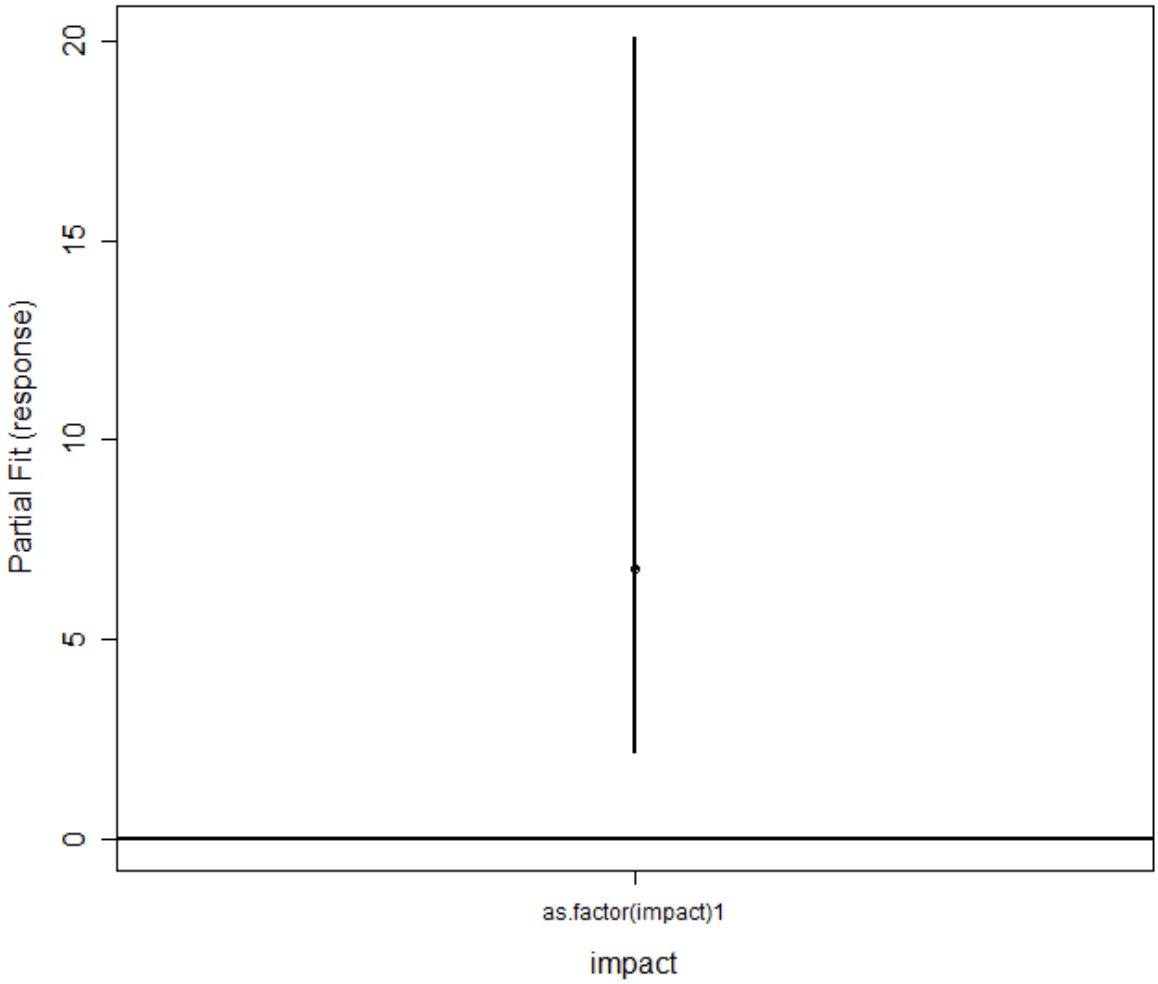

Figure C3.9. Razorbill partial plot of impact.

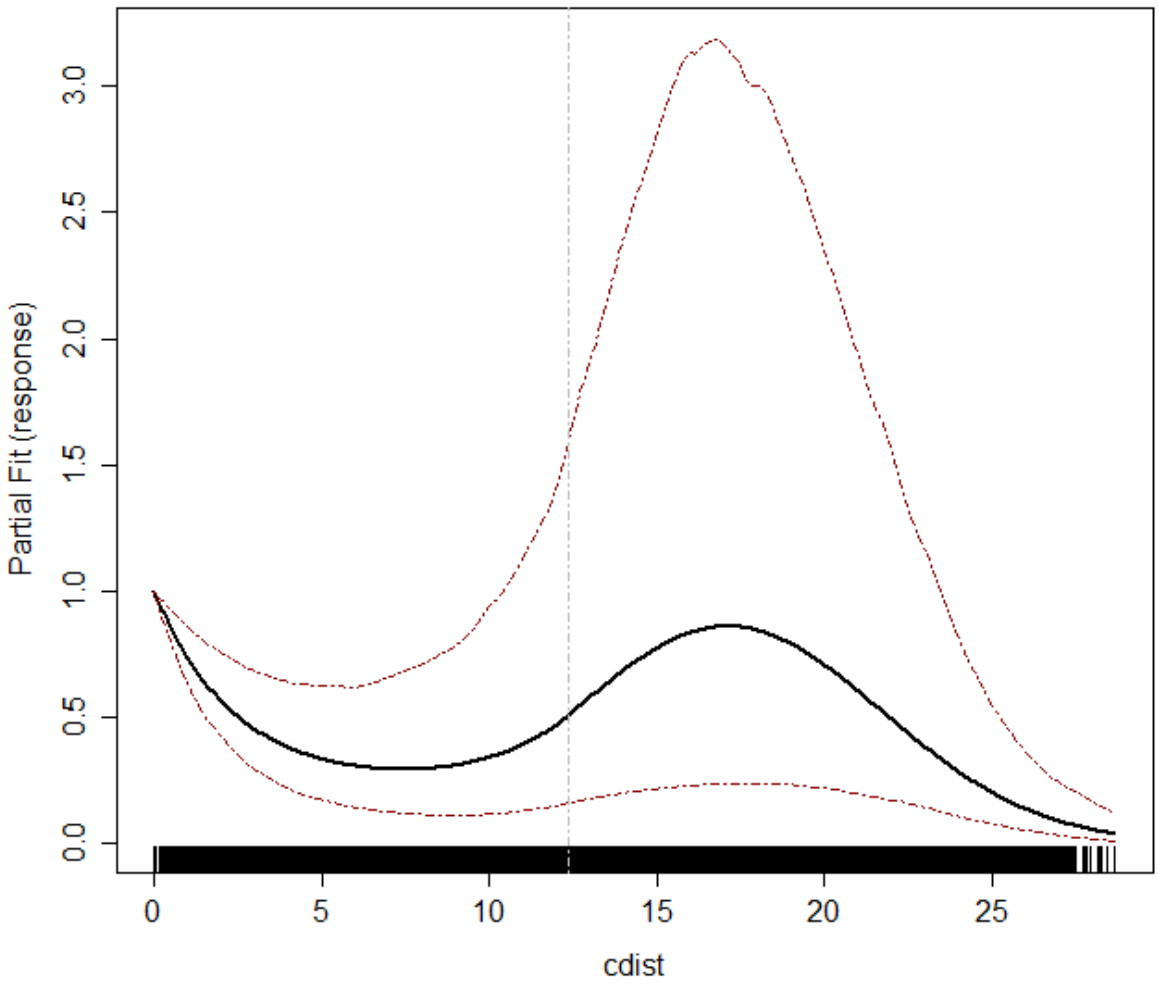

Figure C3.10. Razorbill partial plot of distance to coast (cdist).

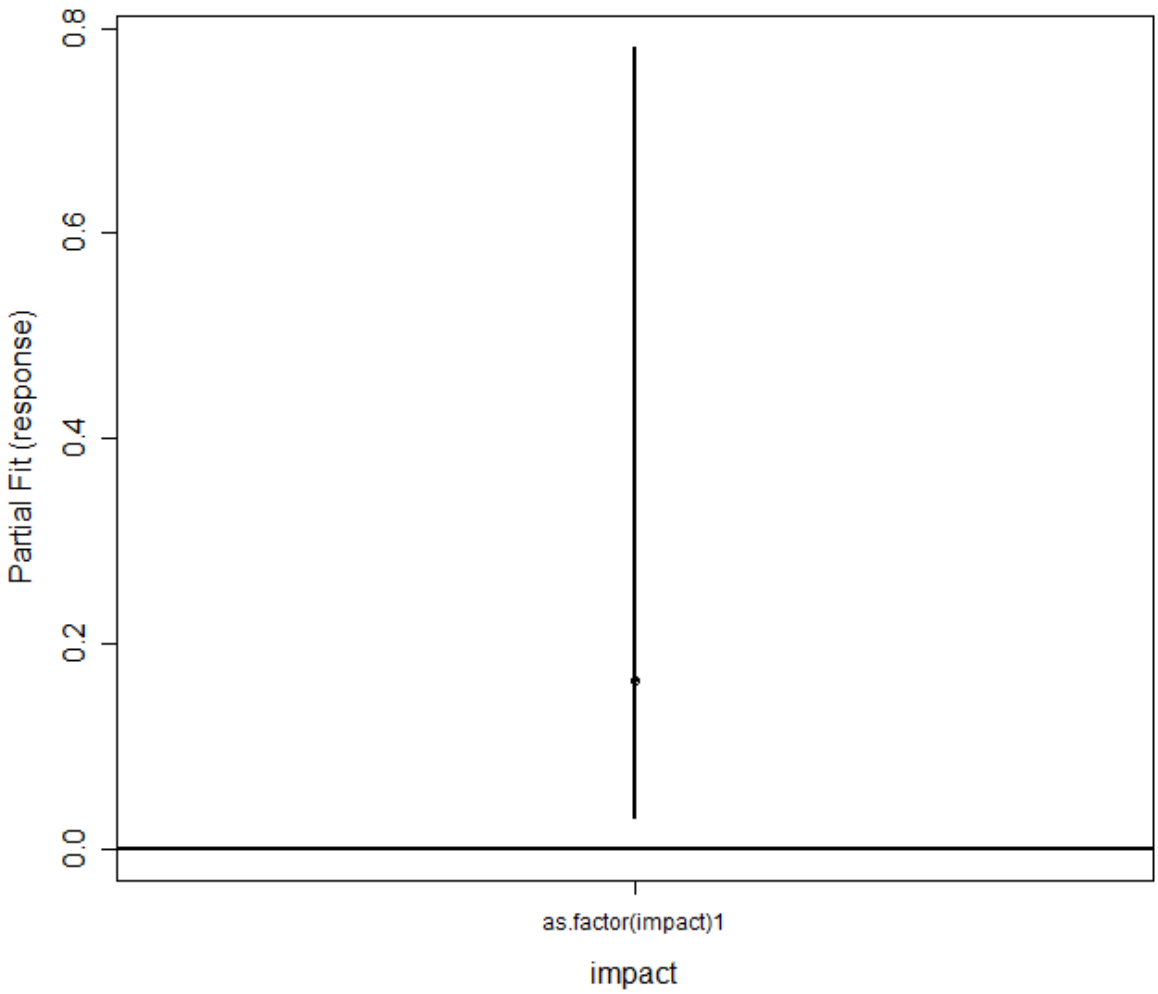

Figure C3.11 Puffin partial plot of impact.

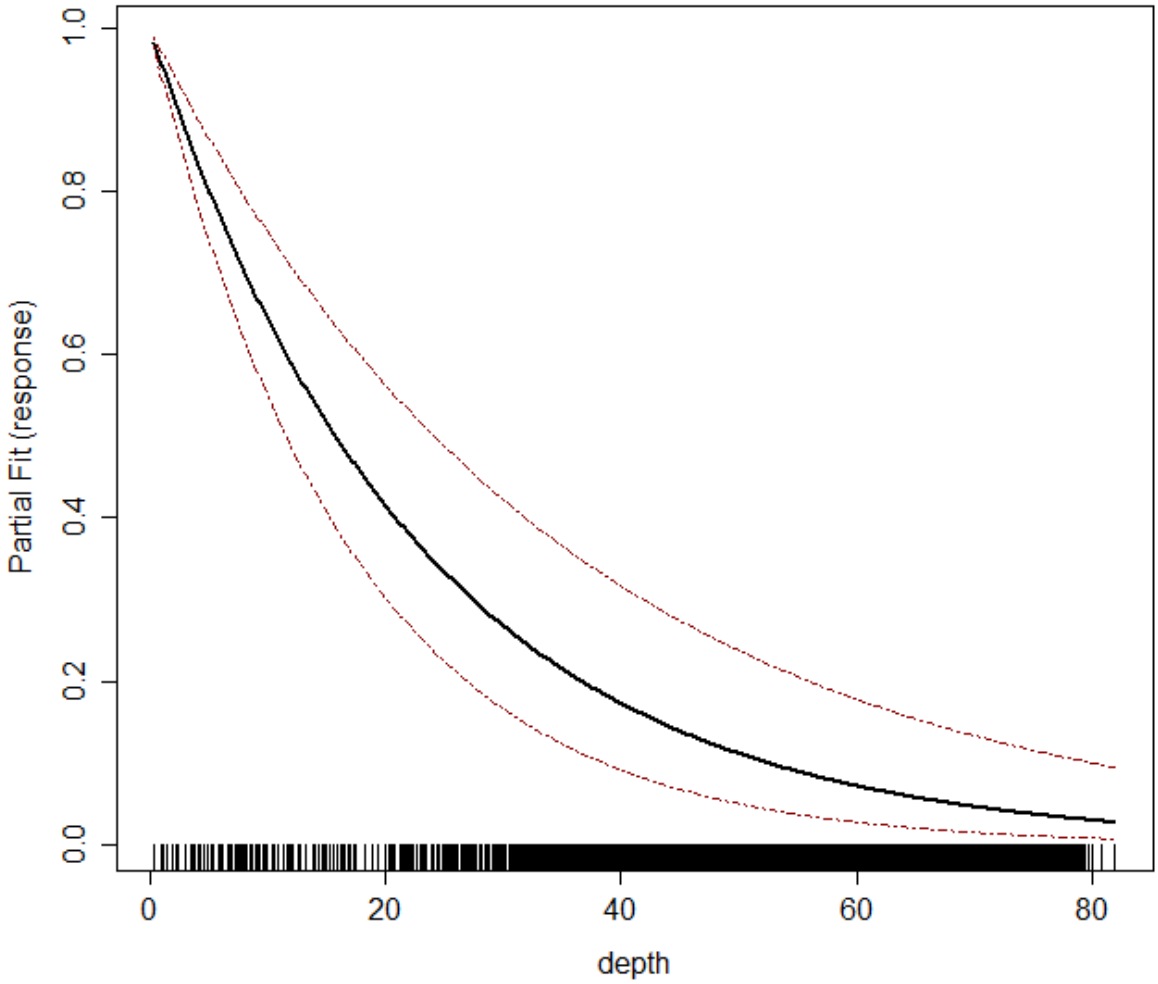

Figure C3.12. Puffin partial plot of depth.

ANNEX D. COVRATIO AND PRESS STATISTICS FOR THE BEFORE-AFTER MODELS

The MRSea function '*runInfluence*' provides two measures of the potential influence of individual blocks within the data. The covratio statistic indicates the change in the precision of the parameter estimates when each block is omitted, while the press statistic quantifies the sensitivity of the model predictions to removal of each block. Values of covratio >1 indicate inflation of model standard errors when the block is removed, and <1 indicate the opposite (reduction in standard errors). Relatively large values of the press statistic indicate the model is sensitive to the corresponding block. In both cases outputs are provided with 95% confidence intervals to assist identification of more influential blocks. It is important to bear in mind that, as stated in the MRSea guidance, there will always be values outside the 95% confidence intervals.

For the current analysis two levels of block were considered: survey number (1-12) and a combined survey number and transect ID (12 surveys x 16 transects = 192). This permitted identification of influential surveys and the transects within those surveys which had the potential to influence the overall result obtained.

Gannet

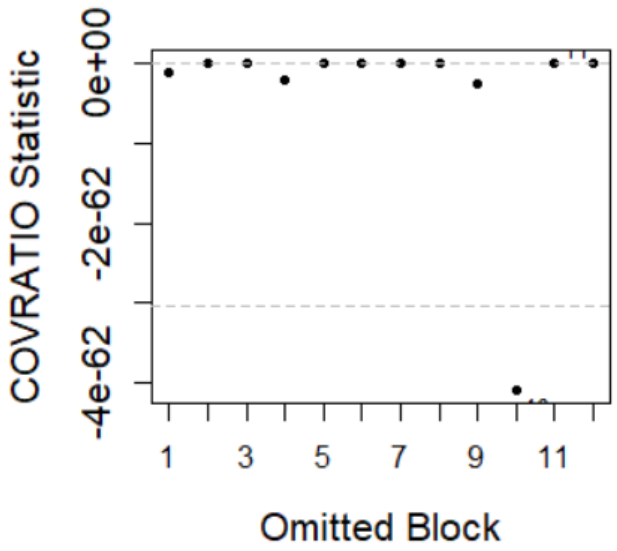

Figure D1. Gannet covratio plot at the level of survey.

Inclusion of survey 10 (survey 4 in 2019) in the results appeared to result in inflation of the standard errors (i.e. making detection of a significant impact less likely). This indicates the before-after impact result was precautionary.

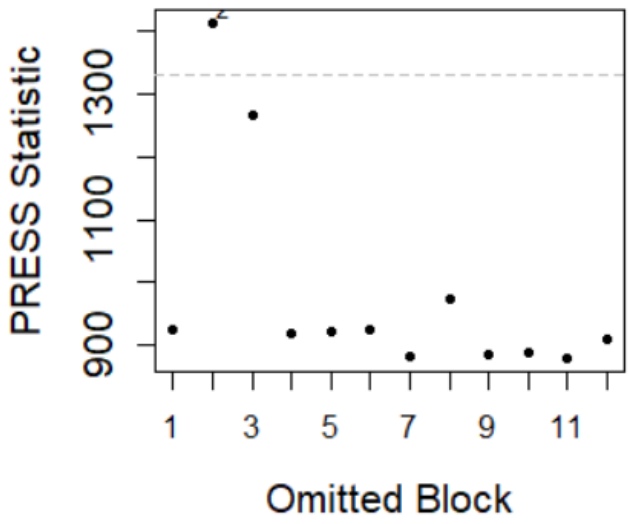

Figure D2. Gannet press plot at the level of survey.

Survey 2 (survey 2 in 2015) had a large press value indicating that the overall result was most sensitive to the data recorded on this survey. However, as this was a survey with a hotspot recorded within the wind farm, this is not an unexpected outcome.

Consideration of the influence of transects within surveys (plots not shown) found that individual transects on surveys 1, 2 and 3 in 2015 and 3, 4, 5 and 6 in 2019 gave covratio and press values outside the 95% range. The distribution of outliers among multiple surveys in both years is therefore considered to be an indication of the varied distributions recorded rather than a systematic problem in the data.

Guilllemot

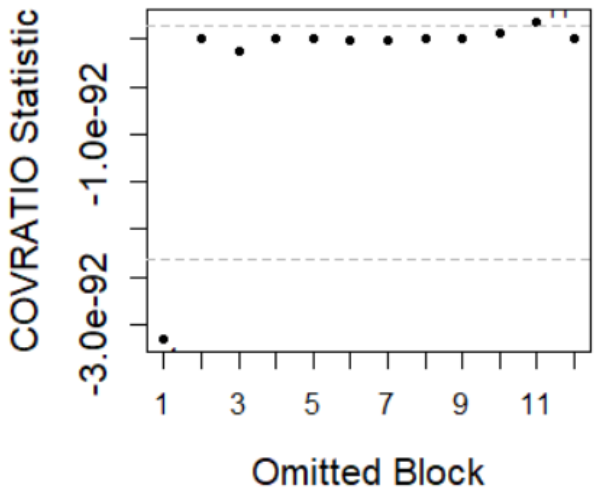

Figure D3. Guillemot covratio plot at the level of survey.

Inclusion of survey 1 (survey 1 in 2015) in the results appeared to result in inflation of the standard errors (i.e. making detection of a significant impact less likely), while survey 11 (survey 5 in 2019) was slightly above the 95% interval (i.e. slightly reducing standard errors). On balance, given the relative position of these outliers it appears that the before-after impact result was precautionary.

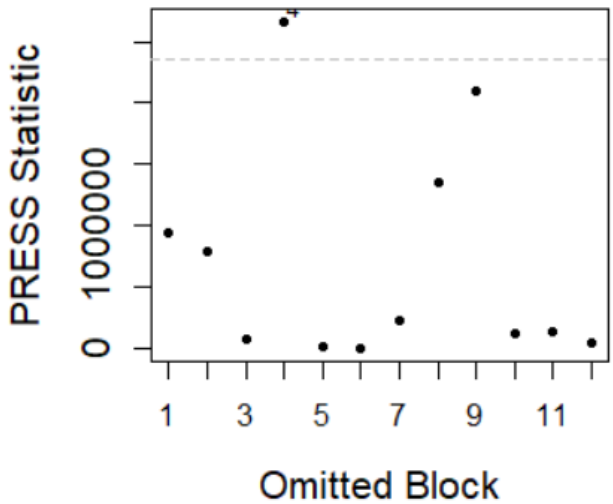

Figure D4. Guillemot press plot at the level of survey.

Survey 4 (survey 4 in 2015) had a large press value indicating that the overall result was most sensitive to the data recorded on this survey. However, this value is not far beyond the range of the other values and is not considered of concern.

Consideration of the influence of transects within surveys (plots not shown) found that individual transects on surveys 1 , 2 and 4 in 2015 and 3, 4 and 5 in 2019 gave covratio and press values outside the 95% range. The distribution of outliers among multiple surveys in both years is therefore considered to be an indication of the varied distributions recorded rather than a systematic problem in the data.

Kittiwake

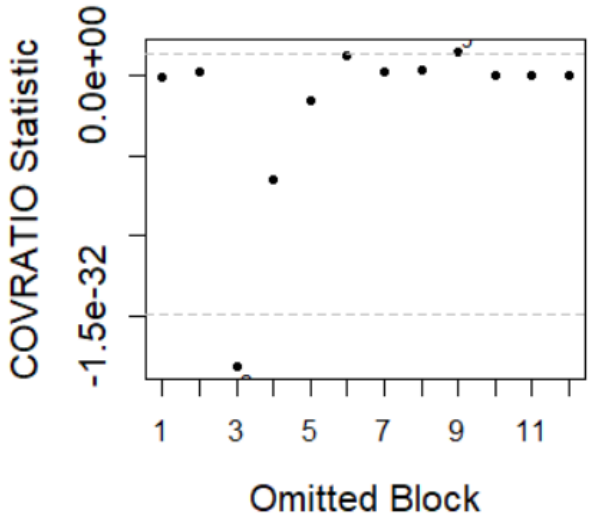

Figure D5. Kittiwake covratio plot at the level of survey.

Inclusion of survey 3 (survey 3 in 2015) in the results appeared to result in inflation of the standard errors (i.e. making detection of a significant impact less likely), while survey 9 (survey 3 in 2019) was slightly above the 95% interval (i.e. slightly reducing standard errors). On balance, given the relative position of these outliers it appears that the before-after impact result was little affected by these data.

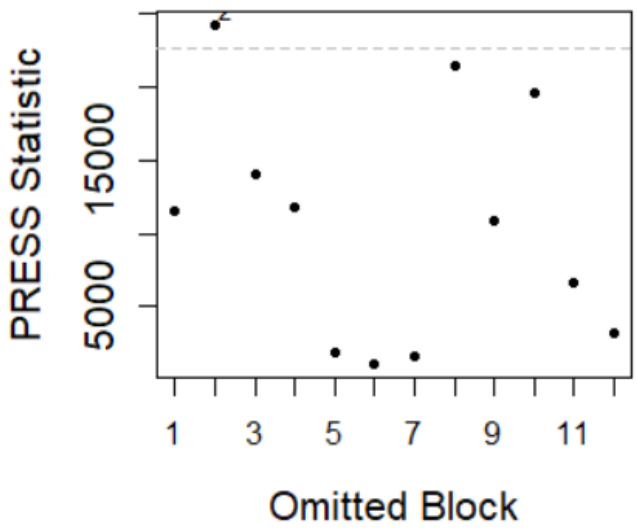

Figure D6. Kittiwake press plot at the level of survey.

Survey 2 (survey 2 in 2015) had a large press value indicating that the overall result was most sensitive to the data recorded on this survey. However, this value is not far beyond the range of the other values and is not considered of concern.

Consideration of the influence of transects within surveys (plots not shown) found that individual transects on surveys 1, 2, 3, 4 and 5 in 2015 and 2, 3, 4 and 5 in 2019 gave covratio and press values outside the 95% range. The distribution of outliers among multiple surveys in both years is therefore considered to be an indication of the varied distributions recorded rather than a systematic problem in the data.

Razorbill

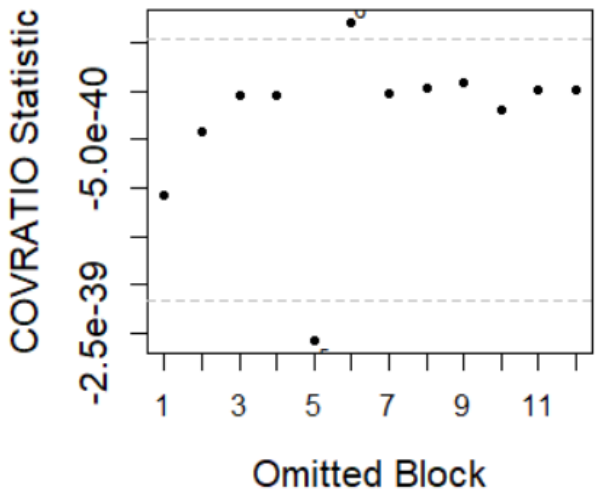

Figure D7. Razorbill covratio plot at the level of survey.

Inclusion of survey 5 (survey 5 in 2015) in the results appeared to result in inflation of the standard errors (i.e. making detection of a significant impact less likely), while survey 6 (survey 6 in 2015) was slightly above the 95% interval (i.e. slightly reducing standard errors). On balance, given the relative position of these outliers it appears that the before-after impact result was precautionary.

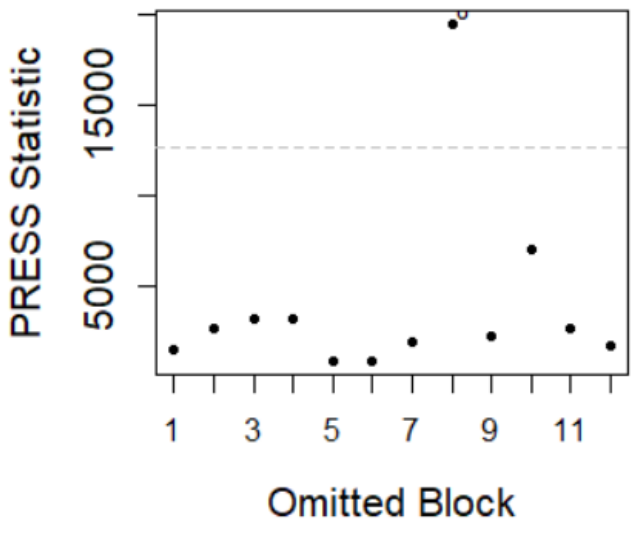

Figure D8. Razorbill press plot at the level of survey.

Survey 8 (survey 2 in 2019) had a large press value indicating that the overall result was most sensitive to the data recorded on this survey. However, this value is not far beyond the range of the other values and is not considered of concern.

Consideration of the influence of transects within surveys (plots not shown) found that individual transects on surveys 2, 3 and 4 in 2015 and 2, 4 and 5 in 2019 gave covratio and press values outside the 95% range. The distribution of outliers among multiple surveys in both years is therefore considered to be an indication of the varied distributions recorded rather than a systematic problem in the data.

Puffin

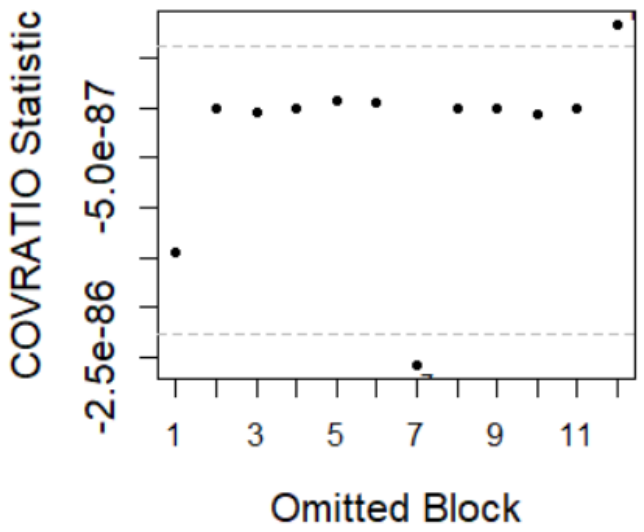

Figure D9. Puffin covratio plot at the level of survey.

Inclusion of survey 7 (survey 1 in 2019) in the results appeared to result in inflation of the standard errors (i.e. making detection of a significant impact less likely), while survey 12 (survey 6 in 2019) was slightly above the 95% interval (i.e. slightly reducing standard errors). On balance, given the relative position of these outliers it appears that the before-after impact result was precautionary.

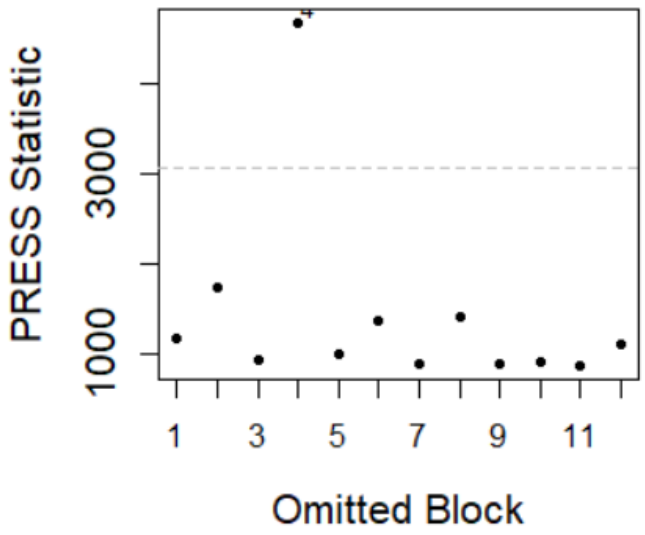

Figure D10. Puffin press plot at the level of survey.

Survey 4 (survey 4 in 2015) had a large press value indicating that the overall result was most sensitive to the data recorded on this survey. However, this value is not far beyond the range of the other values and is not considered of concern.

Consideration of the influence of transects within surveys (plots not shown) found that individual transects on surveys 1, 2, 4 and 6 in 2015 and 2 and 6 in 2019 gave covratio and press values outside the 95% range. The distribution of outliers among multiple surveys in both years is therefore considered to be an indication of the varied distributions recorded rather than a systematic problem in the data.

ANNEX E. LOCATIONS OF CONSTRUCTION ACTIVITY IN MORAY EAST DURING SURVEY PERIOD

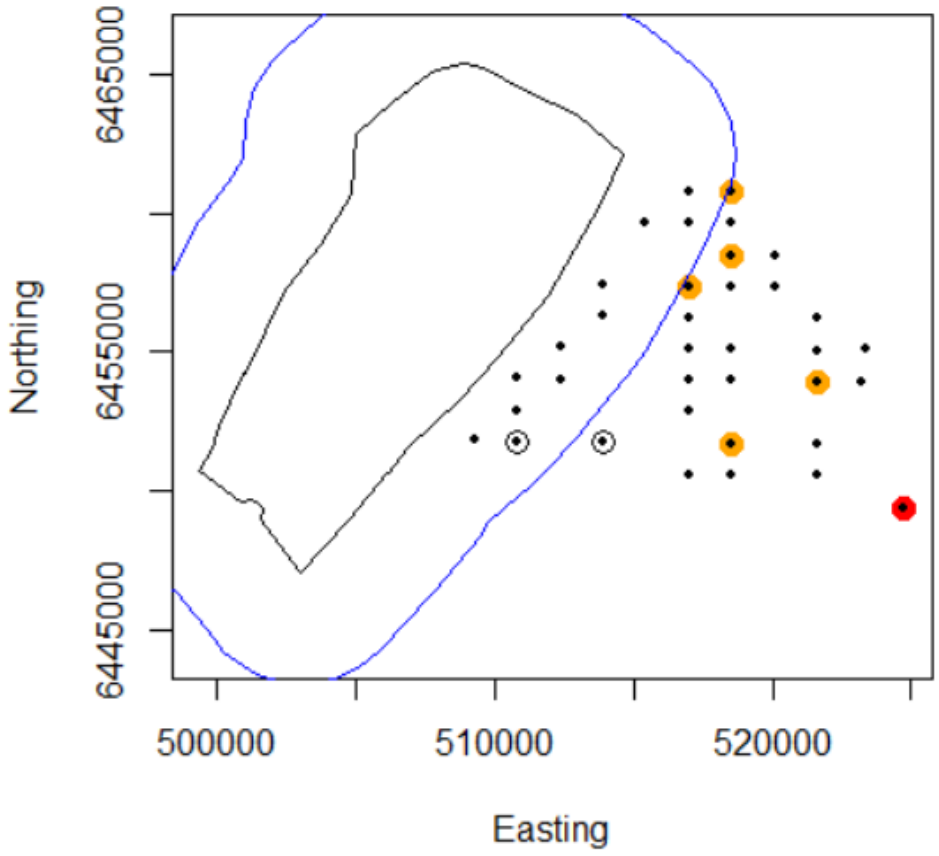

Figure D1. Locations of construction activity at the Moray East Wind Farm during the period of the 2019 surveys (May 28th to July 25th, inclusive). The Beatrice Wind Farm (black line) and 4km buffer (blue line) are indicated. Black dots are locations that piling took place within the overall period, orange circles indicate location that piling occurred on the day *prior* to a survey and the red circle indicates a location where piling occurred on the same day as a survey (survey 6, 25th July). The two dots with black circles indicate locations where jackets were installed (on the 5th and 11th July, between surveys 4 and 5 on the 29th June and 19th July respectively).

ANNEX F. TURBINE AVOIDANCE PLOTS IN RELATION TO RPM

To check whether the turbine avoidance results for presented in section 3.6 were influenced by turbine RPM the analysis was run on data subsets grouped using the average RPM for each turbine recorded during the surveys. Each bird record had the average RPM (recorded during the survey) of the closest turbine appended to it.

Histograms for each species (guillemot, puffin, razorbill, kittiwake and herring gull) analysed for each RPM range (0-2, 2-4, 4-6, 6-8, 8+) are provided below, grouped by RPM. The results are summarised in section 3.6.

On each figure the vertical red line is the observed density within the relevant distance to turbines and the bars are the results of reanalysis of 1,000 re-runs of the analysis with randomised turbine positions (all turbines together to maintain their relative positions). If the red line is in the middle of the bar graph this indicates no difference in the distribution compared with that expected by chance. If the red line is to the left of the peak on the bar graph this indicates lower densities than expected by chance (consistent with avoidance), and if it is to the right this indicates higher densities than expected by chance (consistent with attraction).

RPM 0 - 2

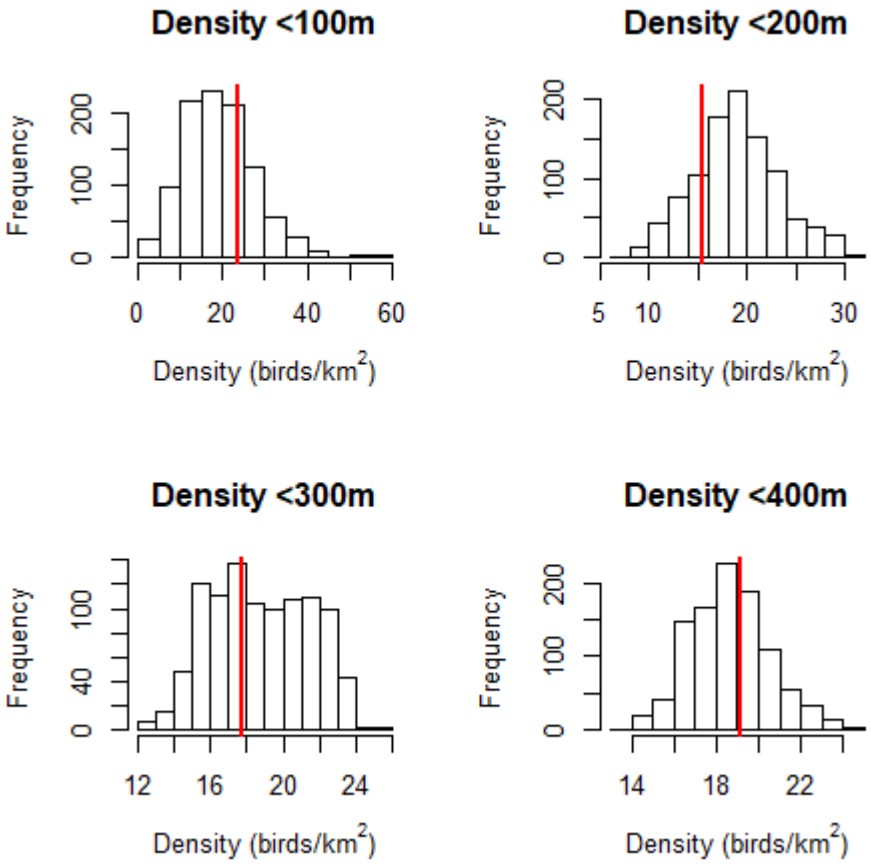

Figure F1. Guillemot densities within 100/200/300/400m of turbine locations (red lines) and distribution of densities estimated for 1,000 simulations with randomly re-positioned turbines (relative turbine positions maintained) at RPM <2.

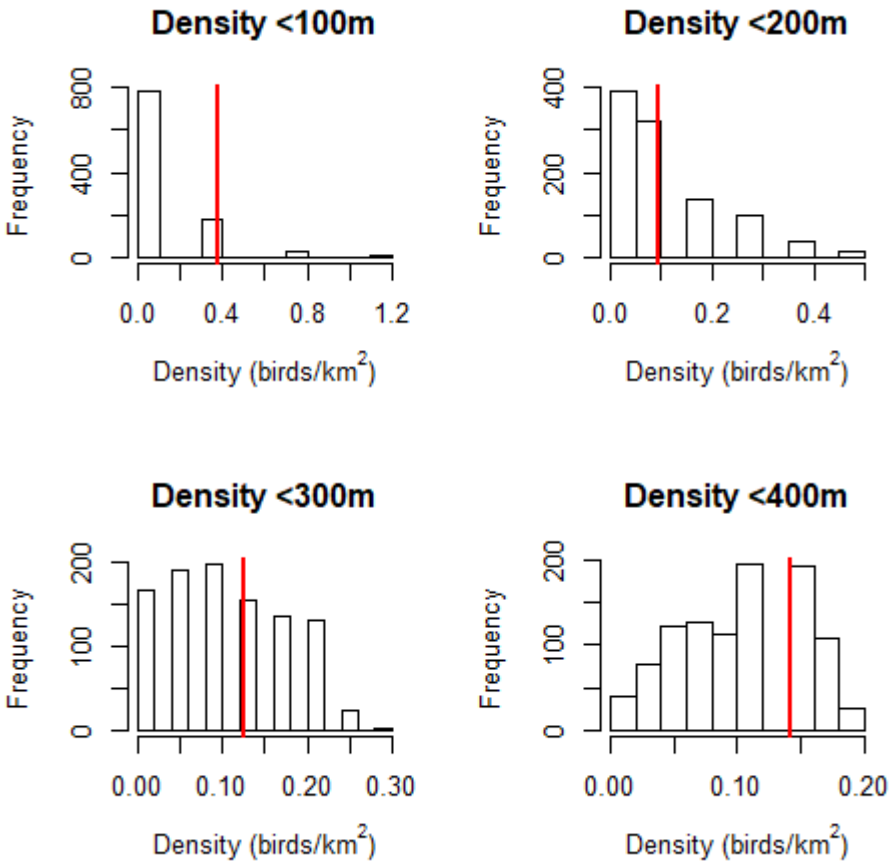

Figure F2. Puffin densities within 100/200/300/400m of turbine locations (red lines) and distribution of densities estimated for 1,000 simulations with randomly re-positioned turbines (relative turbine positions maintained) at RPM <2.

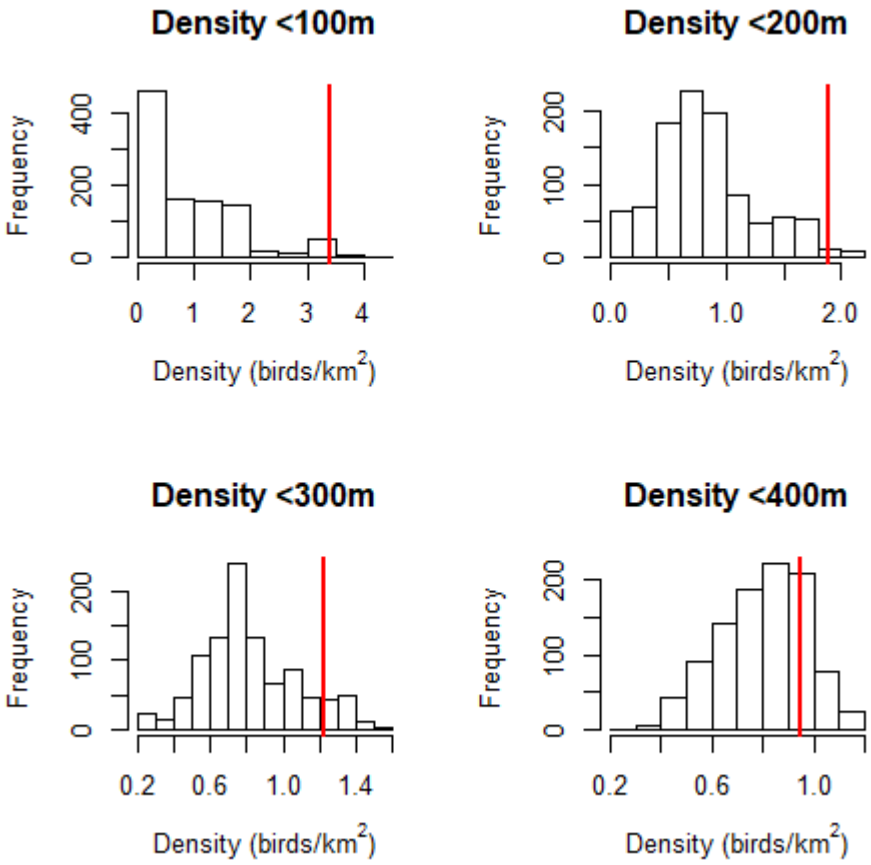

Figure F3. Razorbill densities within 100/200/300/400m of turbine locations (red lines) and distribution of densities estimated for 1,000 simulations with randomly re-positioned turbines (relative turbine positions maintained) at RPM <2.

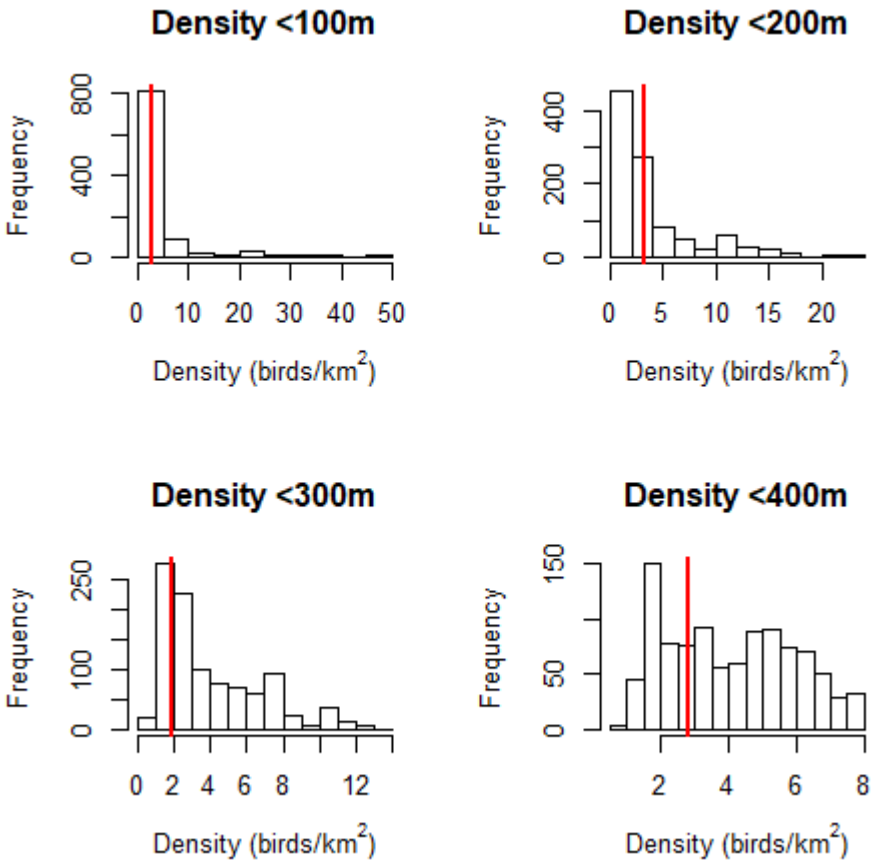

Figure F4. Kittiwake densities within 100/200/300/400m of turbine locations (red lines) and distribution of densities estimated for 1,000 simulations with randomly re-positioned turbines (relative turbine positions maintained) at RPM <2.

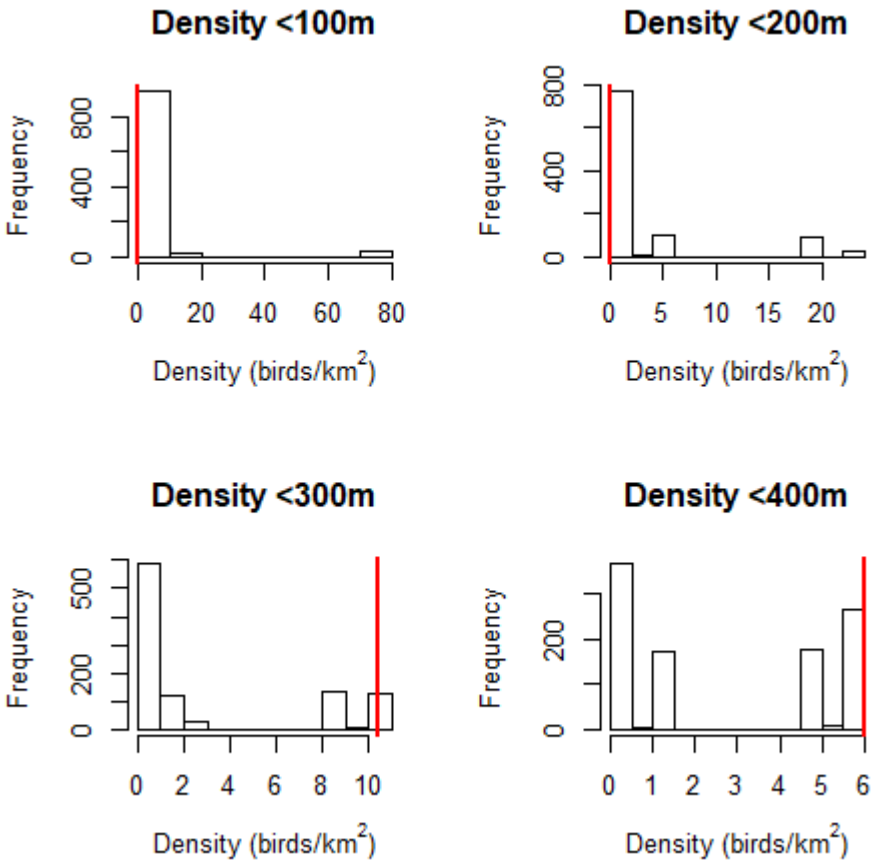

Figure F5. Herring gull densities within 100/200/300/400m of turbine locations (red lines) and distribution of densities estimated for 1,000 simulations with randomly re-positioned turbines (relative turbine positions maintained) at RPM <2.

RPM 2 - 4

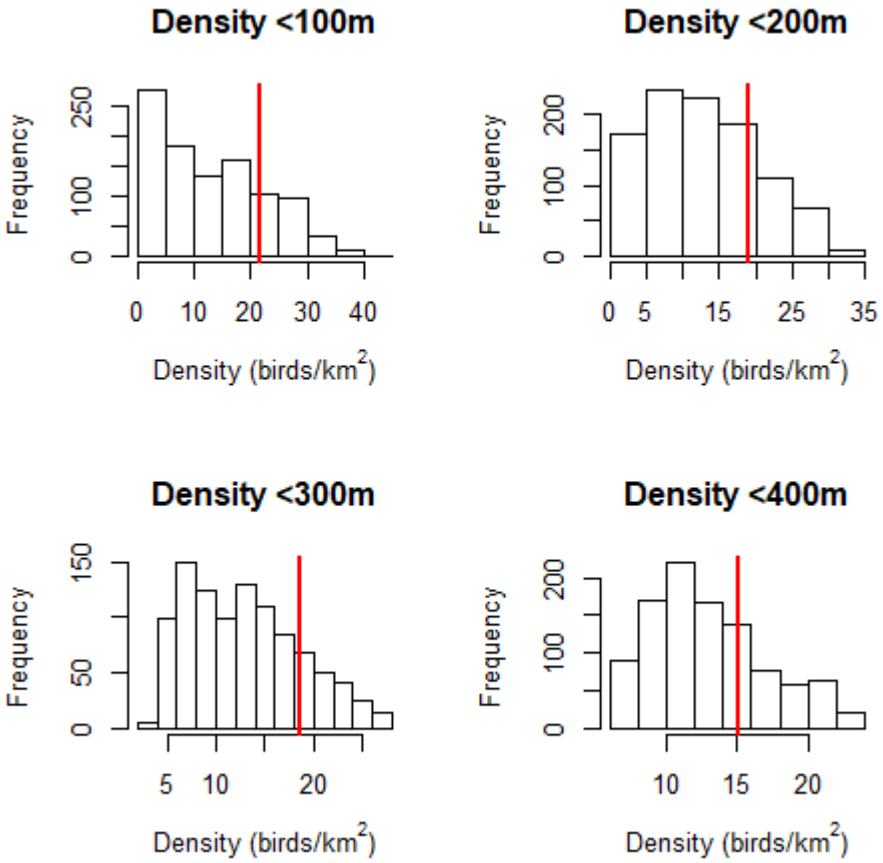

Figure F6. Guillemot densities within 100/200/300/400m of turbine locations (red lines) and distribution of densities estimated for 1,000 simulations with randomly re-positioned turbines (relative turbine positions maintained) at RPM >=2 <4.

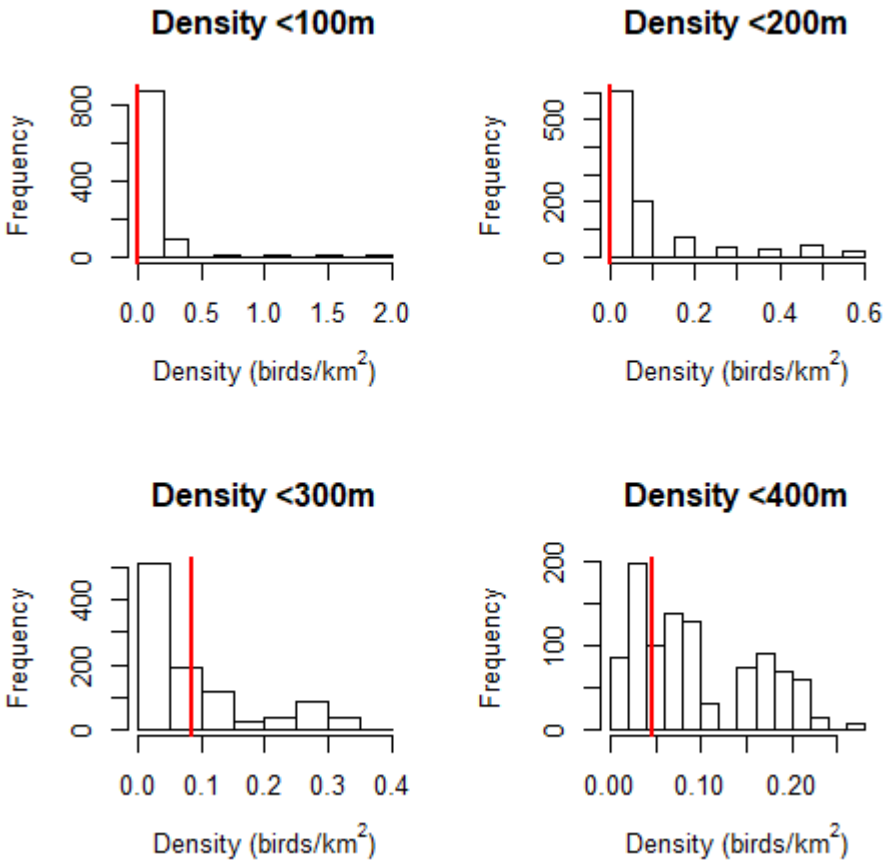

Figure F7. Puffin densities within 100/200/300/400m of turbine locations (red lines) and distribution of densities estimated for 1,000 simulations with randomly re-positioned turbines (relative turbine positions maintained) at RPM >=2 <4.

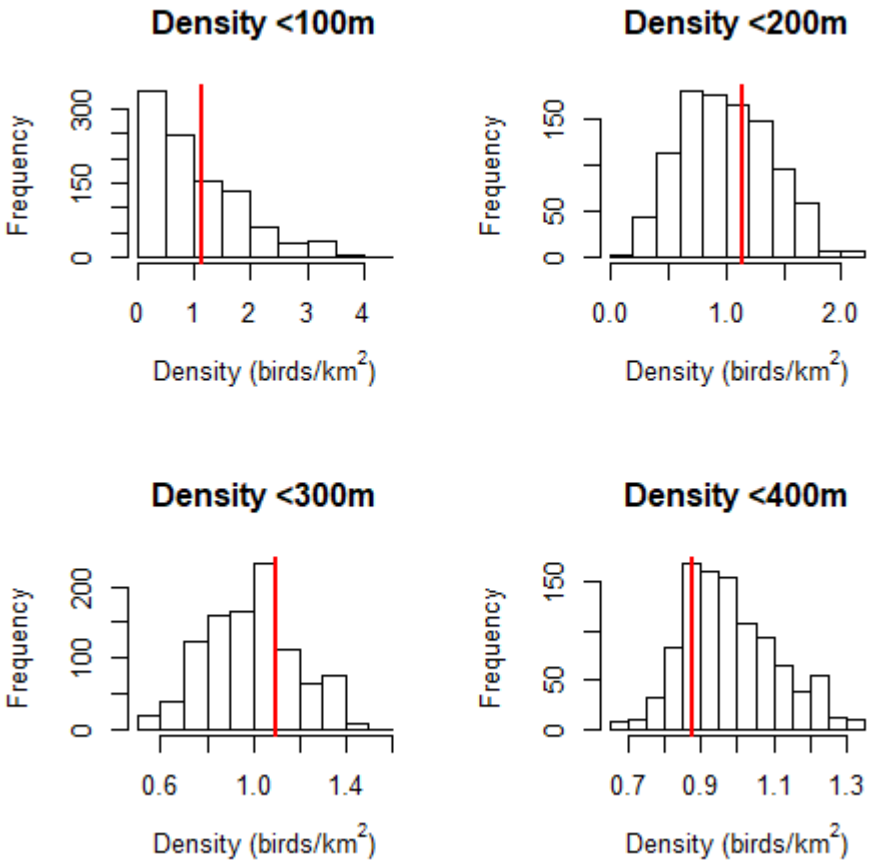

Figure F8. Razorbill densities within 100/200/300/400m of turbine locations (red lines) and distribution of densities estimated for 1,000 simulations with randomly re-positioned turbines (relative turbine positions maintained) at RPM >=2 <4.

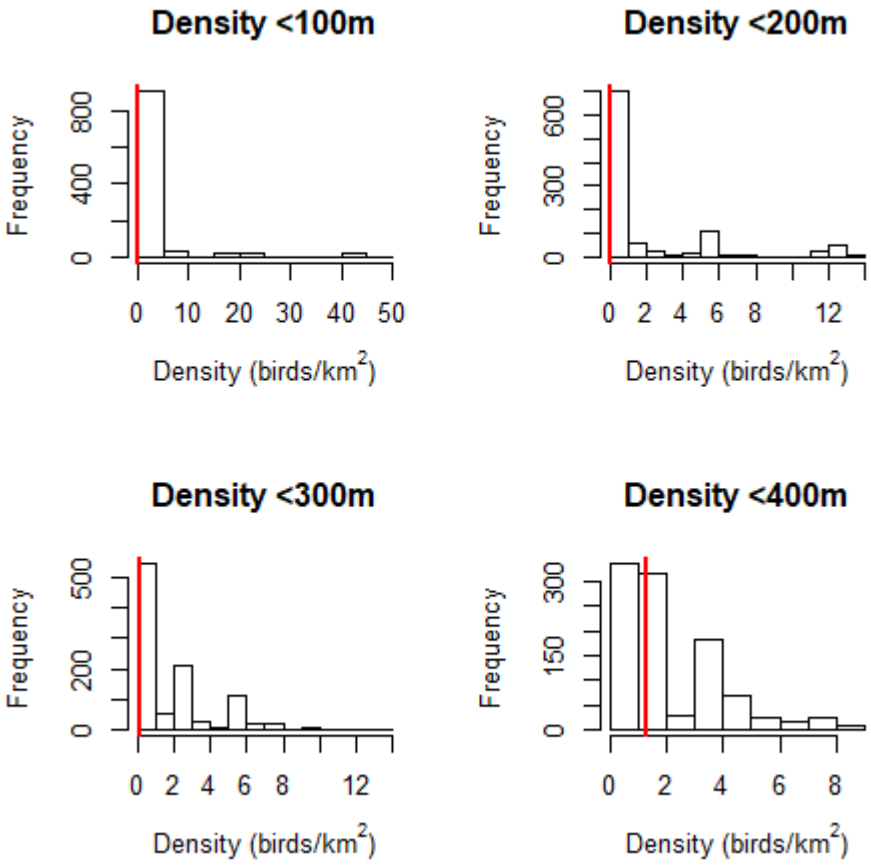

Figure F9. Kittiwake densities within 100/200/300/400m of turbine locations (red lines) and distribution of densities estimated for 1,000 simulations with randomly re-positioned turbines (relative turbine positions maintained) at RPM >=2 <4.

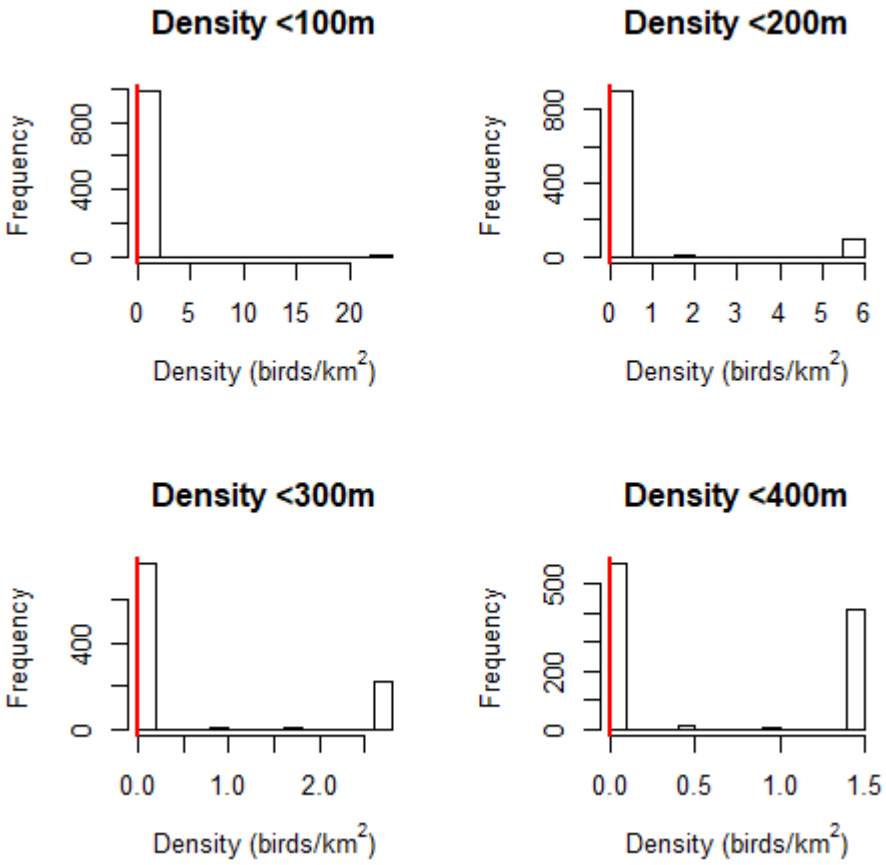

Figure F10. Herring gull densities within 100/200/300/400 m of turbine locations (red lines) and distribution of densities estimated for 1,000 simulations with randomly re-positioned turbines (relative turbine positions maintained) at RPM >=2 <4.

RPM 4 - 6

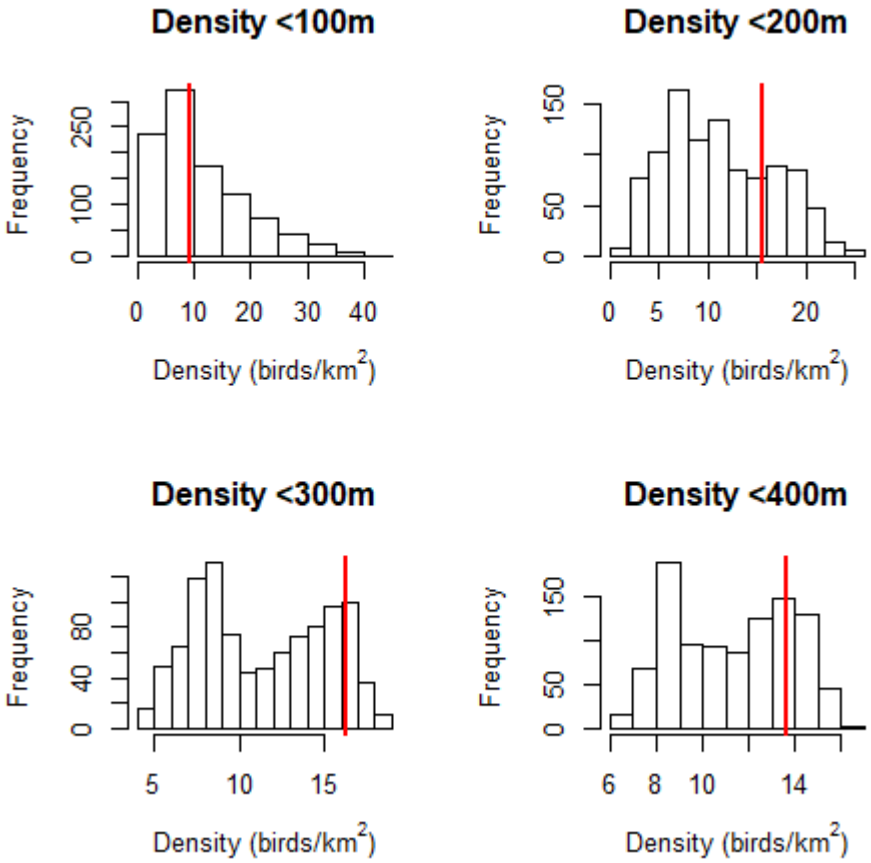

Figure F11. Guillemot densities within 100/200/300/400m of turbine locations (red lines) and distribution of densities estimated for 1,000 simulations with randomly re-positioned turbines (relative turbine positions maintained) at RPM >=4 <6.

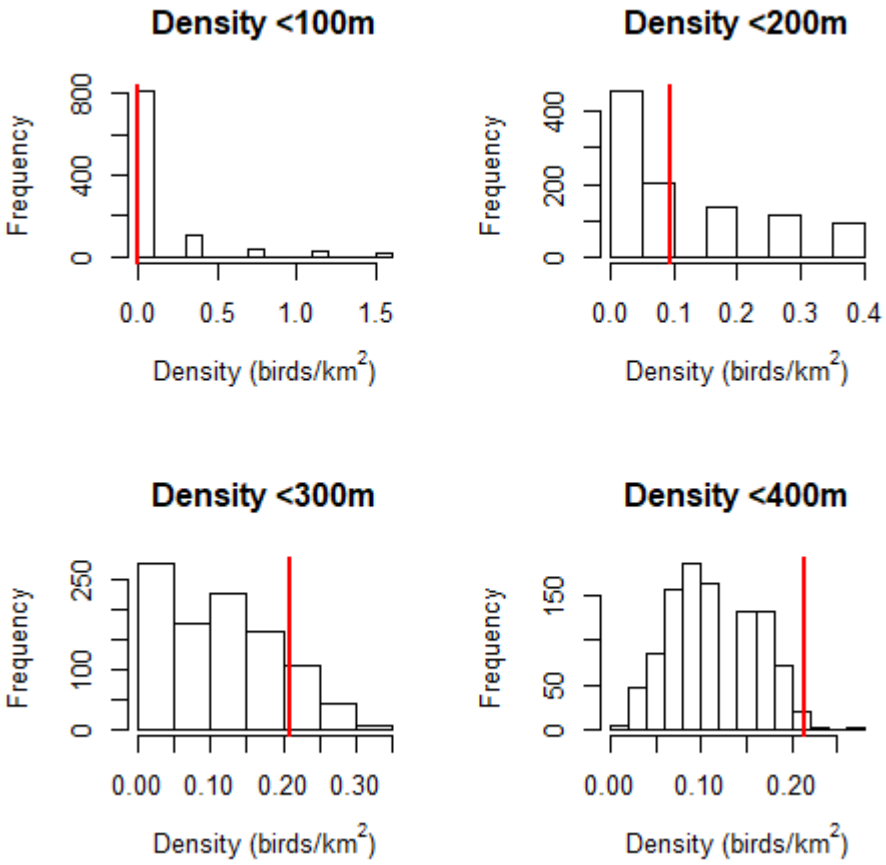

Figure F12. Puffin densities within 100/200/300/400m of turbine locations (red lines) and distribution of densities estimated for 1,000 simulations with randomly re-positioned turbines (relative turbine positions maintained) at RPM >=4 <6.

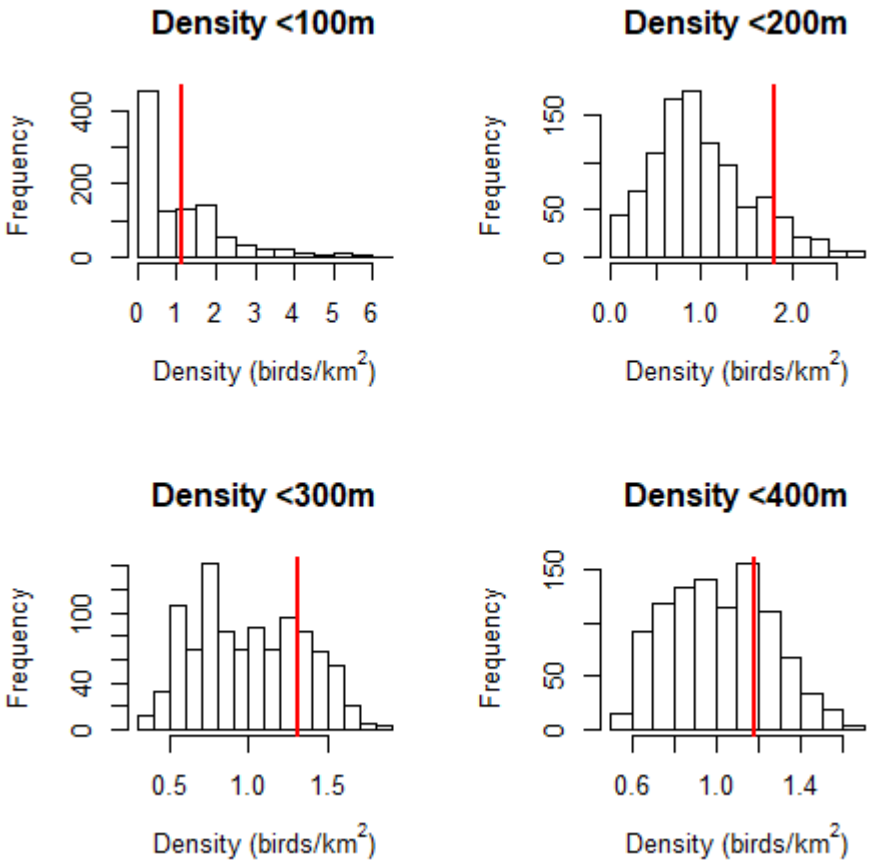

Figure F13. Razorbill densities within 100/200/300/400 m of turbine locations (red lines) and distribution of densities estimated for 1,000 simulations with randomly re-positioned turbines (relative turbine positions maintained) at RPM >=4 <6.

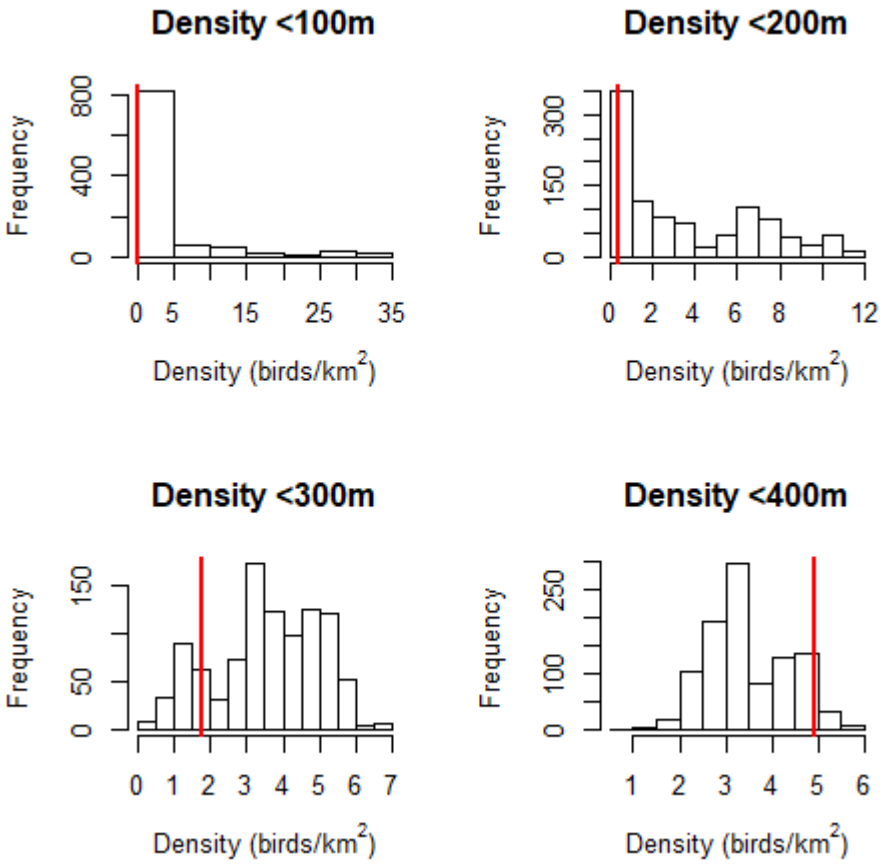

Figure F14. Kittiwake densities within 100/200/300/400 m of turbine locations (red lines) and distribution of densities estimated for 1,000 simulations with randomly re-positioned turbines (relative turbine positions maintained) at RPM >=4 <6.

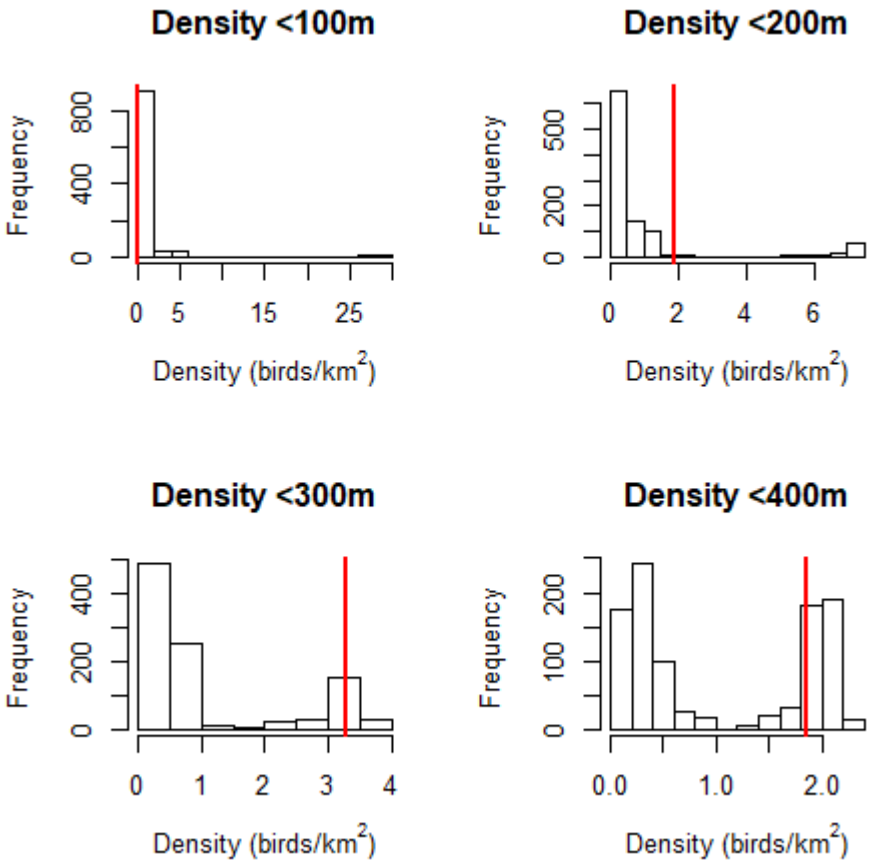

Figure F15. Herring gull densities within 100/200/300/400 m of turbine locations (red lines) and distribution of densities estimated for 1,000 simulations with randomly re-positioned turbines (relative turbine positions maintained) at RPM >=4 <6.

RPM 6 - 8

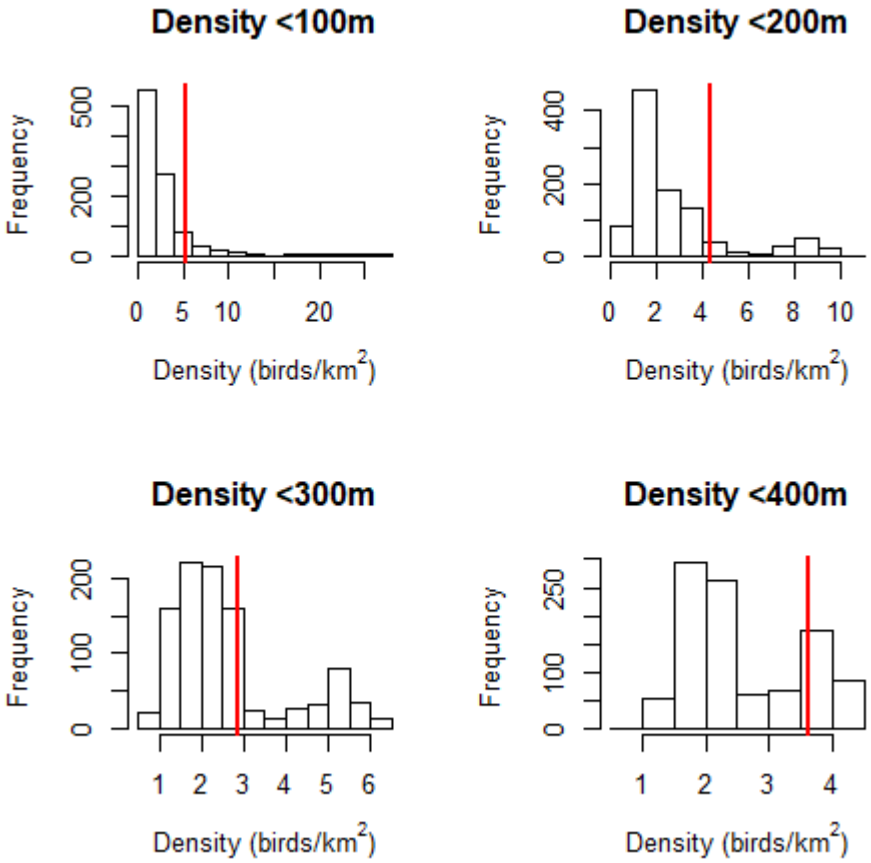

Figure F16. Guillemot densities within 100/200/300/400 m of turbine locations (red lines) and distribution of densities estimated for 1,000 simulations with randomly re-positioned turbines (relative turbine positions maintained) at RPM >=6 <8.

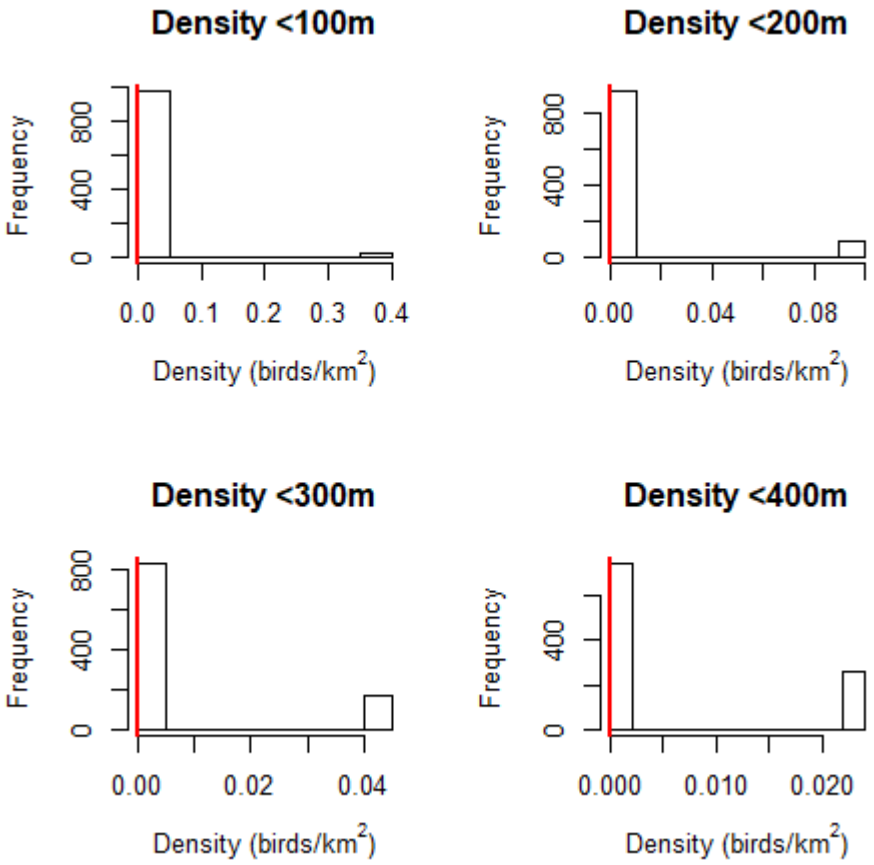

Figure F17. Puffin densities within 100/200/300/400 m of turbine locations (red lines) and distribution of densities estimated for 1,000 simulations with randomly re-positioned turbines (relative turbine positions maintained) at RPM >=6 <8.

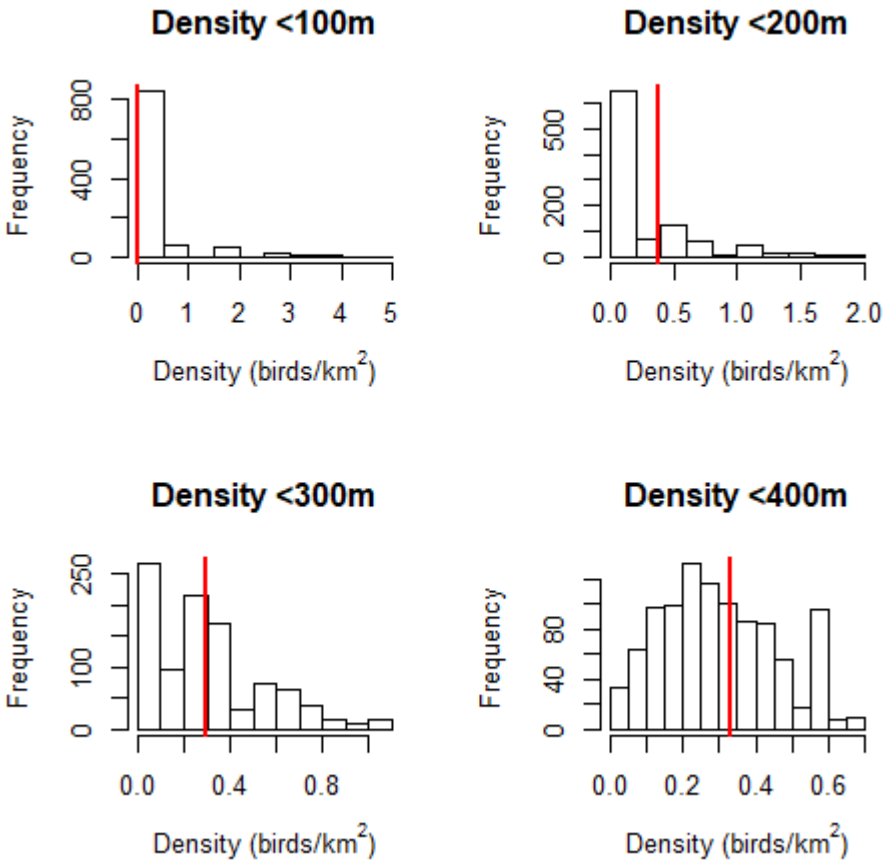

Figure F18. Razorbill densities within 100/200/300/400 m of turbine locations (red lines) and distribution of densities estimated for 1,000 simulations with randomly re-positioned turbines (relative turbine positions maintained) at RPM >=6 <8.

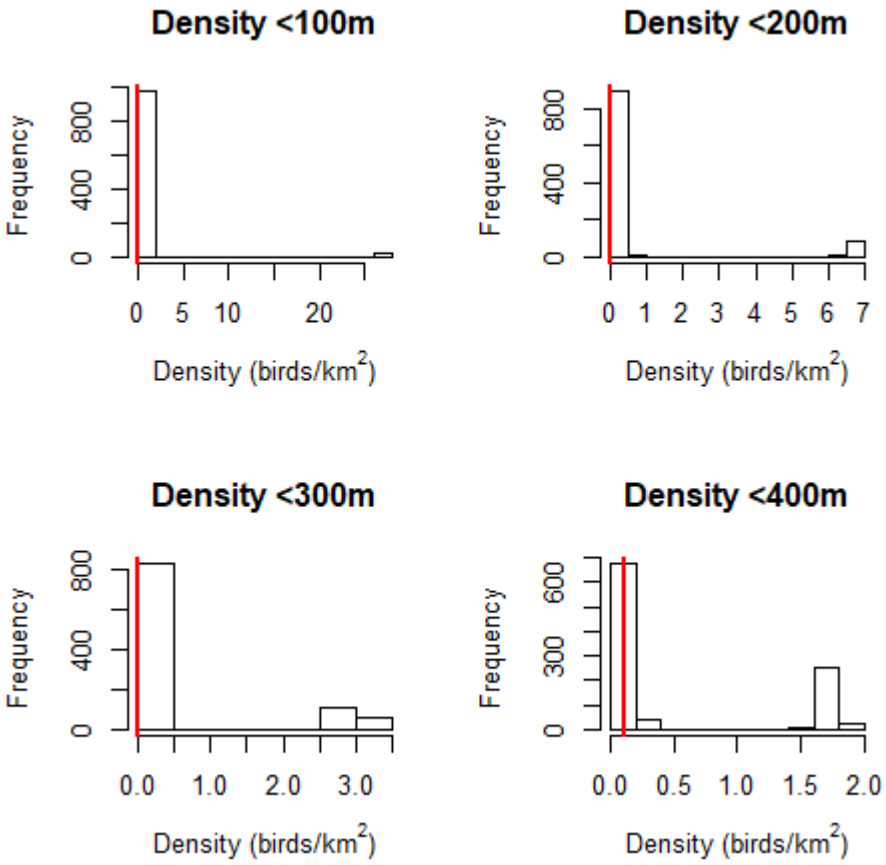

Figure F19. Kittiwake densities within 100/200/300/400 m of turbine locations (red lines) and distribution of densities estimated for 1,000 simulations with randomly re-positioned turbines (relative turbine positions maintained) at RPM >=6 <8.

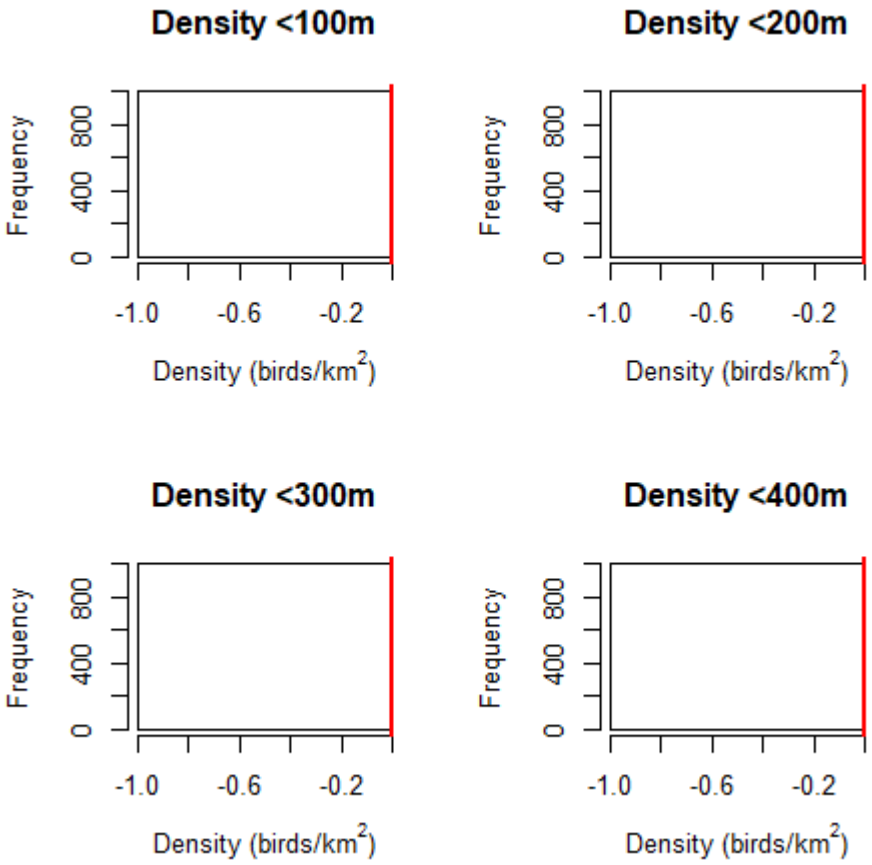

Figure F20. Herring gull densities within 100/200/300/400 m of turbine locations (red lines) and distribution of densities estimated for 1,000 simulations with randomly re-positioned turbines (relative turbine positions maintained) at RPM >=6 <8.

RPM >8

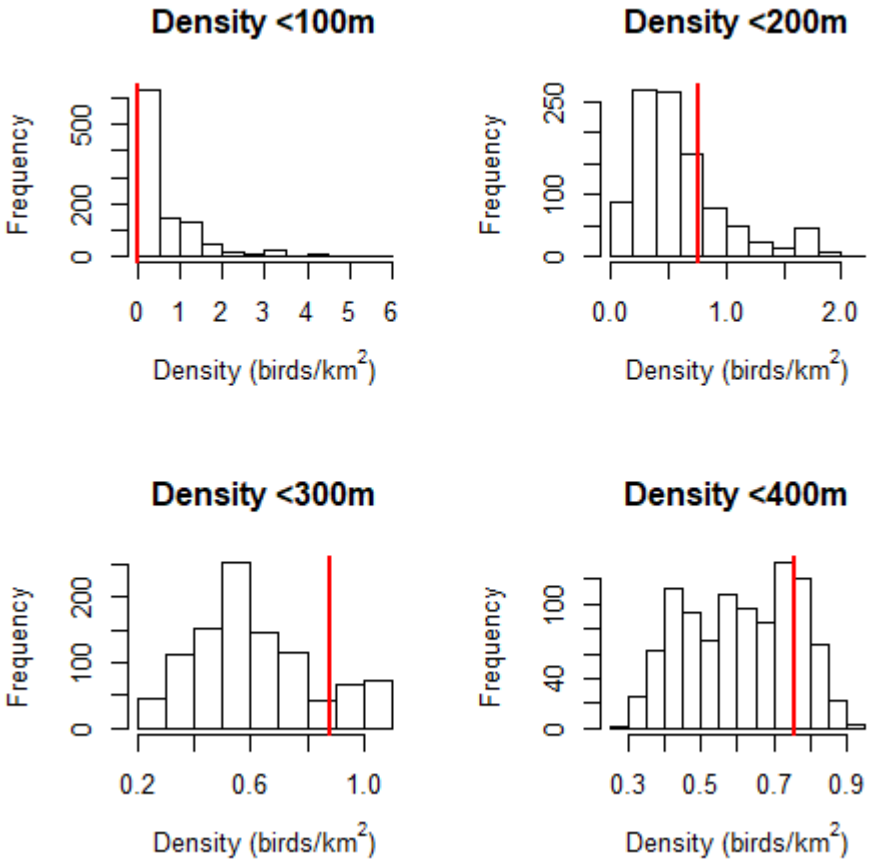

Figure F21. Guillemot densities within 100/200/300/400 m of turbine locations (red lines) and distribution of densities estimated for 1,000 simulations with randomly re-positioned turbines (relative turbine positions maintained) at RPM >=8.

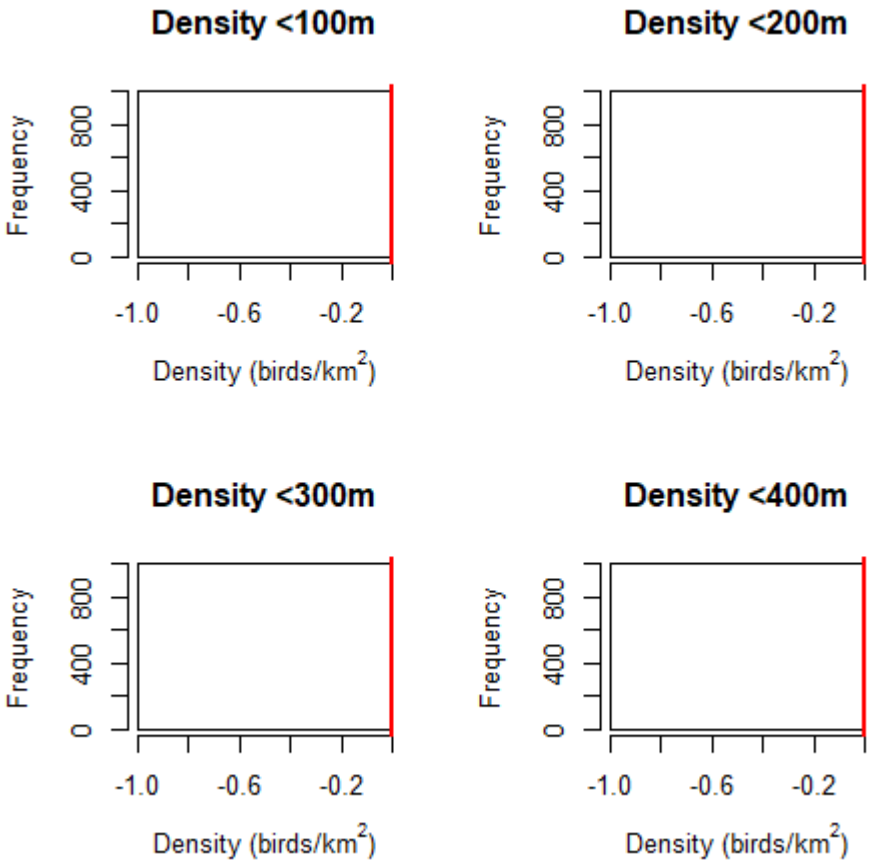

Figure F22. Puffin densities within 100/200/300/400 m of turbine locations (red lines) and distribution of densities estimated for 1,000 simulations with randomly re-positioned turbines (relative turbine positions maintained) at RPM >=8.

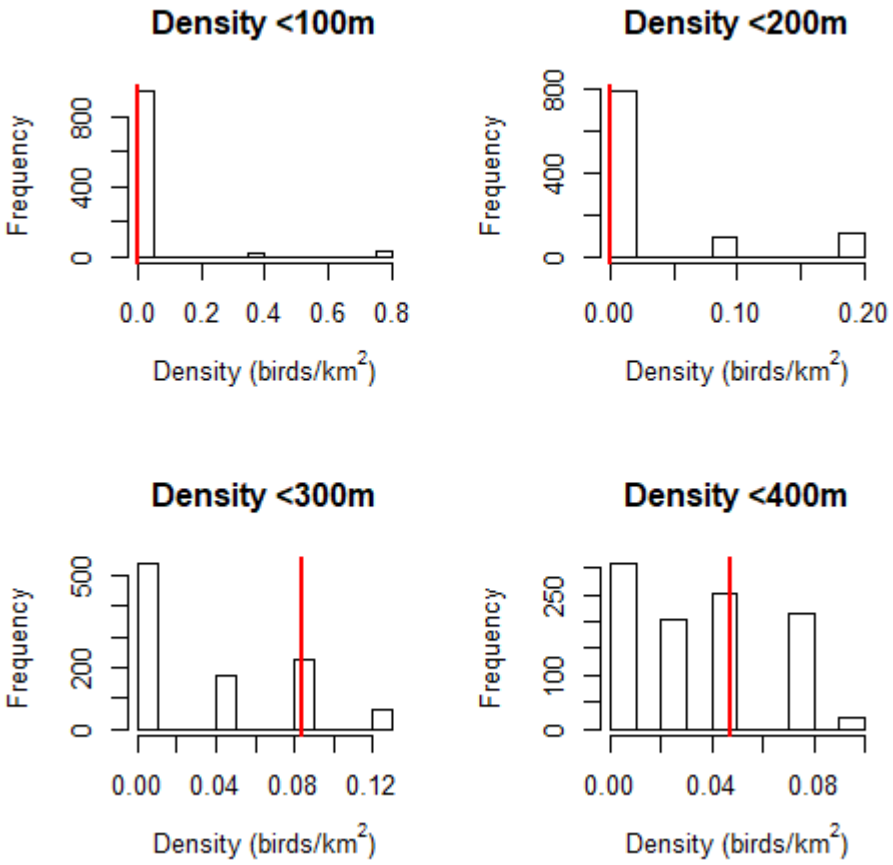

Figure F23. Razorbill densities within 100/200/300/400 m of turbine locations (red lines) and distribution of densities estimated for 1,000 simulations with randomly re-positioned turbines (relative turbine positions maintained) at RPM >=8.

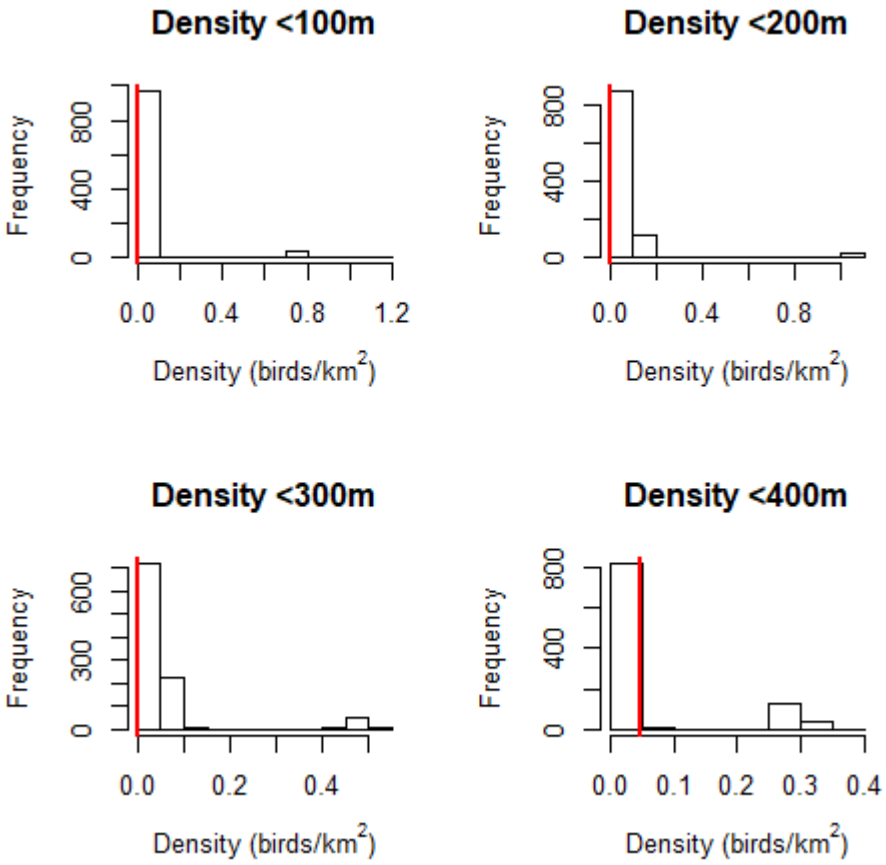

Figure F24. Kittiwake densities within 100/200/300/400 m of turbine locations (red lines) and distribution of densities estimated for 1,000 simulations with randomly re-positioned turbines (relative turbine positions maintained) at RPM >=8.

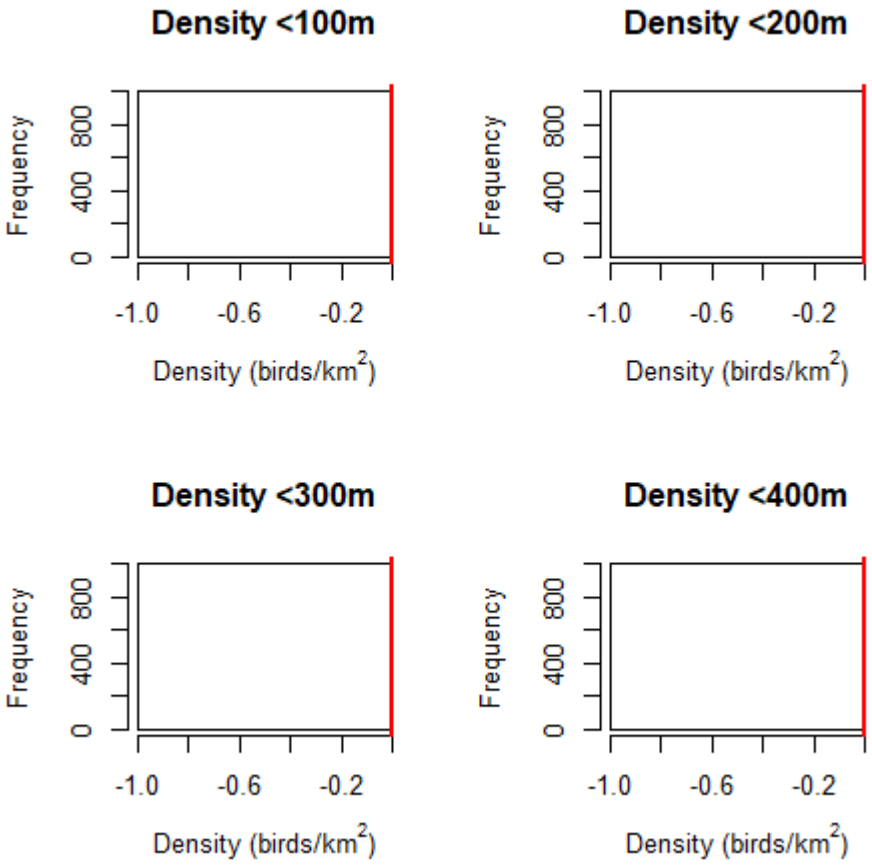

Figure F25. Herring gull densities within 100/200/300/400 m of turbine locations (red lines) and distribution of densities estimated for 1,000 simulations with randomly re-positioned turbines (relative turbine positions maintained) at RPM >=8.